Supporting Information

Kinetics-Controlled Amphiphiles Self-Assembly Processes

Xiaoyan Zheng,[†,‡] Lizhe Zhu,[†] Xiangze Zeng,[†] Luming Meng,[†] Lu Zhang,[†] Dong Wang,[§] and Xuhui Huang[*,†,‡]

[†]Department of Chemistry and Hong Kong Branch of Chinese National Engineering Research Center for Tissue Restoration & Reconstruction, The Hong Kong University of Science and Technology, Clear Water Bay, Kowloon, Hong Kong

[‡]HKUST-Shenzhen Research Institute, Nanshan, Shenzhen 518057, P.R. China

[§]Key Laboratory of Organic OptoElectronics and Molecular Engineering, Department of Chemistry, Tsinghua University, Beijing 100084, P. R. China

Email: xuhuihuang@ust.hk

Supplementary Methods and Discussions

The critical packing parameter of PYR and PYN. The critical packing parameter $P = v/a_0 l_c$ has been widely applied to predict the assembled structure for conventional surfactants.[1] Here, v is the volume of the hydrophobic tail, a_0 is the effective head group surface area and l_c is the length of the extended hydrophobic tail (visualized in Figure S2). When $0 < P \leq 1/3$, only spherical micelles should exist in solution. When $1/3 < P \leq 1/2$, the aggregates are in a rod-like or hexagonal shape. When $1/2 < P \leq 1$, the aggregates are bilayer-like structure.

Because a_0 is related to the interfacial free energy per unit area of the amphiphiles and sensitive to its shape, concentration and solvent condition, we adopt a recent QM-MM hybrid method[2] to predict the shape of aggregates at critical aggregation concentration (*cac*). We used the optimized structure of PYR and PYN (the same structures as the RESP charge fitting) for the calculations. The hydrophobic tail and the hydrophilic head group of both PYR and PYN were represented by the green and pink colors respectively (see Figure S2). The length of the extended hydrophobic tail, l_c of both molecules were also labeled in Figure S2. In addition, we used g_sas tool in Gromacs (version 4.5.4) to calculate the v and a_0. The obtained P values for PYR and PYN at *cac* were 0.269 and 0.163 respectively (see Table S1), indicating that they should both assemble into spherical micelles. Clearly, these P values are insufficient to predict the distinction between PYR-tubes and PYN-vesicles.

Fitting the force field parameters of PYR and PYN for the all-atom (AA) and coarse-grained (CG) simulations. We performed the large-scale molecular dynamics simulations at both the all-atom (AA) and coarse-grained (CG) resolution to obtain enough information for understanding amphiphilic molecules self-assembly mechanism, as summarized in Table S2. (1) We preformed the systematic dihedral angle scan by both the quantum mechanism (QM) and molecular mechanism (MM) calculations to fit new sets of force field parameters for the dihedral angles C=C-C-O of PYR and C=C-C-N of PYN. We also carried out two independent 150 ns AAMD simulations to valid the new fitted force field parameters. Based on the above two sets of AAMD simulations, we fit the coarse-grained (CG) force-field parameters for both PYR and PYN (see **1** and **2** in Table S2, and Figure S1). (2) We ran two serials of 100 independent 12 μs CGMD simulations to obtain sufficient samplings, based on which the kinetic network models (KNMs) for PYR and PYN could be

constructed (see **3** and **4** in Table S2). (3) We performed two serials of 50 independent 1.2 μs CGMD simulations for PYR and PYN to calculate the adhesion rate during two micelles adhesion process (see **5** and **6** in Table S2).

Check the force field parameters in the General Amber Force Field (GAFF) based on the quantum mechanism (QM) calculations. Here, all the atom types and force field parameters of PYR and PYN were built based on the General Amber Force Field (GAFF)[3]. Before performing the AAMD simulations, we need to check and validate the force field parameters of the dihedral angles C=C-C-O of PYR and C=C-C-N of PYN in GAFF first, because these two dihedral angles play important roles in the conformational difference between PYR and PYN (see Figure S1). The details of the force field parameters validation were as follows:

(1) We extracted the representative fragments from PYR and PYN by replacing the carbon chain into the methyl group. Then, we preformed the geometry optimization for each fragment by the QM calculations at B3LYP/6-31G** level using Gaussian 09 package[4].

(2) We scanned the dihedral angle C=C-C-O of PYR and C=C-C-N of PYN through rotating the middle C-C single bond by 360° with an interval of 5° and performed the geometry optimization at each step by QM method at B3LYP/6-31G** level, yielding the QM energy profiles for PYR and PYN (see Figure S3a-b).

(3) We calculated the corresponding MM energy profiles by MM method based on the optimized QM structures (see Figure S3a-b).

Obviously, the obtained MM energy profile for the dihedral angle C=C-C-N of PYN was consistent with the QM profile (see Figure S3b). Yet the MM and QM profiles for the dihedral angle C=C-C-O of PYR were different (see Figure S3a, blue and black lines), which urged us to perform further fitting and to obtain new set of MM parameters for the PYR dihedral angle.

In addition, the partial charge of each atom in both PYR and PYN, as well as the extracted fragments were obtained by the Restrained Electrostatic Potential (RESP) method[5-6] at HF/6-31G* level based on the optimized structures at B3LYP/6-31G* level.

Force field parameters fitting for the dihedral angle C=C-C-O of PYR. The dihedral angle parameters fitting was performed based on the Ryckaert-Bellemans (RB) function[7] as follows:

(1) Calculate the QM and MM energy profiles of the PYR fragment.

(2) Calculate the energy difference (ΔE) between the QM and MM energy profiles.

(3) Fit a new set of dihedral angle parameters to ΔE based on the RB function.

(4) Calculate the MM energy profile again on top of the new fitted parameters and compare it with the QM result.

(5) Repeat steps (2) – (4) iteratively until ΔE within a certain threshold.

As shown in Figure S3a (green), the new MM energy profile for C=C-C-O of PYR after fitting could well-reproduce the QM result.

Validation of the force field parameters of PYR and PYN. We further validate the obtained new force field parameters by performing 2 independent 150 ns AAMD simulations for PYR and PYN, respectively (see **1** and **2** in Table S2). The initial configuration for AAMD simulation were generated by placing one target PYR or PYN in a cubic box with edge length of 50 Å. Then, we solvated it by ~ 4100 pre-equilibrated TIP3P waters. One bromide ion was added in each system to neutralize the positive charged pyridinium group. For each system, we first performed energy minimization using the steepest descent algorithm. After that, we carried out two independent 150 ns production AAMD simulations under NPT (T = 300 K and P = 1 atm) ensemble with a time step of 2 fs. Weak couplings to the external heat and pressure baths were applied based on the V-rescale[8] and Parrinello-Rahman[9] schemes, respectively. Periodic boundary conditions were applied in all the three dimensions. The electrostatic interactions were treated via the particle mesh Ewald (PME) method[10-11] with truncation at 1.2 nm. The cutoff distance for the Van der Waals interactions was also 1.2 nm. In this work, all MD simulations were performed by the GROMACS software (version 4.5.4)[12].

The distribution of dihedral angles C=C-C-O of PYR and C=C-C-N of PYN were illustrated in Figure S4. Clearly the dihedral angle C=C-C-O of PYR sat mainly at 75° and 275°, while the corresponding dihedral angle C=C-C-N of PYN was centered at 90° and 270°. Such distribution from AAMD simulations was consistent with the positions of the local minimum in the final MM profiles in Figure S3, meaning that the force field parameters were sufficient to describe the dynamics of PYR and PYN in aqueous solution.

Site mapping between the All-atom model and the Coarse-grained (CG) model. Based on the mapping rule of the MARTINI force field[13], we setup CG models for PYR and PYN. Here, four types of beads were adopted: polar (P), non-polar (N), apolar (C) and charged (Q), representing the chemical insights of the atomistic structures. The prefix “S” was used to label the beads of the

aromatic rings. After mapping, both PYR and PYN were represented by the 15 CG beads (see Figure S1). The pyrenyl ring was represented by seven CG beads with type SC5 (gray in Figure S1). To keep the large pyrenyl ring planar, we assigned the mass of the whole pyrenyl group only onto three real beads (see the triangles in light blue, Figure S1) and set the other four beads as the massless virtual sites. The carbon chains (with ten carbon atoms) were divided sequentially into propyl, butyl and propyl groups, labeled by the beads with types C2, C1 and C2, respectively (gray in Figure S1). The positive charged pyridinium group was mapped into an equilateral triangular ring by three beads with types SC3, SC3, and SQ0 (with unit positive charge) respectively (magenta in Figure S1). The solvated bromide ion was represented by one CG bead with type Qa (with unit negative charge, magenta in Figure S1). The ester group of PYR and the amide group of PYN were represented by the CG bead with type Na and P4, respectively (in gray and magenta, highlighted by the black dashed circle in Figure S1). For solvent, four real water molecules were grouped together and represented by one bead with type P4. Here, all real CG beads were assigned the real mass, see more details in the force field parameters part in the SI.

Fitting the CG force-field parameters based on the All-atom MD simulations. In the present study, the equilibrium bond lengths and bond angles for the CG model of PYN and PYR were fitted from AAMD trajectories. The force constants of the bond length, bond angle and the non-bonded parameters were directly inherited from the MARTINI force field[13]. After converting the AA trajectories into CG representations via the site-mapping rule, we fit the distribution of each CG bond length and angle into a Gaussian function. Subsequently, we took the peak value of each fitted Gaussian curve as the equilibrium bond length and bond angle in the CG model. The force field parameters of waters were directly inherited from the MARTINI force field[13].

Because of the smoother potential energy surface in the CG model than that in AA model, the dynamics of the CGMD simulation is significantly faster than the AAMD simulation, thus a scaling factor of 4 is used for the timescale interpretation[13]. All the simulation time presented in this work is the effective time obtained by the real simulation time multiplied by 4.

Coarse-Grained Molecular Dynamics (CGMD) simulation set-up. To obtain sufficient samplings for the construction of the kinetic network models (KNMs), we performed large scale CGMD simulations for PYR and PYN. The initial configurations were generated by randomly placing 125 amphiphiles PYR or PYN in the cubic box with edge length of 278.6 Å (see **3** and **4** in

Table S2). Such simulation boxes contained 182,208 and 181,974 beads, corresponding to 2,173,246 and 2,170,563 atoms in total for PYR and PYN, respectively. Notable, the concentrations for both systems were set at 0.1 mol/L, three orders of magnitude higher than those in experiments (1×10^{-4} mol/L)[14-15]. Such high concentration is necessary to reduce the overall computational cost. For each system, after energy minimization, we preformed 100 independent 12 μs CGMD production simulations with different initial velocities under NPT ensemble (see Figures S5-S6). The couplings to both external heat and pressure were applied via the Berendsen schemes[16]. Periodic boundary conditions were applied in all three dimensions. The LINCS algorithm was used to restrain all bond lengths[17]. Particle Mesh Ewald (PME) method[10-11] was applied to calculate the long range electrostatic potential. The cutoff distances of both short range electrostatic potential and van der Waals potential were set to 1.1 nm. The time step was 30 fs. The configurations were stored with the time interval of 2.4 ns for analysis. The total simulation time for both PYR and PYN is 1,200 μs. In total, we collected 500,000 conformations from the CGMD simulations for both PYR and PYN.

Construction of the kinetic network models (KNMs)

Extracting aggregates from CGMD trajectories. We defined two molecules belong to the same aggregate when there exists at least six pairs of contact beads between them (i.e. six pairs of beads with distance shorter than 7 Å). Based on this definition, we extracted 2,696,987 and 2,586,926 aggregates for PYR and PYN respectively.

Order parameters to describe the aggregate conformation. We chose aggregate size and morphology as the order parameters to describe the conformation of each aggregate. Here, the aggregate size (*N*), *i.e.* the number of monomers of each aggregate, is a natural choice to trace the aggregate growth process. In addition to aggregate size, the morphology (shape) of each aggregate was also a widely applied order parameter in previous self-assembly studies by both the experimentalists or theorists[18-24]. Here, the aggregate morphology is quantified by the asphericity parameter (Ap)[25-30]:

$$A_p = \frac{\left(\lambda_1^2-\lambda_2^2\right)^2+\left(\lambda_1^2-\lambda_3^2\right)^2+\left(\lambda_3^2-\lambda_2^2\right)^2}{2\left(\lambda_1^2+\lambda_2^2+\lambda_3^2\right)^2} \quad \text{(S1)}$$

where $\lambda_1, \lambda_2, \lambda_3$ are three eigenvalues of the radius of gyration tensor *A* of each aggregate. *A* is

defined as $A=\begin{bmatrix} S_{xx} & S_{xy} & S_{xz} \\ S_{yx} & S_{yy} & S_{yz} \\ S_{zx} & S_{zy} & S_{zz} \end{bmatrix}$, where $S_{xx}=\frac{1}{n}\sum_i (x_i - x_c)^2$, $S_{xy}=\frac{1}{n}\sum_i (x_i - x_c)(y_i - y_c)$, n is the number of beads of each aggregate. x_i is the coordinate of the i^{th} bead. x_c is the center-of-mass (COM) of each aggregate. According to the general classification of the aggregate morphology, the aggregate is a sphere-like micelle, when Ap ≤ 0.1; a disk-like micelle, when 0.1 < Ap ≤ 0.6; a rod-like micelle, when Ap > 0.6[26, 31-32].

As shown in Figure S7, the projections of all collected aggregates on *N* and Ap span a wide range, indicating that the aggregates grow along the assembled pathways with various conformations states. A few snapshots of the representative aggregates with different size and shape were shown in Figure S7 to demonstrate the aggregate conformations.

Identifying conformational states by clustering. To construct the kinetic network model, we need to divide all the extracted aggregates into different conformational states. To do this, we first partitioned all extracted aggregates into 30 conformational states based on the size *N* by the k-centers clustering algorithm[33]. Here, *N* covered the whole size range from 1 (monomer) to 125 (the total number of amphiphiles), see Figure S8. We then grouped all aggregates into 3 based on their shapes, according to Ap: sphere-like (Ap ≤ 0.1), disk-like (0.1 < Ap ≤ 0.6) and rod-like (Ap > 0.6) micelles. Finally, we constructed a product basis containing 30×3 possible combined conformational states. After removing the empty states, we obtained 76 and 75 conformational states for PYR and PYN, respectively (details in Figure S8 and also in Tables S3, S4).

Constructing the mass flow matrix. Because the self-assembly processes of amphiphiles PYR and PYN were strong energetically downhill, the transitions corresponding to the aggregate dissociation were rarely sampled in our finite-length CGMD simulations. Consequently, the Transition Path Theory (TPT)[34-35] cannot be directly applicable to our dataset as it is formulated under the assumption of the equilibrium sampling, where the detailed balance is satisfied. To address this issue, we followed our previous work[36] to identify the self-assembly pathways based on the mass flow matrix $\{\mu_{ij}\}$ rather than the equilibrium flux matrix used in TPT. Each element μ_{ij} was defined as the collective mass of all amphiphilic molecules going through transition from the conformational state *i* to the conformational state *j* after a lag time Δt in all CGMD trajectories.

$$\mu_{ij} = \sum_{traj}\sum_{k}\sum_{n=1}^{N-1} m L_k^i \delta^i_{x(k,n\Delta t)} \delta^j_{x(k',(n+1)\Delta t)} \quad \text{(S2)}$$

where *traj* and *k* represent the identity of the trajectory and the aggregate, respectively. *m* is the mass of one amphiphilic molecule PYR or PYN. L_k is the size of aggregate k. $\delta^i_{x(k,n\tau)}$ was the conformational state indicator function: $\delta^i_{x(k,n\tau)} = \begin{cases} 1, x(k,n\Delta t) = i \\ 0, x(k,n\Delta t) \neq i \end{cases}$, where $x(k,n\Delta t)$ denotes the conformational state that the aggregate k belongs to at time $n\Delta t$. When two aggregates adhere, the size of both aggregates changed simultaneously. To avoid double count, the mass flow was counted only if: $L_{(k,n\Delta t)} \geq L_{(k,(n+1)\Delta t)} - L_{(k,n\Delta t)}$, where $L_{(k,n\Delta t)}$ and $L_{(k,(n+1)\Delta t)}$ representing the aggregate size at $n\Delta t$ and $(n+1)\Delta t$, respectively. In other words, we only traced the transitions of the larger aggregate at each time.

Identifying the self-assembly pathways

Obtaining an ensemble of self-assembly pathways from kinetic network models. The self-assembly pathways were identified from the kinetic network models (mass flow matrix) by the modified Dijkstra's algorithm[37]. We chose small-size aggregates ($N \leq 5$ for PYN and $N \leq 6$ for PYR) as the initial state, denoted by **I**, and the large-size aggregates with $N \geq 113$ and $0.1 < \mathrm{Ap} \leq 0.6$ were chosen as the final state, denoted by **F**. All remaining conformational states were assigned as the intermediate states (**M**). The detailed procedure is listed below.

(1) Identify the widest pathway (with largest flux) from the mass flow matrix. The flux of each pathway is defined as the minimum mass flow between two adjacent states along it, i.e. the kinetic bottleneck f_{bn} for this pathway.

(2) Remove the flux of the identified pathway from the mass flow matrix by subtracting $\min\left\{f_{\max,bn}/100, f_{bn}\right\}$ from each edge along this pathway. The upper bound $f_{max,bn}/100$ was set to avoid losing important pathways that share the same edge as the found top flux pathway (see Figure S9).

(3) Repeat (1) (2) until all pathways between **I** and **F** were decomposed.

We present all identified aggregation pathways by a direct node-and-edge graph. In this graph, each node represents each conformational state. The weight of the directed edge corresponds to the

mass flow between these two conformational states. In total, we identified 2033 and 1371 pathways for PYR and PYN, respectively (see Figure S10).

Lumping the microscopic pathways into the metastable path channels. The large number (thousands) of identified paralleled assembly pathways hindered human appreciation of the mechanism of amphiphilic molecules self-assembly. Therefore, we further grouped the kinetically well-connected aggregation pathways into path channels according to their kinetic similarity by the newly developed path lumping algorithm.

The kinetic similarity (S_{MN}) between a pair of pathways was quantified by the accumulated intercrossing flux shared by them. The definition of the S_{MN} is

$$S_{MN} = \frac{1}{2}\sum_{i\in M}\sum_{j\in N}\left(\frac{F_M}{g_i}h_{ij}\frac{F_N}{g_j}+\frac{F_N}{g_j}h_{ji}\frac{F_M}{g_i}\right) \quad \text{(S3)}$$

where F_M and F_N are the flux of pathway M and N, respectively. h_{ij} represents the effective mass flow between nodes *i* and *j*, calculated by the summation over the mass flow of all pathways going through the edge $i \rightarrow j$, namely $h_{ij} = \sum_{M,(i\rightarrow j)\in M} F_M$. g_i is a normalized constant ($g_i = \sum_{M,i\in M} F_M$), reflecting the total effective mass flow going in/out of node *i*. F_M / g_i or F_N / g_j represented the weight of pathway *M* or *N* going through node *i* or *j*.

Based on the calculated similarity matrix $\mathbf{S}_{MN}$, we grouped all identified aggregation pathways into different path channels by the spectral clustering method[38] (Figures S9-S10). The number of path channels of each system was determined by the location of the major gap of the eigenvalues of $\mathbf{S}_{MN}$, corresponding to the largest separation of timescale within the system.

For both PYR and PYN, two metastable path channels were identified: the incremental and hopping channel, respectively. For PYR, the mass flow ratio between the incremental and hopping channel is 69%:31% (the corresponding number of pathways are 1411 and 622, respectively, see Figure S11a, c). For the incremental and hopping channel of PYN, the corresponding mass flow ratio is 41%:59%, and the pathway numbers are 573 and 798, respectively, see Figure S11b,d). The representative top 2 pathways of the major channel for PYR and PYN are shown in Figure 1c-d respectively. Figures S12-S13 demonstrate the top 20 pathways of the incremental and hopping channel of PYR and PYN, respectively.

Assigning individual CGMD simulations to a specific path channel. To explore the dependence of the final assembled structures on the assembly channels (mechanisms), we further assign each assembly CGMD trajectory into a specific path channel based on the kinetic similarity (the inter-crossing fluxes) between the top pathway of each CGMD trajectory and the representative pathways of each path channel. Then, we assign the CGMD trajectory to the specific path channel with larger kinetic similarity to itself. The detailed procedure is listed below.

(1) Construct the mass flow matrix for each CGMD trajectory that arrive at **F**, using the same state definition as for the overall mass flow matrix constructed from all trajectories (see Figure S8, Tables S3 and S4).

(2) Identify all aggregation pathways for each trajectory.

(3) Calculate the kinetic similarity between the top flux pathway of each CGMD trajectory and all representative pathways of the incremental (S_{inc}) and hopping (S_{hop}) channels for PYR and PYN, respectively. Here, the representative pathways of each channel are defined as the top pathways that count for 10% of the total mass flux of each path channel. For PYR, the total number of pathways chosen to calculate the similarity for the incremental and hopping channels were 94 and 155, while for PYN, the corresponding number of pathways were 95 and 53, respectively.

(4) Compare S_{hop} with S_{inc} and assigned the CGMD trajectory to the path channel bearing the larger similarity with itself.

Through this procedure, all the CGMD trajectories were classified into two groups: the incremental group and the hopping group. Statistical analysis can then be performed on all the aggregates at the final conformational state **F** assembled from the different path channels (see Figure S19).

Calculations of the mean first passage times (MFPTs). We computed the mean first passage time (MFPT), i.e. the average time taken for the transition from the conformational state *i* to the conformational state *f* for the first time in all the CGMD trajectories. Both the direct transitions from conformational state *i* to *f* and the transitions through the other intermediate conformational states were included. Here we counted the interstate transitions from the 100 CGMD trajectories directly and calculated the MFPT (F_{if}) by equation (S4):

$$F_{if} = \frac{\sum_{J}^{N}\sum_{m}^{n_J} t_{Jm}^{if}}{\sum_{J}^{N} n_J} \quad \text{(S4)}$$

where *i* and *f* represented the conformational state. *J* and *N* represented the identity of the trajectory and the total number of trajectories, respectively. *m* denotes the aggregate in conformational state *i*. n_J indicated the total number of aggregates in the *J*th trajectory which belongs to conformational state *i* and could transit to conformational state *f* simultaneously. t_{Jm}^{if} represents the interstate transition time of the *m*-th aggregate in *J*-th trajectory from *i* to *f*. The calculated MFPT are demonstrated in Figure S14c.

Calculations of the rate for the two-micelle adhesion process. To better understand the different path channel preference of PYR and PYN, we performed large scale independent CGMD simulations to calculate the adhesion rate in two micelles adhesion process of PYR and PYN (see **5** and **6** in Table S2). The simulations setup was kept identical for PYR and PYN. The detailed procedure is listed below.

(1) Select a sphere-like micelle (*N* = 30, Ap < 0.05) from the original CGMD trajectories, put it in a new cubic box (with edge length of 105 Å) and solvated it by the pre-equilibrated CG waters.

(2) Equilibrate the solvated micelles by 24 ns long CGMD simulations under the NPT ensemble.

(3) Place two equilibrated spherical micelles into the center of the cubic box (edge length 105 Å) with an inter-micellar COM distance of 50 Å and solvate them by the pre-equilibrated CG waters as the initial conformations.

(3) Performed two serials of 50 independent 1,200 ns CGMD simulations with different initial velocities under NPT ensemble (see **5** and **6** in Table S2) after energy minimization of the systems, With a time interval of the snapshots storage at 30 ps, this step generated in total 2,000,000 conformations for PYR and PYN.

(4) Calculate the adhesion rate of two micelles from the initial separated state (**Is**) to the final adhesive state (**Fa**) based on the Mean First Passage Time (MFPT) from **Is** to **Fa**, by equation S5:

$$k_{adhesion} = 1 / MFPT_{adhes} \quad \text{(S5)}$$

Here, we used the inter-micellar COM distance between two micelles to define **Is** (d>5.0 nm) and **Fa** (d<2.9 nm).

The calculated adhesion rate during two micelles adhesion for PYR and PYN are 4.29×10^6 s^{-1} and 7.2×10^6 s^{-1}, respectively (see Figure 2b in the main text).

Packing density and surface positive charge density of each aggregate. We used the *g_sas* tool in GROMACS (version 4.5.4) package[39] to measure the surface area and volume of each aggregate. Here, the probe radius was set to 0.47 nm. Then, we calculated the surface positive charge density of each aggregate by using the total number of positive charges divided by the surface area of each aggregate (see Figure 2c-d in the main text and Figure S17).

The potential energy calculations of the final assembled nanostructures. To evaluate the thermodynamic stability of the final assembled nanostructures formed along the different path channels, we calculated the potential energy of the final assembled aggregates **F** of both PYR and PYN. We first extracted the aggregates from the last 100 frames of each CGMD trajectory of the incremental and hopping channel and then, we calculated the averaged potential energy of all collected aggregates by the GROMACS (version 4.5.4) program. Because the final structures of PYR are all planar, regardless of the growth channel, we evaluate the stability of curved micelles of PYR hypothetically using the conformations of the curved micelles of PYN. This was achieved by replacing the CG bead of the amide group of the curved PYN micelles into the CG bead of the ester group. After replacement, we performed 200 ns CGMD simulations to equilibrate the curved PYR micelles. Finally, we used the curved micelles in the last 50 ns of the CGMD trajectory to calculate the potential energy of PYR aggregates. All calculated averaged potential energy were shown in Figure S22.

Water distributions around each functional group and the distributions of hydrophilic beads within each aggregate. The number of waters within 6.7 Å (cutoff distance) around each functional group of PYR or PYN as a function of time of all CGMD trajectories for both PYR and PYN were obtained by VMD program[40] (Figure S15). The cutoff distance was determined by the range of the first solvation shell of the aggregates based on the radical distribution function of the water molecules around the aggregates (Figure S16). The distribution of hydrophilic bead in the aggregates at **F** of both the incremental and hopping channels were also obtained by VMD program[40] (Figure S23).

The impact of the individual molecular conformations on self-assembly mechanisms. To

examine the impact of the molecular conformation on self-assembly mechanism, we have analyzed the distributions of the monomer conformation for PYR and PYN molecules within the aggregates at all stages of the assembly. The results show that the difference between PYR and PYN conformations is negligible when the aggregate size is sufficiently large (size≥30, see Figure S20), even though there is considerable difference in their molecular conformations when the aggregates are small. For large aggregates with size over 30, the majority (>90%) of molecules in both PYR and PYN systems are linear rather than bent (Figure S21a). We also note that the two kinetic pathways we identified (hopping and incremental pathway) share the same growth mechanism for small aggregates, and only start to deviate at a later assembly stage (aggregates size ≥ 30, see Figure S21b). These observations suggest that no clear correlation exists between the kinetic mechanisms and the individual molecular conformations.

Here, we characterized the bending of individual PYR or PYN molecule in aggregates via $d(S_4, S_{12})$, the distance between site S_4 and S_{12} in each individual molecule (bent if $d(S_4, S_{12})\leq$ 1.0 nm and linear otherwise). Based on our samples of the 100 12,000 ns CGMD simulations, we randomly extracted aggregates at different stages of the self-assembly process to calculate $d(S_4, S_{12})$. From the initial free monomer (size=1) to the final assembled nanostructures (size=125), we randomly extracted 5000 conformations for the free monomers and picked 500 aggregates for other sizes of aggregates:10, 30, 50, 70, 90 and 125, respectively. Figure S20 shows the distribution of $d(S_4, S_{12})$ for all monomers in the aggregates at different stages of the self-assembly process. It is clear that the distribution only differs for small aggregates (size = 1, 10) between PYR and PYN. For larger aggregates (size≥30), the difference between PYR and PYN monomers is negligible (all peaked at 1.55 nm). This can be further illustrated by the fraction of bent monomers in the aggregates (see Figure S21). The fraction of bent monomers is very different between PYR and PYN for small aggregates (76% and 99.5% for free monomers; 13% and 17% when size=10). For all larger aggregates (size ≥30), the fraction further shrinks to <10% without significant difference between PYR and PYN. In contrast, the incremental and hopping mechanisms for PYR and PYN start to deviate from each other at much later assembly stage (size>50), as shown by the averaged size increase (ΔN) of the top 20 pathways of PYR and PYN (Figure S21b). Therefore, no correlation can be found between the difference in individual molecular conformations and the bifurcation of the two kinetic mechanisms. Besides, the broad distributions

of $d(S_4, S_{12})$ at large aggregate size (Figure S20) also indicate that a relatively rigid critical packing conformation cannot be defined. These evidences illustrate that the morphology of the assembled structures are not dependent on the intra-molecular interactions or the critical packing shape of the individual molecules.

Thermodynamic relaxation of PYN and PYR aggregates. The difference in the final assembled structures of PYR and PYN can also be rationalized by further thermodynamic considerations. After micelles adhesion in each fusion stage, the newly formed super-micelle (Figure 2a in the main text) tends to self-reorganize into a thermodynamically more preferred structure (Figure S22). However, the ability for the super-micelle reorganization differs between the two amphiphiles. For PYR, the super-micelle is easy to reorganize because its well-separated hydrophobic and hydrophilic groups. Thus, the super-micelles of PYR can easily relax into the preferred planar disks, regardless of the path channels. While the introduction of the amide group in PYN breaks the hydrophobic tail and reduced the hydrophobic interactions, and thus makes such reorganization more difficult. This is supported by the different number of buried hydrophilic groups in the planar and curved disks of PYN (Figure S23b,e). Notably, the number of buried pyridinium group in the planar PYN disks is considerably smaller than that in the thermodynamically favored curved disks. This suggests a high free energy barrier that prevents a planar disk to reorganize into a curved one, because such transition has to distort the hydrophobic core dramatically so as to bury a larger number of hydrophilic pyridinium groups into the aggregate. Furthermore, we also computed the number of amide-pyridinium contacts (cutoff: 9.0 Å) that are buried in the final PYN aggregates assembled from the two kinetic mechanisms (Figure S23c,f). We found that for both mechanisms, the number of intramolecular amide-pyridinium contacts buried in the final aggregates never exceeds 2. This indicates that the different packing density and charged distribution shown in Figure S17 is mainly brought by the intermolecular interactions among the monomers. What's more, the number of amide-pyridinium contacts of both intra- and inter-molecules in the hopping channel is larger than in the incremental channel. Accordingly, the concerted variation of the number of buried amide and pyridinium groups (Figure S23b,e) is not due to the burial of bent monomers into the aggregates, but instead the intermolecular amide-pyridinium contacts formed among many linear monomers (see Figure S23c,f). Collectively, these results support our conclusion that the self-assembly of PYN is mainly driven by the kinetic mechanisms underlined by the inter-molecular interactions

rather than conformations of individual molecules determined by intramolecular interactions.

The RDF as a function of the distance between B_{12} and the counter-ions: Br^-. To characterize the counter-ion distribution in aqueous solution, we calculated the averaged radical distribution function (RDF) as a function of the distance between the positive charged pyridinium groups and the negative charged counter-ions: Br^- based on the 100 12,000 ns CGMD simulations of PYR. As shown in Figure S18, there is an obvious peak locating at a distance of 5.94 Å, indicating the existing electrostatic interactions among the positive charged pyridinium groups and negative charged counter-ions: Br^- during the self-assembly process The second peak of the B_{12}-Br^- radical distribution function locates at the position with distance about 10 Å. Notably, some counter-ions are also distributed randomly in the bulk solutions, because the counter-ions could diffuse in the aqueous solution.

Supplementary Figures

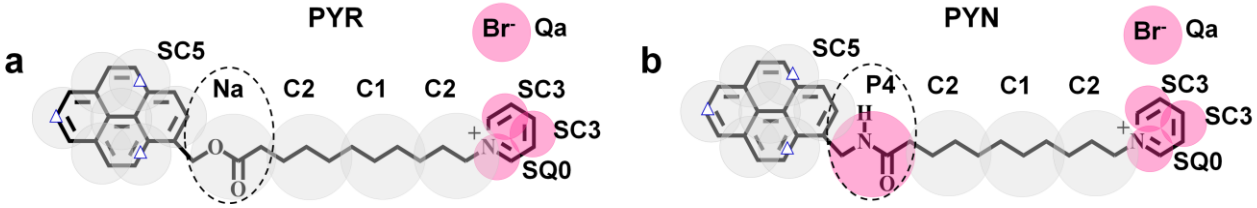

Figure S1. (a) and (b) The coarse-graining scheme used to map PYR and PYN from all-atom to coarse-grained beads, respectively. The beads type of rings are labelled with prefix "S". The pyrenyl group and the alkyl chain are in gray. The pyridinium group with one positive charge, magenta. The ester group of PYR, gray. The amide group of PYN, magenta. The blue triangles label the real beads locations in pyrenyl group for defining the virtual sites to keep aromatic ring planar.

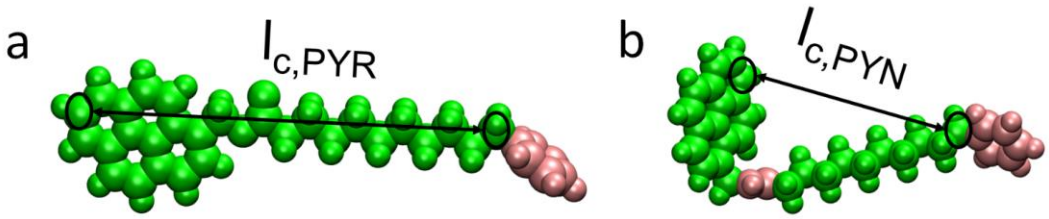

Figure S2. The definition of the length of the extended hydrophobic tail l_c of (a) PYR and (b) PYN. The hydrophobic and hydrophilic part of PYR and PYN were illustrated by the green and pink color, respectively.

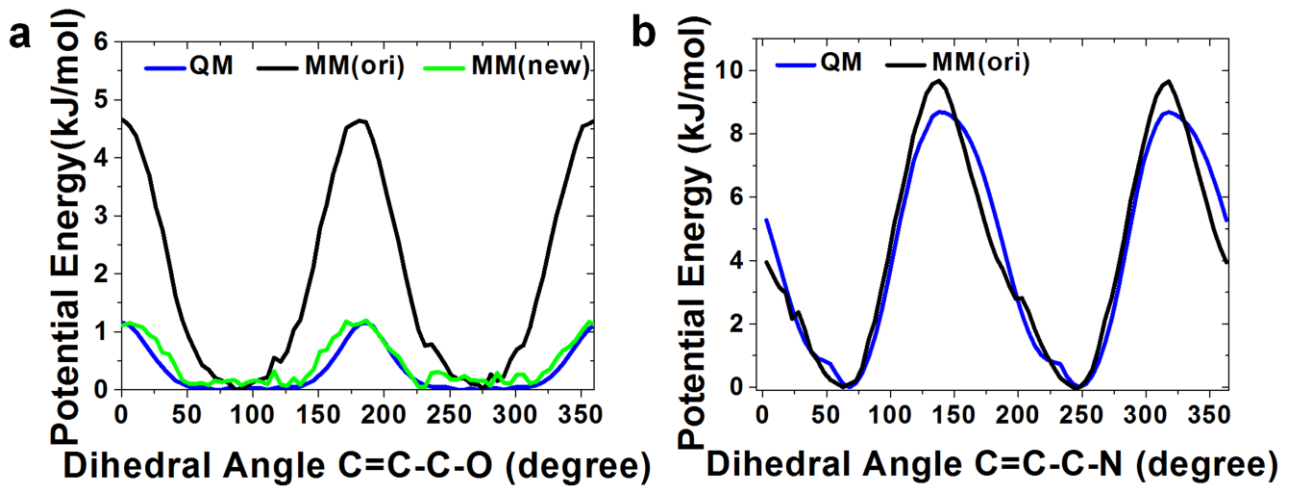

Figure S3. (a) The calculated energy profiles of the dihedral angle C=C-C-O of PYR by the QM (blue), the original MM (black) and the new fitted MM force field parameters (green), respectively. (b) The calculated energy profiles of the dihedral angle C=C-C-N of PYN by the QM (blue) and the original MM force field parameters (black), respectively.

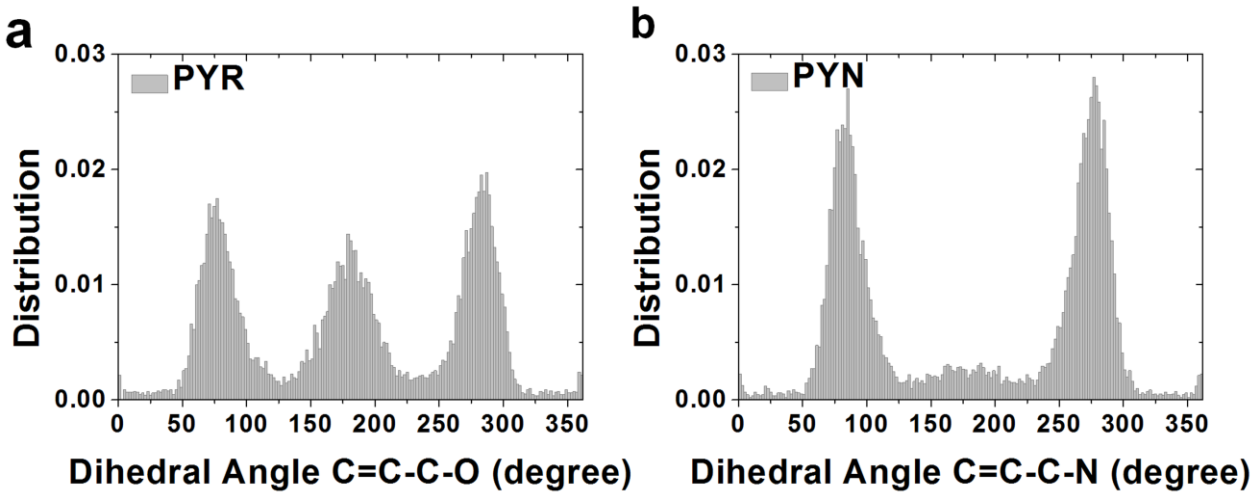

Figure S4. (a) and (b) The distributions of the dihedral angles C=C-C-O of PYR and C=C-C-N of PYN averaged by two independent 150 ns AAMD trajectories, respectively.

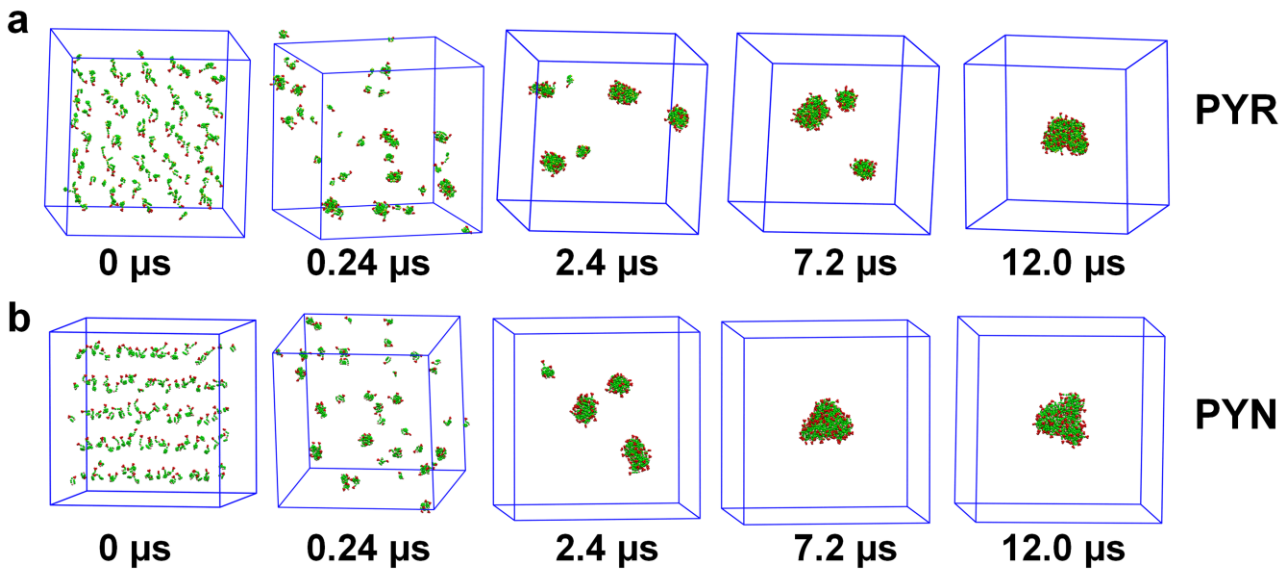

Figure S5. (a) and (b) The snapshots extracted from one representative CGMD trajectory of PYR and PYN to illustrate the aggregation process, respectively. The CG waters were not shown for clarity.

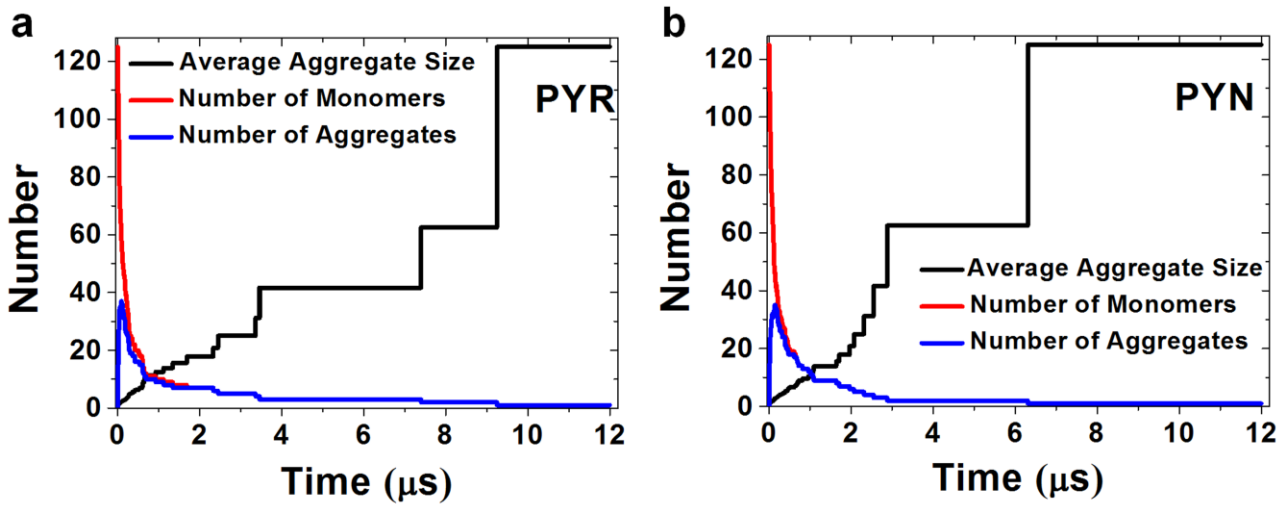

Figure S6. (a) and (b) The time evolution of the average aggregate size, number of monomers and number of aggregates of PYR and PYN averaged by 100 independent CGMD trajectories, respectively.

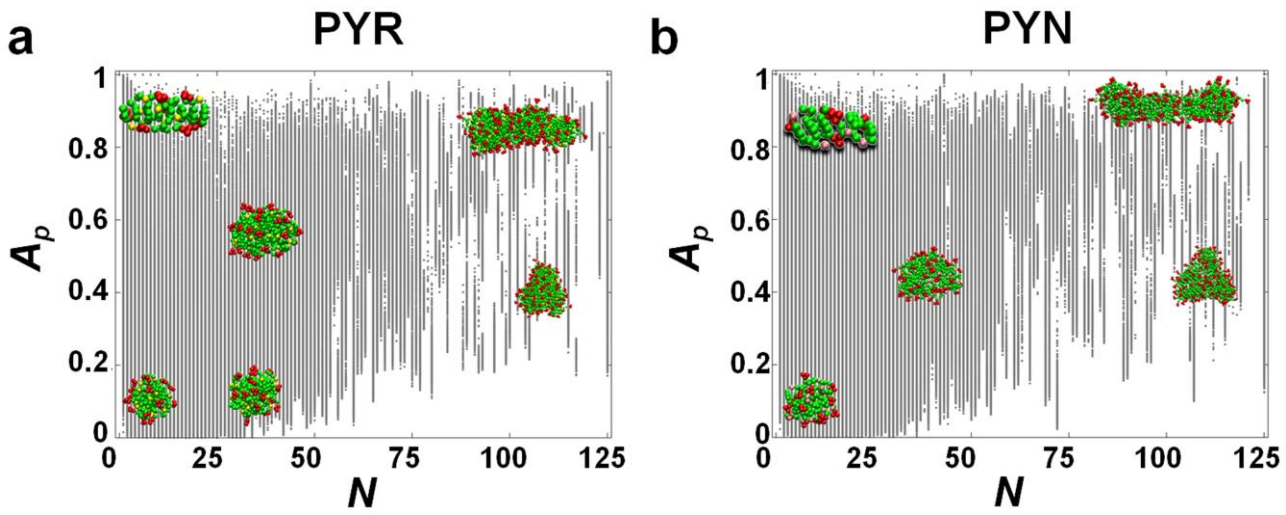

Figure S7. (a) and (b) Projection all the collected aggregates of PYR and PYN onto the size (*N*) and morphology (Ap), respectively. Some representative aggregates in a wide range of *N* and Ap were shown to demonstrate the aggregate conformations. Here, the total number of aggregates for PYR and PYN were 2,696,987 and 2,586,926, respectively.

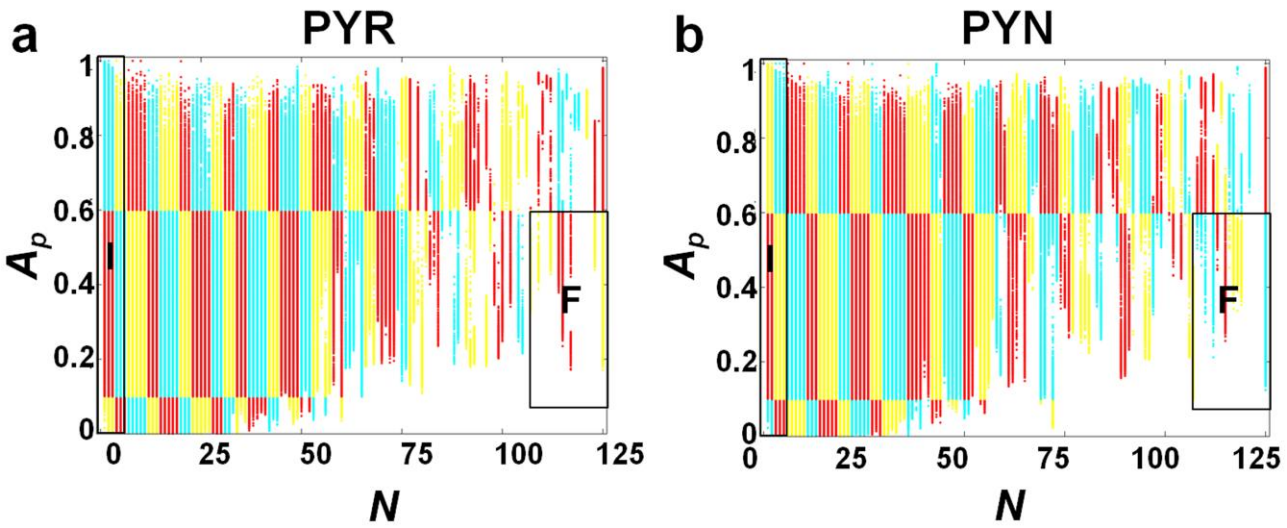

Figure S8. (a) and (b) The overall conformational states partitioned based on both *N* and Ap for PYR and PYN, respectively. **I** and **F** represented the initial and final conformational state that both were for the aggregation pathways identification. Here, we obtained 76 and 75 conformational states for PYR and PYN, respectively. See more details in Table S3 and Table S4.

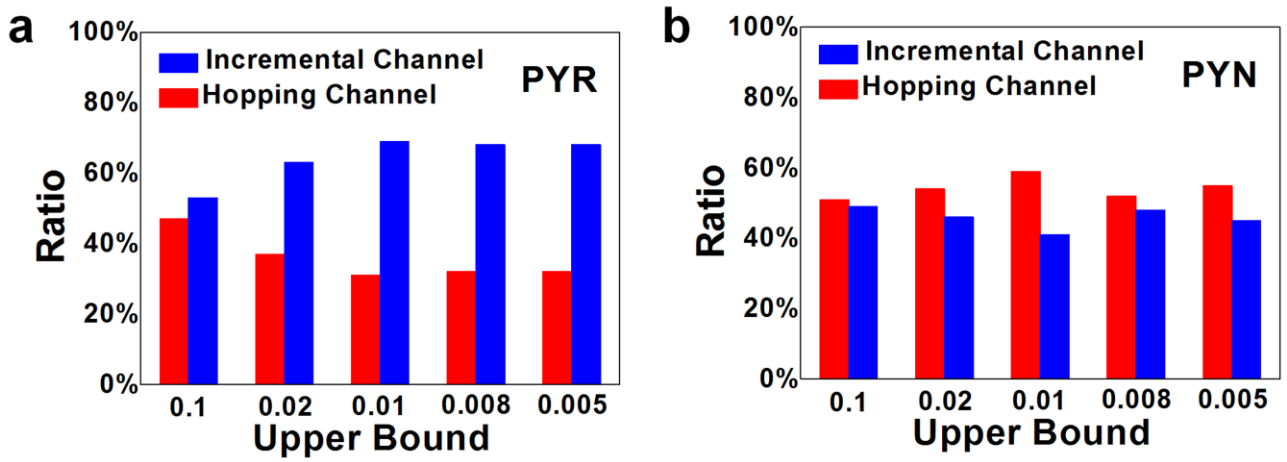

Figure S9. (a) and (b) The influence of the upper bounds on the mass flow ratios of the incremental and hopping channels of PYR and PYN, respectively.

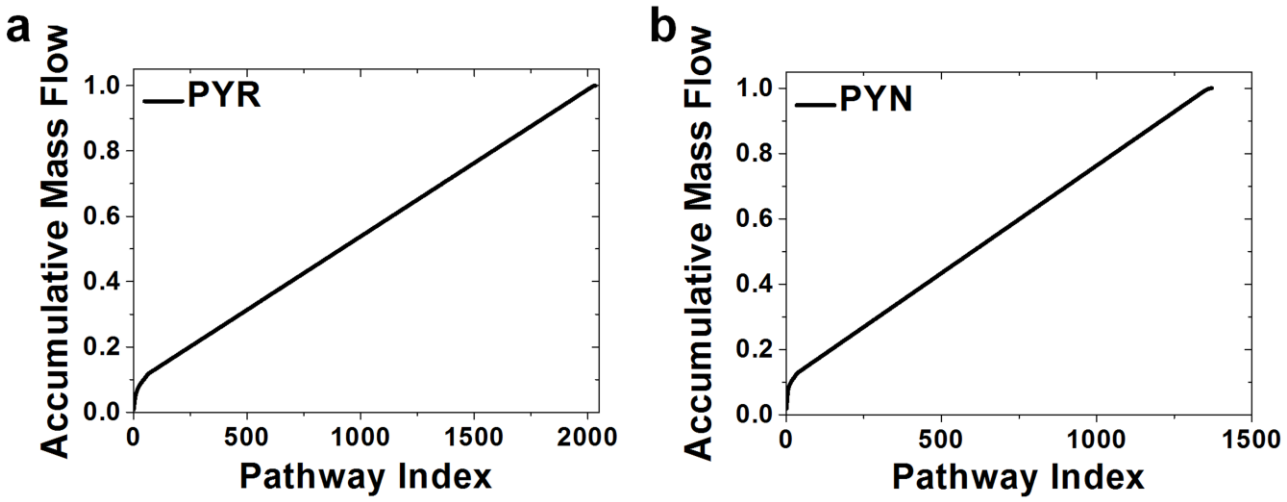

Figure S10. (a) and (b) The accumulative mass flow of all identified aggregation pathways for PYR and PYN, respectively. Here, both PYR and PYN includes a large number of pathways with comparable mass flow. The index of each pathway was assigned according to the mass flow in a descending order.

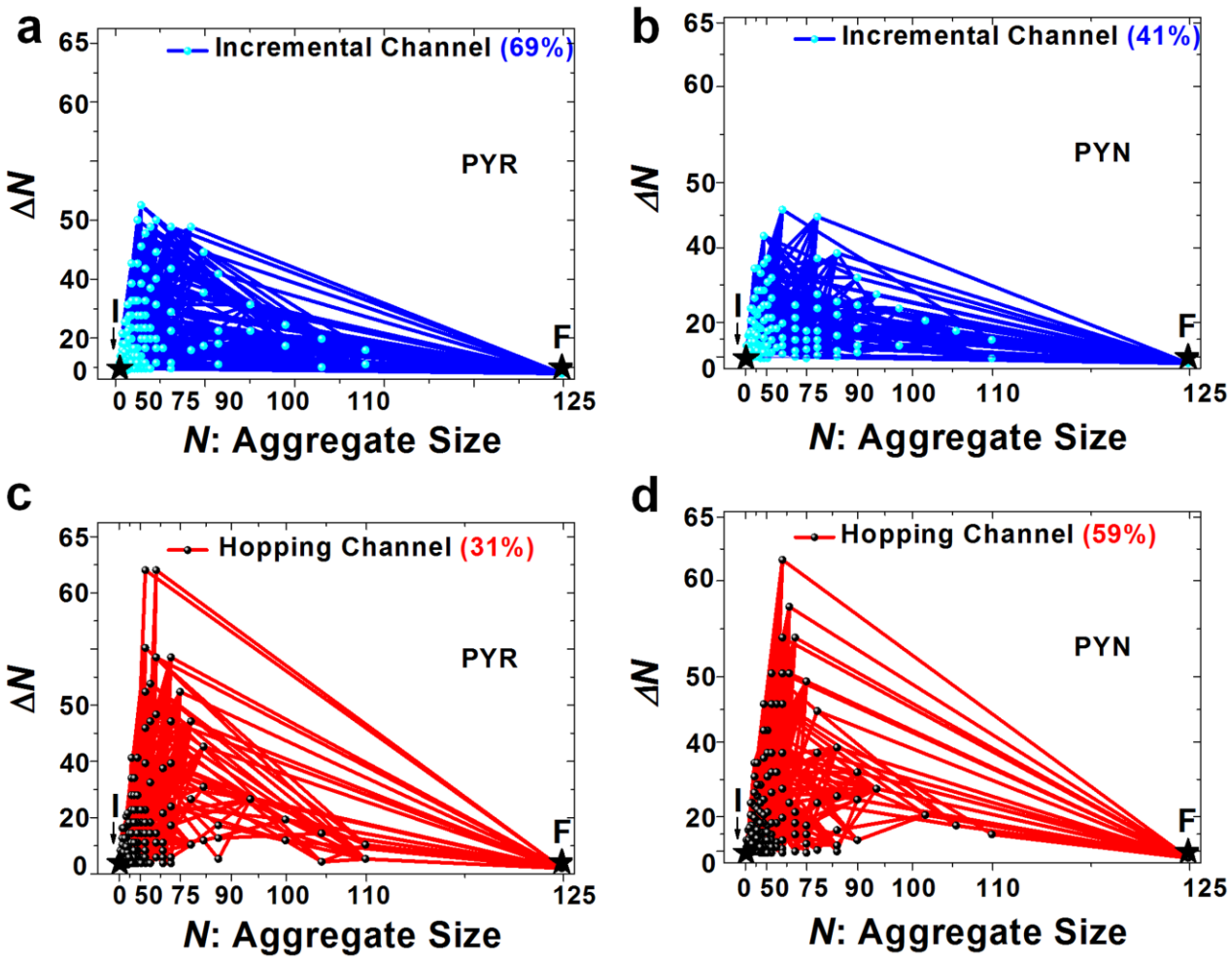

Figure S11. (a), (b) The identified incremental (blue line plus cyan dots) and (c), (d) hopping (red line plus black dots) channels by grouping multiple aggregation pathways for both PYR and PYN, respectively. ΔN, the average size change of each aggregate after pairwise conformational states transition. Here, both two axes are plotted with scaling factor: 125^{-125} exponentially to better characterize the path channels. Here, **I** and **F** represented the initial and final conformational state, respectively.

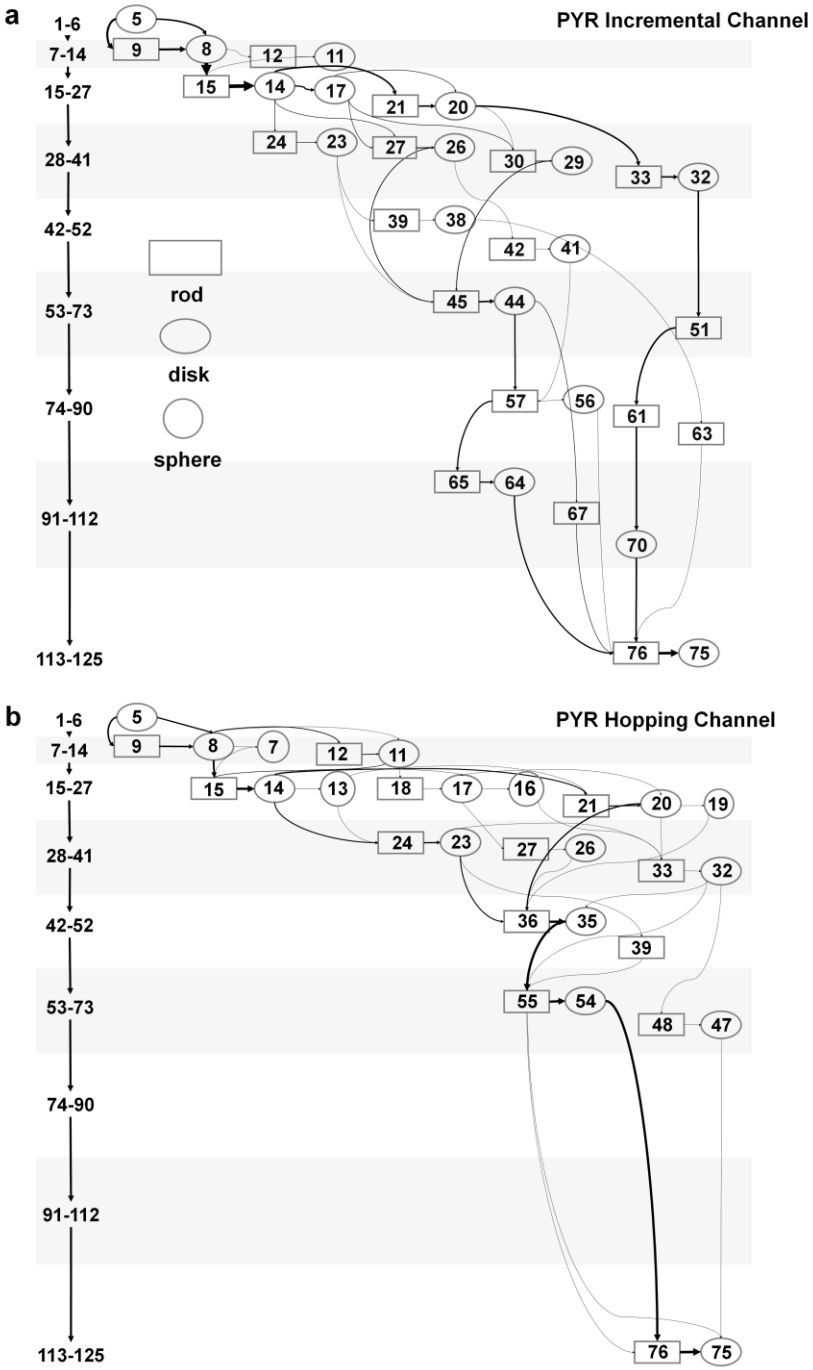

Figure S12. (a) and (b) The top 20 aggregation pathways of the incremental and hopping channels of PYR, with the total mass flow ratios of 13% and 8%, respectively. The rod-like ($0.6 < Ap \leq 1$), disk-like ($0.1 < Ap \leq 0.6$) and sphere-like ($Ap \leq 0.1$) micelles were represented by rectangle, ellipse and circle, respectively. Here, all pathways starting from **I** (the initial conformational state, **5**) and arriving at **F** (the final conformational state, **75**) were represented by the node-and-edge graph. The layers were distinguished by gray and white color alternatively. Some layers were further divided into sub-layers based on the morphology switching. The size range of each layer was labeled on the left hand of each panel. The width of each edge was proportional to the accumulative mass flow of the top 20 aggregation pathways going through it. The conformational state index was inserted in each node, see more details in Table S3.

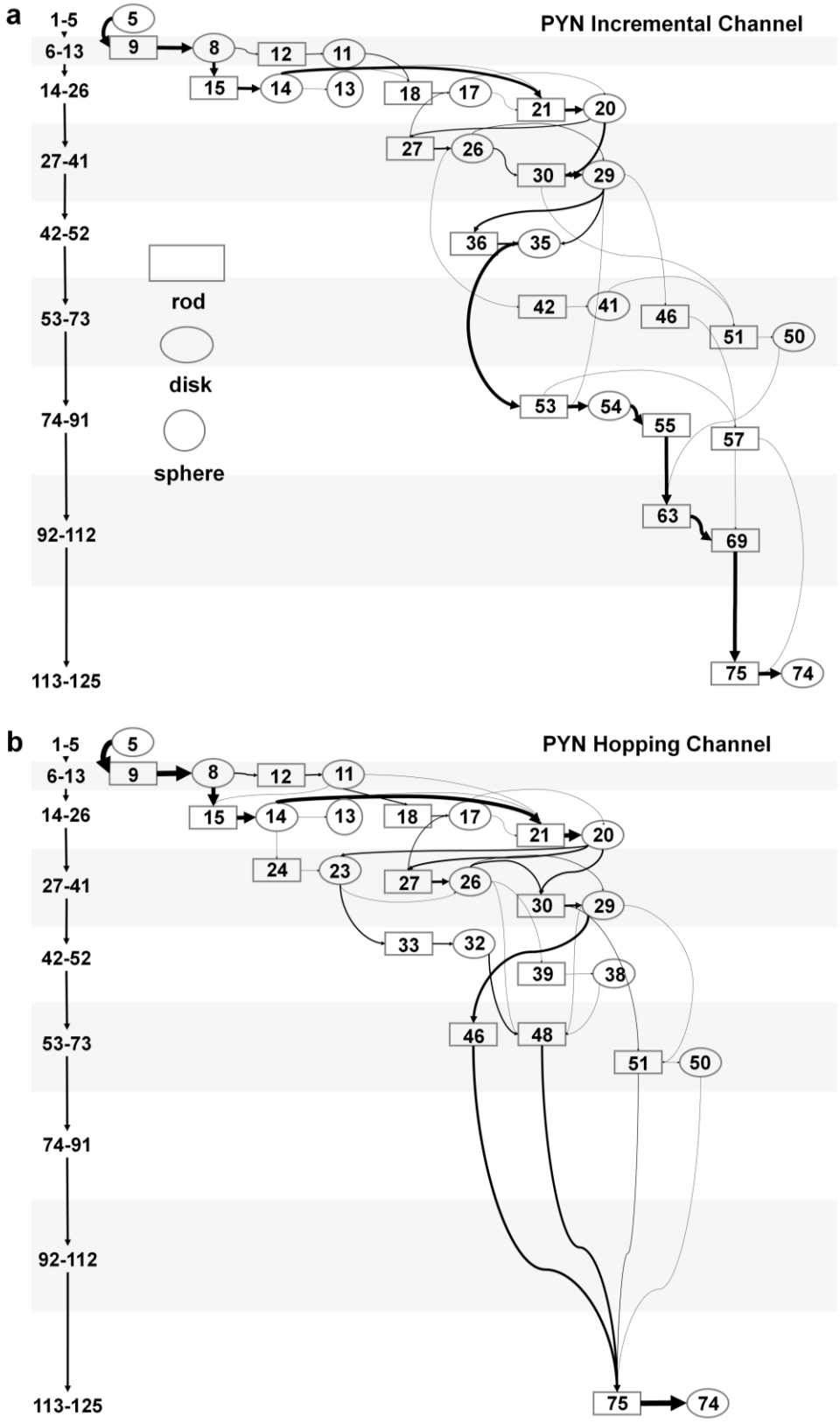

Figure S13. (a) and (b) The top 20 aggregation pathways of the incremental and hopping channels of PYN, with the total mass flow ratios of 14% and 10%, respectively. Here, all pathways starting from **I** (the initial conformational state, **5**) and arriving at **F** (the final conformational state, **74**) were represented by the node-and-edge graph. All other labels here were the same as Figure S12. The conformational state index was labeled on each node, see more details in Table S4.

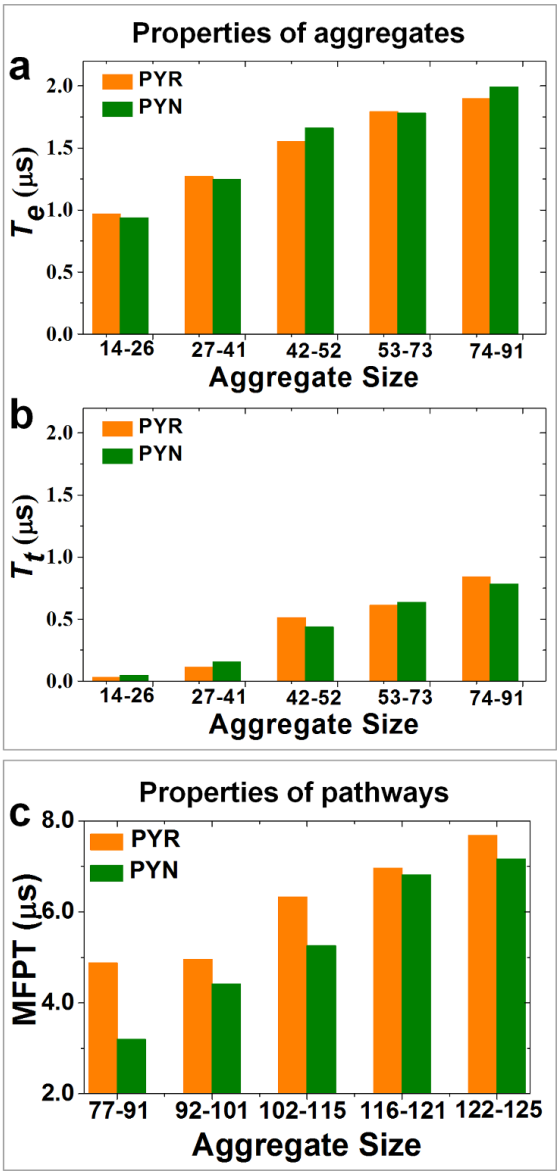

Figure S14. (a) The average encounter time of two aggregates (T_e) in some specific size range. (b) The average transition time from rod to disk (T_t) for each aggregate in some specific size range. (c) The mean first passage times (MFPT) between the chosen pairwise conformational states.

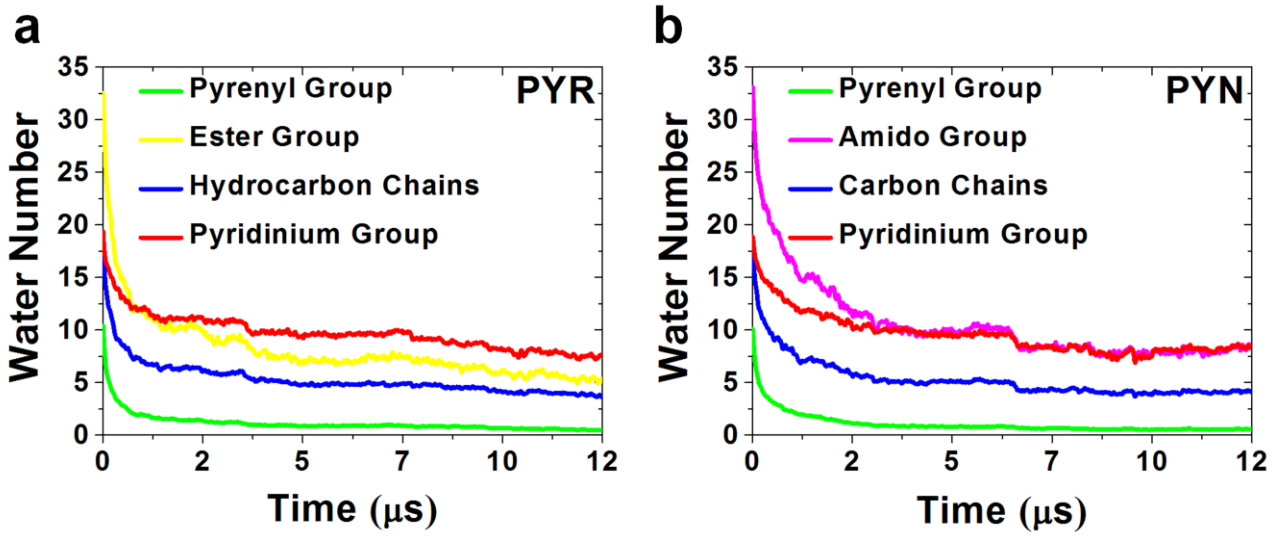

Figure S15. (a) and (b) The time evolution of the number of waters around each functional group of PYR and PYN, respectively. Here the cutoff distance was 6.7 Å, determined based on the radical distribution function shown in Figure S16.

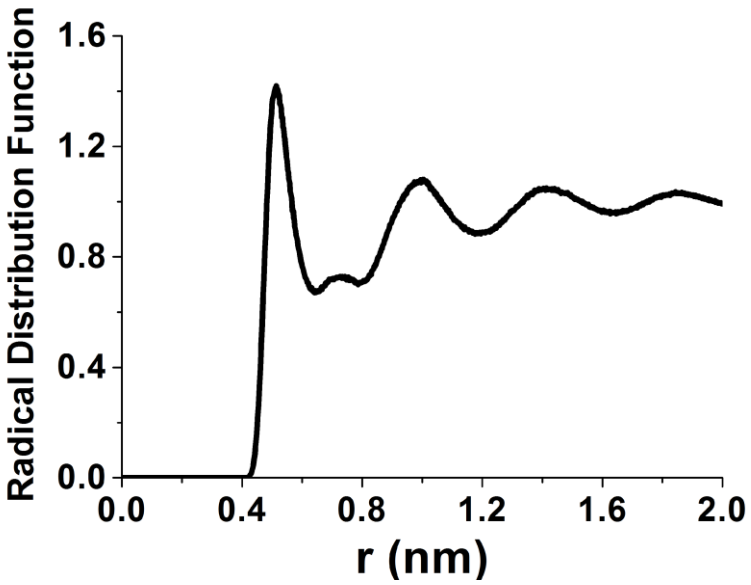

Figure S16. The radical distribution function (RDF) as a function of the center-of-mass (COM) distance between PYR aggregate (with size: 125) and the CG water beads.

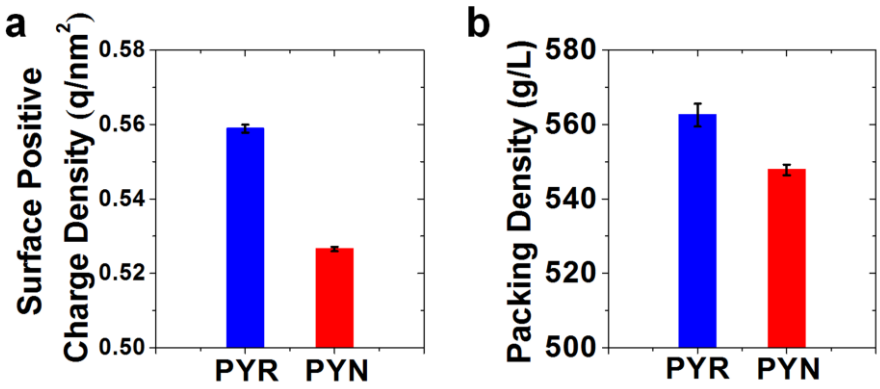

Figure S17. (a) and (b) The surface positive charge density and the packing density of the assembled micelles in the final state (size=125), respectively.

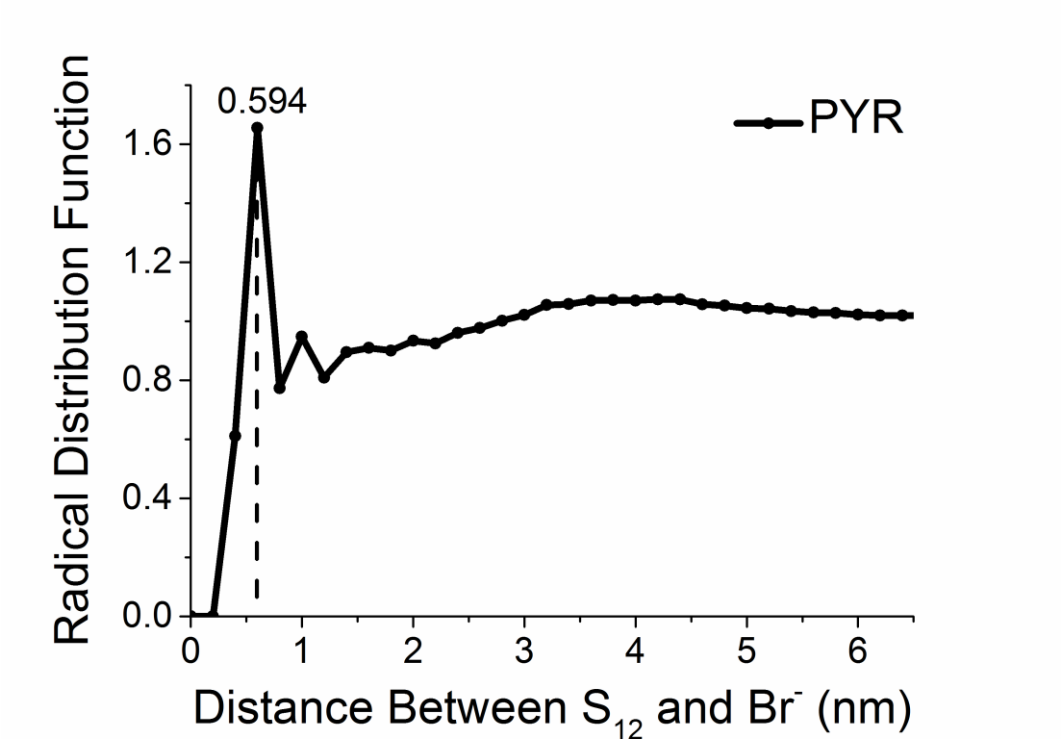

Figure S18. The averaged radical distribution functions (RDF) as a function of the distance between site S_{12} and the counterion Br^- of PYR aggregates at the last 2 μs of each of the 80 CGMD trajectories.

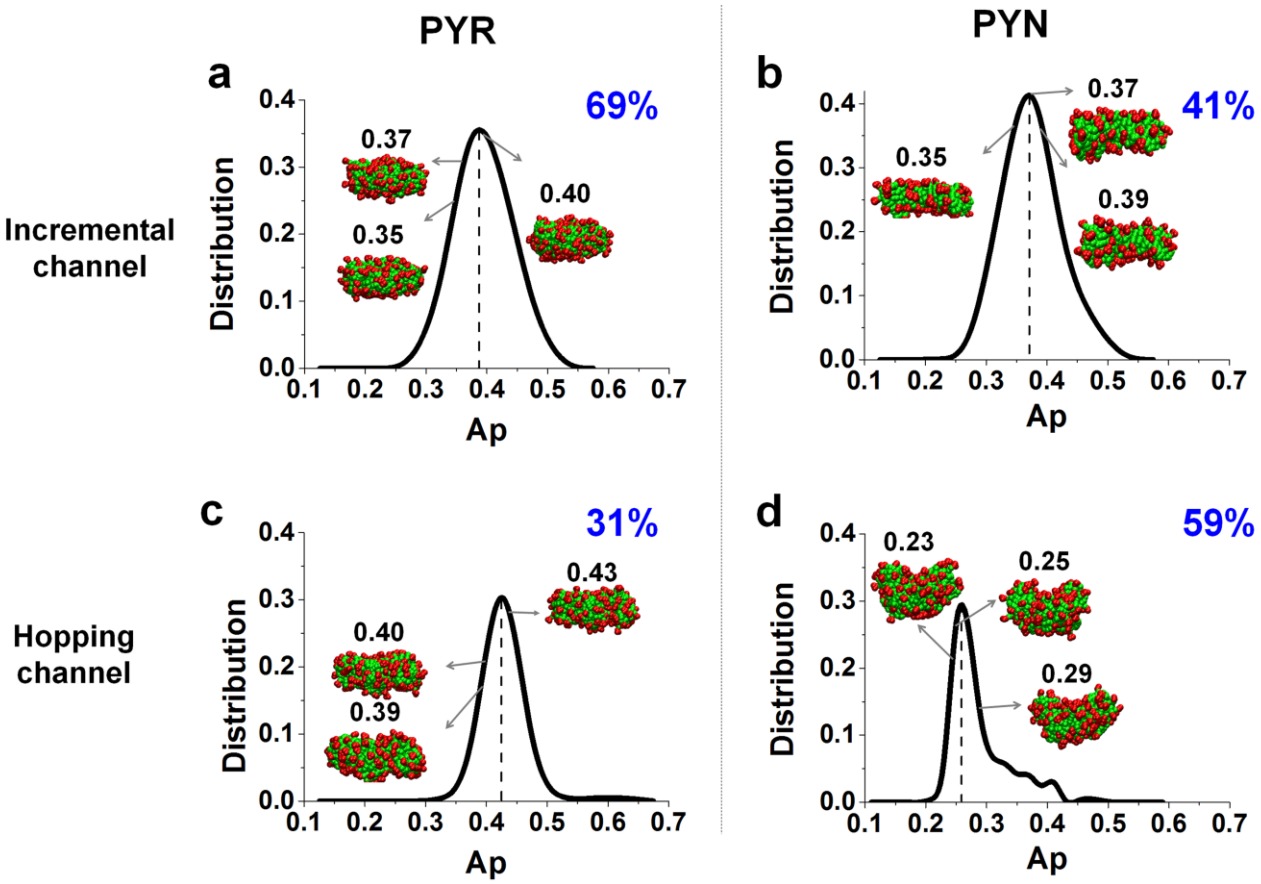

Figure S19. The Ap distribution of the aggregates at the final state **F** assembled along pathways of the (a), (b) incremental and (c), (d) hopping channel of PYR (the left-hand side) and PYN (the right-hand side), respectively. The snapshots of some representative aggregates were shown in each panel. The corresponding peak location for the panels from (a) to (d) were 0.38, 0.37, 0.42 and 0.26, respectively.

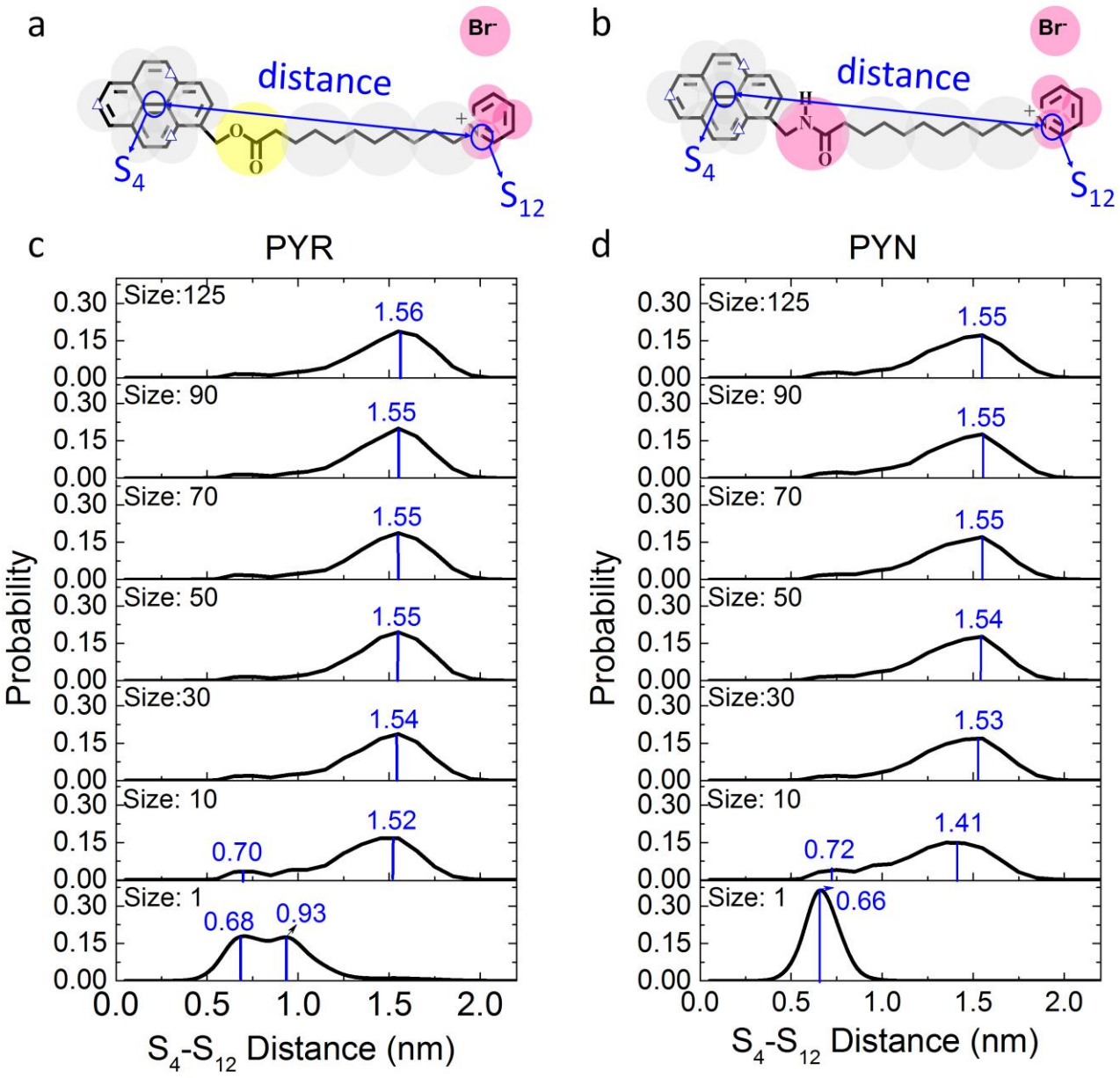

Figure S20. Characterization of the conformations of individual PYR and PYN molecules in aggregates. The definition of distance between sites S_4 and S_{12} of (a) PYR and (b) PYN. The distributions of S_4-S_{12} distance in aggregates with different sizes (1, 10, 30, 50, 70, 90 and 125) for (c) PYR and (d) PYN.

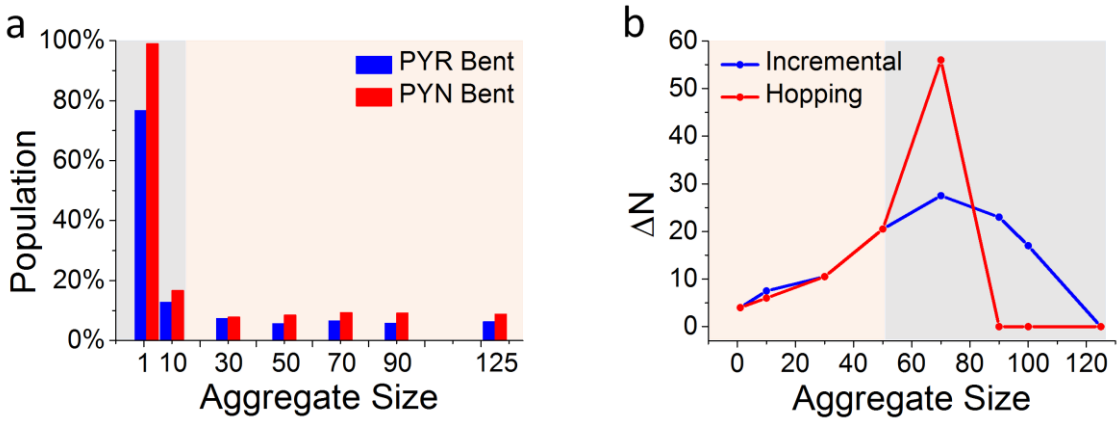

Figure S21. (a) The population of the bent conformations for the molecules in different sizes of PYR and PYN aggregates. (b) The averaged ΔN as a function of aggregate size obtained by the top 20 pathways of each path channel of PYR and PYN. ΔN, the average size change of each aggregate after pairwise conformational states transition.

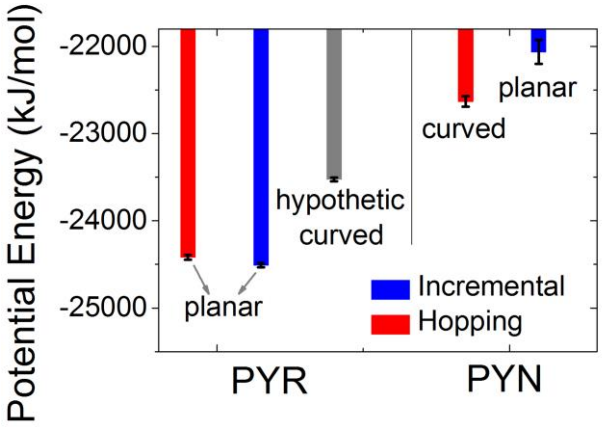

Figure S22. The averaged potential energies of micelles at the final state **F** of PYR and PYN from the incremental (blue) and hopping (red) channel, respectively. The presented "planar" and "curved" labels represent the disk-like micelles with low- and high-curvature respectively. The gray histogram represented the potential energy of the hypothetic curved micelles of PYR. The conformations of the hypothetic curved micelles of PYR were obtained by replacing the CG amide group of the curved PYN micelles into the CG ester group directly. After replacement, we performed 200 ns CGMD simulations to equilibrate the obtained micelles, see more details in the Supplementary Methods and Discussion section.

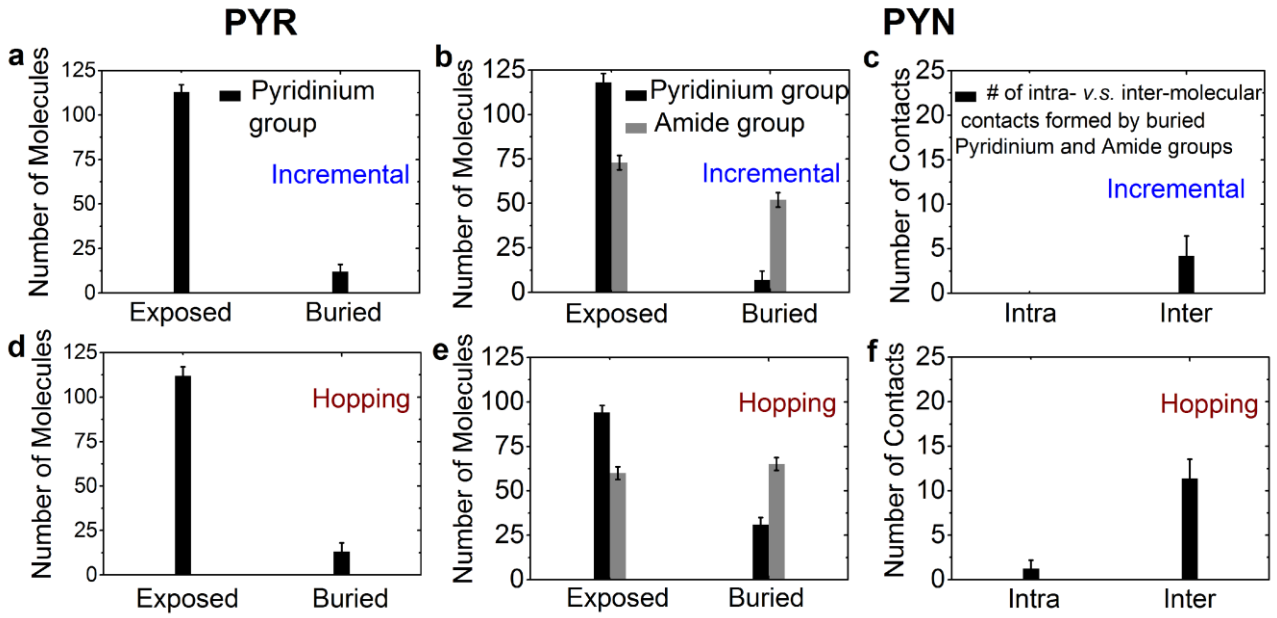

Figure S23. The number of buried and exposed hydrophilic groups at the final state **F** obtained along the aggregation pathways of the (a)(b) incremental and (d)(e) hopping channel for PYR and PYN. The pyridinium and the amide group were labeled in black and dark gray, respectively. (c)(f) present the number of amide-pyridinium contacts buried in **F** for the PYN system.

1. Supplementary Tables

Table S1. The calculated volume of the hydrophobic tail (v), the effective head group surface area (a_0), the length of the extended hydrophobic tail (l_c) and the critical packing parameters (P) for PYR and PYN.

	v (nm^3)	a_0 (nm^2)	l_c (nm)	P
PYR	0.997	2.245	1.650	0.269
PYN	0.910	3.109	1.800	0.163

Table S2 Summary of all MD simulations performed in this work. AA denotes all-atom simulations while CG means coarse-grained simulations.

labels	systems	$N_{surfactant}$	N_{water}[a]	length of cubic simulation box (Å)	time length (μs)	trajectories number	total time (μs)
1	PYR (AA)	1	4,101	50	0.15	2	0.30
2	PYN (AA)	1	4,097	50	0.15	2	0.30
3	PYR (CG)	125	300,428	278.6	12	100	1200
4	PYN (CG)	125	300,450	278.5	12	100	1200
5	PYR (CG)	60	8,682	105	1.2	50	60
6	PYN (CG)	60	8,682	105	1.2	50	60

[a]: The number of water molecules was 4 times of the CG water beads in the studied systems since the MARTINI force field using a 4:1 mapping rule for water molecules.

Table S3. The detailed information of all partitioned conformational states of PYR. Sphere-like micelle, when Ap in range [0, 0.1], disk-like micelle, when Ap in range (0.1, 0.6], rod-like micelle, when Ap > 0.6.

layer ID	size of each	state ID	*N*	size ID index	Ap
1 (**Initial**)	1-6 (**I**)	1	1-3	1	[0, 0.1]
		2			(0.1,0.6]
		3			(0.6, 1]
		4	4-6	2	[0, 0.1]
		5			(0.1,0.6]
		6			(0.6, 1]
2	7-14	7	7-11	3	[0, 0.1]
		8			(0.1,0.6]
		9			(0.6, 1]
		10	12-14	4	[0, 0.1]
		11			(0.1,0.6]
		12			(0.6, 1]
3	15-27	13	15-19	5	[0, 0.1]
		14			(0.1,0.6]
		15			(0.6, 1]
		16	20-22	6	[0, 0.1]
		17			(0.1,0.6]
		18			(0.6, 1]
		19	23-27	7	[0, 0.1]
		20			(0.1,0.6]
		21			(0.6, 1]
4	28-41	22	28-30	8	[0, 0.1]
		23			(0.1,0.6]
		24			(0.6, 1]
		25	31-33	9	[0, 0.1]
		26			(0.1,0.6]
4	28-41	27	31-33	9	(0.6, 1]
		28	34-36	10	[0, 0.1]
		29			(0.1,0.6]
		30			(0.6, 1]
		31	37-41	11	[0, 0.1]
		32			(0.1,0.6]
		33			(0.6, 1]
5	42-52	34	42-44	12	[0, 0.1]
		35			(0.1,0.6]
		36			(0.6, 1]
		37	47-49	13	[0, 0.1]
		38			(0.1,0.6]
		39			(0.6, 1]
		40	50-52	14	[0, 0.1]
		41			(0.1,0.6]
		42			(0.6, 1]
6	53-73	43	53-57	15	[0, 0.1]
		44			(0.1,0.6]
		45			(0.6, 1]
		46	58-60	16	[0, 0.1]
		47			(0.1, 0.6]
		48			(0.6, 1]
		49	61-65	17	[0, 0.1]
		50			(0.1, 0.6]
		51	66-68	18	(0.6, 1]
		52			(0.1, 0.6]
6	53-73	53	66-68	18	(0.6, 1]
		54	69-73	19	(0.1,0.6]
		55			(0.6, 1]
7	74-90	56	74-76	20	(0.1, 0.6]
		57			(0.6, 1]
		58	77-81	21	(0.1, 0.6]
		59			(0.6, 1]
		60	82-84	22	(0.1, 0.6]
		61			(0.6, 1]
		62	85-90	23	(0.1, 0.6]
		63			(0.6, 1]
8	91-112	64	91-97	24	(0.1, 0.6]
		65			(0.6, 1]
		66	98-102	25	(0.1, 0.6]
		67			(0.6, 1]
		68	103-106	26	(0.1, 0.6]
		69			(0.6, 1]
		70	107-112	27	(0.1, 0.6]
		71			(0.6, 1]
9 (**Final**)	113-125 (**F**)	72	113-119	28	(0.1, 0.6]
		73			(0.6, 1]
		74	120-121	29	(0.6, 1]
		75	122-125	30	(0.1, 0.6]
		76			(0.6, 1]

Table S4. The detailed information of each microstate in PYN. Sphere-like micelle, when Ap in range [0, 0.1], disk-like micelle, when Ap in range (0.1, 0.6], rod-like micelle, when Ap > 0.6.

layer size	size of each	state id index	*N*	size id index	Ap	layer size	size range	state id index	*N*	size id index	Ap	layer size	size range	state id index	*N*	size id index	Ap
1 (**Initial**)	1-5 (**I**)	1	1-2	1	[0, 0.1]	**4**	27-41	26	30-35	9	(0.1,0.6]	**7**	74-91	51	69-73	18	(0.6, 1]
		2			(0.1,0.6]			27			(0.6, 1]			52	74-76	19	(0.1,0.6]
		3			(0.6, 1]			28			[0, 0.1]			53			(0.6, 1]
		4			[0, 0.1]			29	36-41	10	(0.1,0.6]			54	77-82	20	(0.1,0.6]
		5	3-5	2	(0.1,0.6]			30			(0.6, 1]			55			(0.6, 1]
		6			(0.6, 1]	**5**	42-52	31	42-45	11	[0, 0.1]			56	83-88	21	(0.1,0.6]
2	6-13	7	6-10	3	[0, 0.1]			32			(0.1,0.6]			57			(0.6, 1]
		8			(0.1,0.6]			33			(0.6, 1]			58	89-91	22	(0.1,0.6]
		9			(0.6, 1]			34			[0, 0.1]			59			(0.6, 1]
		10			[0, 0.1]			35	46-49	12	(0.1,0.6]	**8**	92-112	60	92-96	23	(0.1,0.6]
		11	11-13	4	(0.1,0.6]			36			(0.6, 1]			61			(0.6, 1]
		12			(0.6, 1]			37			[0, 0.1]			62	97-99	24	(0.1,0.6]
3	14-26	13	14-18	5	[0, 0.1]			38	50-52	13	(0.1,0.6]			63			(0.6, 1]
		14			(0.1,0.6]			39			(0.6, 1]			64	101-104	25	(0.1,0.6]
		15			(0.6, 1]	**6**	53-73	40	53-57	14	[0, 0.1]			65			(0.6, 1]
		16			[0, 0.1]			41			(0.1,0.6]			66	105-107	26	(0.1,0.6]
		17	19-21	6	(0.1,0.6]			42			(0.6, 1]			67			(0.6, 1]
		18			(0.6, 1]			43	58-60	15	(0.1,0.6]			68	108-112	27	(0.1,0.6]
		19			[0, 0.1]			44			(0.6, 1]			69			(0.6, 1]
		20	22-26	7	(0.1,0.6]			45	61-65	16	(0.1,0.6]	**9** (**Final**)	113-125 (**F**)	70	113-115	28	(0.1,0.6]
		21			(0.6, 1]			46			(0.6, 1]			71			(0.6, 1]
4	27-41	22	27-29	8	[0, 0.1]			47	66-68	17	(0.1,0.6]			72	116-121	29	(0.1,0.6]
		23			(0.1,0.6]			48			(0.6, 1]			73			(0.6, 1]
		24			(0.6, 1]	**7**	74-91	49	69-73	18	[0, 0.1]			74	122-125	30	(0.1,0.6]
		25	30-35	9	[0, 0.1]			50			(0.1,0.6]			75			(0.6, 1]

Force field parameters for PYR and PYN at both all-atom and coarse-grained resolutions implemented in Gromacs 4.5x

(1) Force field parameters for PYR in all atom resolution.

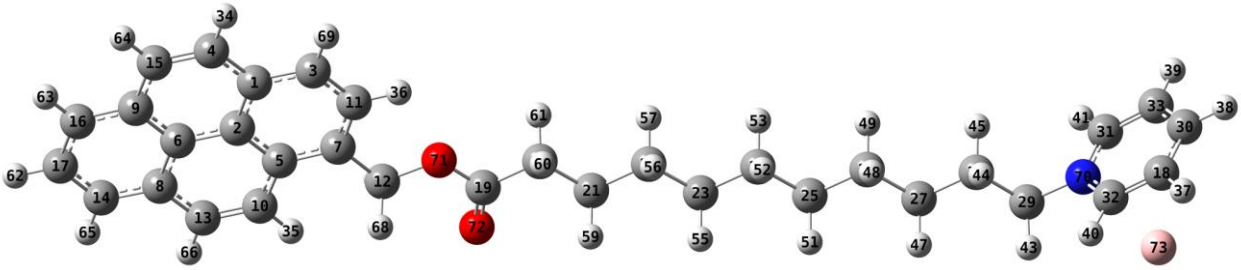

Snapshot of PYR in all atom representation (the index of each atom was also labeled in the above Figure).

The details of PYR force field in all atom resolution in Gromacs format are as follows:

; PYR-AA.top

; head.itp for PYR

[defaults]

nbfunc	comb-rule	gen-pairs	fudgeLJ	fudgeQQ
1	2	yes	0.5	0.8333

[atomtypes]

;name	bond_type	mass	charge	ptype	sigma	epsilon
ca	ca	0.00000	0.00000	A	3.39967e-01	3.59824e-01
c3	c3	0.00000	0.00000	A	3.39967e-01	4.57730e-01
c	c	0.00000	0.00000	A	3.39967e-01	3.59824e-01
ha	ha	0.00000	0.00000	A	2.59964e-01	6.27600e-02
h4	h4	0.00000	0.00000	A	2.51055e-01	6.27600e-02
h1	h1	0.00000	0.00000	A	2.47135e-01	6.56888e-02
hc	hc	0.00000	0.00000	A	2.64953e-01	6.56888e-02
na	na	0.00000	0.00000	A	3.25000e-01	7.11280e-01
os	os	0.00000	0.00000	A	3.00001e-01	7.11280e-01
o	o	0.00000	0.00000	A	2.95992e-01	8.78640e-01
IM	IM	0.00000	0.00000	A	3.95559e-01	1.33888e+00

[moleculetype]

;name nrexcl

PYR 3

[atoms]

; nr	type	resi	res	atom	cgnr	charge	mass
1	ca	1	PYR	C1	1	0.167975	12.01000
2	ca	1	PYR	C2	2	0.017551	12.01000
3	ca	1	PYR	C3	3	-0.291045	12.01000
4	ca	1	PYR	C4	4	-0.226023	12.01000
5	ca	1	PYR	C5	5	0.040960	12.01000
6	ca	1	PYR	C6	6	-0.029377	12.01000
7	ca	1	PYR	C7	7	-0.153472	12.01000
8	ca	1	PYR	C8	8	0.187055	12.01000
9	ca	1	PYR	C9	9	0.177985	12.01000
10	ca	1	PYR	C10	10	-0.171733	12.01000
11	ca	1	PYR	C11	11	-0.106858	12.01000
12	c3	1	PYR	C12	12	0.457272	12.01000
13	ca	1	PYR	C13	13	-0.249727	12.01000
14	ca	1	PYR	C14	14	-0.273432	12.01000
15	ca	1	PYR	C15	15	-0.238608	12.01000
16	ca	1	PYR	C16	16	-0.268200	12.01000
17	ca	1	PYR	C17	17	-0.096378	12.01000
18	ca	1	PYR	C18	18	-0.226126	12.01000
19	c	1	PYR	C19	19	0.921118	12.01000
20	c3	1	PYR	C20	20	-0.318857	12.01000
21	c3	1	PYR	C21	21	0.060167	12.01000
22	c3	1	PYR	C22	22	0.011301	12.01000
23	c3	1	PYR	C23	23	-0.068721	12.01000
24	c3	1	PYR	C24	24	0.021128	12.01000
25	c3	1	PYR	C25	25	0.034555	12.01000

26	c3	1	PYR	C26	26	-0.090753	12.01000
27	c3	1	PYR	C27	27	-0.004294	12.01000
28	c3	1	PYR	C28	28	0.098931	12.01000
29	c3	1	PYR	C29	29	-0.278451	12.01000
30	ca	1	PYR	C30	30	0.116938	12.01000
31	ca	1	PYR	C31	31	0.020970	12.01000
32	ca	1	PYR	C32	32	0.020970	12.01000
33	ca	1	PYR	C33	33	-0.226126	12.01000
34	ha	1	PYR	H1	34	0.156856	1.00800
35	ha	1	PYR	H2	35	0.124401	1.00800
36	ha	1	PYR	H3	36	0.146424	1.00800
37	ha	1	PYR	H4	37	0.196658	1.00800
38	ha	1	PYR	H5	38	0.159729	1.00800
39	ha	1	PYR	H6	39	0.196658	1.00800
40	h4	1	PYR	H7	40	0.204006	1.00800
41	h4	1	PYR	H8	41	0.204006	1.00800
42	h1	1	PYR	H9	42	0.140615	1.00800
43	h1	1	PYR	H10	43	0.140615	1.00800
44	hc	1	PYR	H11	44	0.012970	1.00800
45	hc	1	PYR	H12	45	0.012970	1.00800
46	hc	1	PYR	H13	46	0.026596	1.00800
47	hc	1	PYR	H14	47	0.026596	1.00800
48	hc	1	PYR	H15	48	0.027026	1.00800
49	hc	1	PYR	H16	49	0.027026	1.00800
50	hc	1	PYR	H17	50	0.001626	1.00800
51	hc	1	PYR	H18	51	0.001626	1.00800
52	hc	1	PYR	H19	52	0.001190	1.00800
53	hc	1	PYR	H20	53	0.001190	1.00800
54	hc	1	PYR	H21	54	0.020556	1.00800
55	hc	1	PYR	H22	55	0.020556	1.00800

56	hc	1	PYR	H23	56	0.007543	1.00800
57	hc	1	PYR	H24	57	0.007543	1.00800
58	hc	1	PYR	H25	58	0.011886	1.00800
59	hc	1	PYR	H26	59	0.011886	1.00800
60	hc	1	PYR	H27	60	0.094965	1.00800
61	hc	1	PYR	H28	61	0.094965	1.00800
62	ha	1	PYR	H29	62	0.144613	1.00800
63	ha	1	PYR	H30	63	0.165450	1.00800
64	ha	1	PYR	H31	64	0.161556	1.00800
65	ha	1	PYR	H32	65	0.165598	1.00800
66	ha	1	PYR	H33	66	0.166712	1.00800
67	h1	1	PYR	H34	67	0.007823	1.00800
68	h1	1	PYR	H35	68	0.007823	1.00800
69	ha	1	PYR	H36	69	0.170865	1.00800
70	na	1	PYR	N1	70	0.126797	14.01000
71	os	1	PYR	O1	71	-0.590109	16.00000
72	o	1	PYR	O2	72	-0.642509	16.00000
73	IM	1	PYR	Br-	73	-1.000000	79.90000

[bonds]

; ai	aj	funct	r	k	
1	2	1	1.3870e-01	4.0033e+05 ;	C1 - C2
1	3	1	1.3870e-01	4.0033e+05 ;	C1 - C3
1	4	1	1.3870e-01	4.0033e+05 ;	C1 - C4
2	5	1	1.3870e-01	4.0033e+05 ;	C2 - C5
2	6	1	1.3870e-01	4.0033e+05 ;	C2 - C6
3	11	1	1.3870e-01	4.0033e+05 ;	C3 - C11
3	69	1	1.0870e-01	2.8811e+05 ;	C3 - H36
4	15	1	1.3870e-01	4.0033e+05 ;	C4 - C15
4	34	1	1.0870e-01	2.8811e+05 ;	C4 - H1
5	7	1	1.3870e-01	4.0033e+05 ;	C5 - C7

5	10	1	1.3870e-01	4.0033e+05 ;	C5 - C10
6	8	1	1.3870e-01	4.0033e+05 ;	C6 - C8
6	9	1	1.3870e-01	4.0033e+05 ;	C6 - C9
7	11	1	1.3870e-01	4.0033e+05 ;	C7 - C11
7	12	1	1.5130e-01	2.7070e+05 ;	C7 - C12
8	13	1	1.3870e-01	4.0033e+05 ;	C8 - C13
8	14	1	1.3870e-01	4.0033e+05 ;	C8 - C14
9	15	1	1.3870e-01	4.0033e+05 ;	C9 - C15
9	16	1	1.3870e-01	4.0033e+05 ;	C9 - C16
10	13	1	1.3870e-01	4.0033e+05 ;	C10 - C13
10	35	1	1.0870e-01	2.8811e+05 ;	C10 - H2
11	36	1	1.0870e-01	2.8811e+05 ;	C11 - H3
12	67	1	1.0930e-01	2.8108e+05 ;	C12 - H34
12	68	1	1.0930e-01	2.8108e+05 ;	C12 - H35
12	71	1	1.4390e-01	2.5230e+05 ;	C12 - O1
13	66	1	1.0870e-01	2.8811e+05 ;	C13 - H33
14	17	1	1.3870e-01	4.0033e+05 ;	C14 - C17
14	65	1	1.0870e-01	2.8811e+05 ;	C14 - H32
15	64	1	1.0870e-01	2.8811e+05 ;	C15 - H31
16	17	1	1.3870e-01	4.0033e+05 ;	C16 - C17
16	63	1	1.0870e-01	2.8811e+05 ;	C16 - H30
17	62	1	1.0870e-01	2.8811e+05 ;	C17 - H29
18	30	1	1.3870e-01	4.0033e+05 ;	C18 - C30
18	32	1	1.3870e-01	4.0033e+05 ;	C18 - C32
18	37	1	1.0870e-01	2.8811e+05 ;	C18 - H4
19	20	1	1.5080e-01	2.7472e+05 ;	C19 - C20
19	71	1	1.3430e-01	3.4418e+05 ;	C19 - O1
19	72	1	1.2140e-01	5.4225e+05 ;	C19 - O2
20	21	1	1.5350e-01	2.5363e+05 ;	C20 - C21
20	60	1	1.0920e-01	2.8225e+05 ;	C20 - H27

20	61	1	1.0920e-01	2.8225e+05 ;	C20 - H28
21	22	1	1.5350e-01	2.5363e+05 ;	C21 - C22
21	58	1	1.0920e-01	2.8225e+05 ;	C21 - H25
21	59	1	1.0920e-01	2.8225e+05 ;	C21 - H26
22	23	1	1.5350e-01	2.5363e+05 ;	C22 - C23
22	56	1	1.0920e-01	2.8225e+05 ;	C22 - H23
22	57	1	1.0920e-01	2.8225e+05 ;	C22 - H24
23	24	1	1.5350e-01	2.5363e+05 ;	C23 - C24
23	54	1	1.0920e-01	2.8225e+05 ;	C23 - H21
23	55	1	1.0920e-01	2.8225e+05 ;	C23 - H22
24	25	1	1.5350e-01	2.5363e+05 ;	C24 - C25
24	52	1	1.0920e-01	2.8225e+05 ;	C24 - H19
24	53	1	1.0920e-01	2.8225e+05 ;	C24 - H20
25	26	1	1.5350e-01	2.5363e+05 ;	C25 - C26
25	50	1	1.0920e-01	2.8225e+05 ;	C25 - H17
25	51	1	1.0920e-01	2.8225e+05 ;	C25 - H18
26	27	1	1.5350e-01	2.5363e+05 ;	C26 - C27
26	48	1	1.0920e-01	2.8225e+05 ;	C26 - H15
26	49	1	1.0920e-01	2.8225e+05 ;	C26 - H16
27	28	1	1.5350e-01	2.5363e+05 ;	C27 - C28
27	46	1	1.0920e-01	2.8225e+05 ;	C27 - H13
27	47	1	1.0920e-01	2.8225e+05 ;	C27 - H14
28	29	1	1.5350e-01	2.5363e+05 ;	C28 - C29
28	44	1	1.0920e-01	2.8225e+05 ;	C28 - H11
28	45	1	1.0920e-01	2.8225e+05 ;	C28 - H12
29	42	1	1.0930e-01	2.8108e+05 ;	C29 - H9
29	43	1	1.0930e-01	2.8108e+05 ;	C29 - H10
29	70	1	1.4560e-01	2.8008e+05 ;	C29 - N1
30	33	1	1.3870e-01	4.0033e+05 ;	C30 - C33
30	38	1	1.0870e-01	2.8811e+05 ;	C30 - H5

```
    31     33     1      1.3870e-01     4.0033e+05 ;   C31 - C33
    31     41     1      1.0880e-01     2.8694e+05 ;   C31 - H8
    31     70     1      1.3500e-01     3.9355e+05 ;   C31 - N1
    32     40     1      1.0880e-01     2.8694e+05 ;   C32 - H7
    32     70     1      1.3500e-01     3.9355e+05 ;   C32 - N1
    33     39     1      1.0870e-01     2.8811e+05 ;   C33 - H6

[ pairs ]

;    ai     aj     funct
     1      7      1 ;     C1 - C7
     1      8      1 ;     C1 - C8
     1      9      1 ;     C1 - C9
     1      10     1 ;     C1 - C10
     1      36     1 ;     C1 - H3
     1      64     1 ;     C1 - H31
     2      11     1 ;     C2 - C11
     2      12     1 ;     C2 - C12
     2      13     1 ;     C2 - C13
     2      14     1 ;     C2 - C14
     2      15     1 ;     C2 - C15
     2      16     1 ;     C2 - C16
     2      34     1 ;     C2 - H1
     2      35     1 ;     C2 - H2
     2      69     1 ;     C2 - H36
     3      5      1 ;     C3 - C5
     3      6      1 ;     C3 - C6
     3      12     1 ;     C3 - C12
     3      15     1 ;     C3 - C15
     3      34     1 ;     C3 - H1
     4      5      1 ;     C4 - C5
     4      6      1 ;     C4 - C6
```

4	11	1 ;	C4 - C11
4	16	1 ;	C4 - C16
4	69	1 ;	C4 - H36
5	8	1 ;	C5 - C8
5	9	1 ;	C5 - C9
5	36	1 ;	C5 - H3
5	66	1 ;	C5 - H33
5	67	1 ;	C5 - H34
5	68	1 ;	C5 - H35
5	71	1 ;	C5 - O1
6	7	1 ;	C6 - C7
6	10	1 ;	C6 - C10
6	17	1 ;	C6 - C17
6	63	1 ;	C6 - H30
6	64	1 ;	C6 - H31
6	65	1 ;	C6 - H32
6	66	1 ;	C6 - H33
7	13	1 ;	C7 - C13
7	19	1 ;	C7 - C19
7	35	1 ;	C7 - H2
7	69	1 ;	C7 - H36
8	15	1 ;	C8 - C15
8	16	1 ;	C8 - C16
8	35	1 ;	C8 - H2
8	62	1 ;	C8 - H29
9	13	1 ;	C9 - C13
9	14	1 ;	C9 - C14
9	34	1 ;	C9 - H1
9	62	1 ;	C9 - H29
10	11	1 ;	C10 - C11

10 12 1 ; C10 - C12

10 14 1 ; C10 - C14

11 67 1 ; C11 - H34

11 68 1 ; C11 - H35

11 71 1 ; C11 - O1

12 20 1 ; C12 - C20

12 36 1 ; C12 - H3

12 72 1 ; C12 - O2

13 17 1 ; C13 - C17

13 65 1 ; C13 - H32

14 63 1 ; C14 - H30

14 66 1 ; C14 - H33

15 17 1 ; C15 - C17

15 63 1 ; C15 - H30

16 64 1 ; C16 - H31

16 65 1 ; C16 - H32

18 29 1 ; C18 - C29

18 31 1 ; C18 - C31

18 39 1 ; C18 - H6

19 22 1 ; C19 - C22

19 58 1 ; C19 - H25

19 59 1 ; C19 - H26

19 67 1 ; C19 - H34

19 68 1 ; C19 - H35

20 23 1 ; C20 - C23

20 56 1 ; C20 - H23

20 57 1 ; C20 - H24

21 24 1 ; C21 - C24

21 54 1 ; C21 - H21

21 55 1 ; C21 - H22

21	71	1 ;	C21 - O1
21	72	1 ;	C21 - O2
22	25	1 ;	C22 - C25
22	52	1 ;	C22 - H19
22	53	1 ;	C22 - H20
22	60	1 ;	C22 - H27
22	61	1 ;	C22 - H28
23	26	1 ;	C23 - C26
23	50	1 ;	C23 - H17
23	51	1 ;	C23 - H18
23	58	1 ;	C23 - H25
23	59	1 ;	C23 - H26
24	27	1 ;	C24 - C27
24	48	1 ;	C24 - H15
24	49	1 ;	C24 - H16
24	56	1 ;	C24 - H23
24	57	1 ;	C24 - H24
25	28	1 ;	C25 - C28
25	46	1 ;	C25 - H13
25	47	1 ;	C25 - H14
25	54	1 ;	C25 - H21
25	55	1 ;	C25 - H22
26	29	1 ;	C26 - C29
26	44	1 ;	C26 - H11
26	45	1 ;	C26 - H12
26	52	1 ;	C26 - H19
26	53	1 ;	C26 - H20
27	42	1 ;	C27 - H9
27	43	1 ;	C27 - H10
27	50	1 ;	C27 - H17

27 51 1 ; C27 - H18

27 70 1 ; C27 - N1

28 31 1 ; C28 - C31

28 32 1 ; C28 - C32

28 48 1 ; C28 - H15

28 49 1 ; C28 - H16

29 33 1 ; C29 - C33

29 40 1 ; C29 - H7

29 41 1 ; C29 - H8

29 46 1 ; C29 - H13

29 47 1 ; C29 - H14

30 40 1 ; C30 - H7

30 41 1 ; C30 - H8

30 70 1 ; C30 - N1

31 38 1 ; C31 - H5

31 40 1 ; C31 - H7

31 42 1 ; C31 - H9

31 43 1 ; C31 - H10

32 33 1 ; C32 - C33

32 38 1 ; C32 - H5

32 41 1 ; C32 - H8

32 42 1 ; C32 - H9

32 43 1 ; C32 - H10

33 37 1 ; C33 - H4

34 64 1 ; H1 - H31

35 66 1 ; H2 - H33

36 69 1 ; H3 - H36

37 38 1 ; H4 - H5

37 40 1 ; H4 - H7

37 70 1 ; H4 - N1

38 39 1 ; H5 - H6

39 41 1 ; H6 - H8

39 70 1 ; H6 - N1

42 44 1 ; H9 - H11

42 45 1 ; H9 - H12

43 44 1 ; H10 - H11

43 45 1 ; H10 - H12

44 46 1 ; H11 - H13

44 47 1 ; H11 - H14

44 70 1 ; H11 - N1

45 46 1 ; H12 - H13

45 47 1 ; H12 - H14

45 70 1 ; H12 - N1

46 48 1 ; H13 - H15

46 49 1 ; H13 - H16

47 48 1 ; H14 - H15

47 49 1 ; H14 - H16

48 50 1 ; H15 - H17

48 51 1 ; H15 - H18

49 50 1 ; H16 - H17

49 51 1 ; H16 - H18

50 52 1 ; H17 - H19

50 53 1 ; H17 - H20

51 52 1 ; H18 - H19

51 53 1 ; H18 - H20

52 54 1 ; H19 - H21

52 55 1 ; H19 - H22

53 54 1 ; H20 - H21

53 55 1 ; H20 - H22

54 56 1 ; H21 - H23

```
    54      57      1 ;     H21 - H24
    55      56      1 ;     H22 - H23
    55      57      1 ;     H22 - H24
    56      58      1 ;     H23 - H25
    56      59      1 ;     H23 - H26
    57      58      1 ;     H24 - H25
    57      59      1 ;     H24 - H26
    58      60      1 ;     H25 - H27
    58      61      1 ;     H25 - H28
    59      60      1 ;     H26 - H27
    59      61      1 ;     H26 - H28
    60      71      1 ;     H27 - O1
    60      72      1 ;     H27 - O2
    61      71      1 ;     H28 - O1
    61      72      1 ;     H28 - O2
    62      63      1 ;     H29 - H30
    62      65      1 ;     H29 - H32

[ angles ]
;   ai      aj      ak      funct       theta           cth
    1       2       5       1       1.1997e+02      5.6233e+02 ; C1 - C2 - C5
    1       2       6       1       1.1997e+02      5.6233e+02 ; C1 - C2 - C6
    1       3       11      1       1.1997e+02      5.6233e+02 ; C1 - C3 - C11
    1       3       69      1       1.2001e+02      4.0585e+02 ; C1 - C3 - H36
    1       4       15      1       1.1997e+02      5.6233e+02 ; C1 - C4 - C15
    1       4       34      1       1.2001e+02      4.0585e+02 ; C1 - C4 - H1
    2       1       3       1       1.1997e+02      5.6233e+02 ; C2 - C1 - C3
    2       1       4       1       1.1997e+02      5.6233e+02 ; C2 - C1 - C4
    2       5       7       1       1.1997e+02      5.6233e+02 ; C2 - C5 - C7
    2       5       10      1       1.1997e+02      5.6233e+02 ; C2 - C5 - C10
```

2	6	8	1	1.1997e+02	5.6233e+02 ; C2 - C6 - C8
2	6	9	1	1.1997e+02	5.6233e+02 ; C2 - C6 - C9
3	1	4	1	1.1997e+02	5.6233e+02 ; C3 - C1 - C4
3	11	7	1	1.1997e+02	5.6233e+02 ; C3 - C11- C7
3	11	36	1	1.2001e+02	4.0585e+02 ; C3 - C11- H3
4	15	9	1	1.1997e+02	5.6233e+02 ; C4 - C15- C9
4	15	64	1	1.2001e+02	4.0585e+02 ; C4 - C15- H31
5	2	6	1	1.1997e+02	5.6233e+02 ; C5 - C2 - C6
5	7	11	1	1.1997e+02	5.6233e+02 ; C5 - C7 - C11
5	7	12	1	1.2063e+02	5.3388e+02 ; C5 - C7 - C12
5	10	13	1	1.1997e+02	5.6233e+02 ; C5 - C10- C13
5	10	35	1	1.2001e+02	4.0585e+02 ; C5 - C10- H2
6	8	13	1	1.1997e+02	5.6233e+02 ; C6 - C8 - C13
6	8	14	1	1.1997e+02	5.6233e+02 ; C6 - C8 - C14
6	9	15	1	1.1997e+02	5.6233e+02 ; C6 - C9 - C15
6	9	16	1	1.1997e+02	5.6233e+02 ; C6 - C9 - C16
7	5	10	1	1.1997e+02	5.6233e+02 ; C7 - C5 - C10
7	11	36	1	1.2001e+02	4.0585e+02 ; C7 - C11- H3
7	12	67	1	1.1095e+02	3.9162e+02 ; C7 - C12- H34
7	12	68	1	1.1095e+02	3.9162e+02 ; C7 - C12- H35
7	12	71	1	1.1051e+02	5.6651e+02 ; C7 - C12- O1
8	6	9	1	1.1997e+02	5.6233e+02 ; C8 - C6 - C9
8	13	10	1	1.1997e+02	5.6233e+02 ; C8 - C13- C10
8	13	66	1	1.2001e+02	4.0585e+02 ; C8 - C13- H33
8	14	17	1	1.1997e+02	5.6233e+02 ; C8 - C14- C17
8	14	65	1	1.2001e+02	4.0585e+02 ; C8 - C14- H32
9	15	64	1	1.2001e+02	4.0585e+02 ; C9 - C15- H31
9	16	17	1	1.1997e+02	5.6233e+02 ; C9 - C16- C17
9	16	63	1	1.2001e+02	4.0585e+02 ; C9 - C16- H30
10	13	66	1	1.2001e+02	4.0585e+02 ;C10 - C13- H33

11	3	69	1	1.2001e+02	4.0585e+02 ;C11 - C3 - H36
11	7	12	1	1.2063e+02	5.3388e+02 ;C11 - C7 - C12
12	71	19	1	1.1514e+02	5.3220e+02 ;C12 - O1 - C19
13	8	14	1	1.1997e+02	5.6233e+02 ;C13 - C8 - C14
13	10	35	1	1.2001e+02	4.0585e+02 ;C13 - C10- H2
14	17	16	1	1.1997e+02	5.6233e+02 ;C14 - C17- C16
14	17	62	1	1.2001e+02	4.0585e+02 ;C14 - C17- H29
15	4	34	1	1.2001e+02	4.0585e+02 ;C15 - C4 - H1
15	9	16	1	1.1997e+02	5.6233e+02 ;C15 - C9 - C16
16	17	62	1	1.2001e+02	4.0585e+02 ;C16 - C17- H29
17	14	65	1	1.2001e+02	4.0585e+02 ;C17 - C14- H32
17	16	63	1	1.2001e+02	4.0585e+02 ;C17 - C16- H30
18	30	33	1	1.1997e+02	5.6233e+02 ;C18 - C30- C33
18	30	38	1	1.2001e+02	4.0585e+02 ;C18 - C30- H5
18	32	40	1	1.2109e+02	4.0334e+02 ;C18 - C32- H7
18	32	70	1	1.1834e+02	5.8743e+02 ;C18 - C32- N1
19	20	21	1	1.1053e+02	5.3388e+02 ;C19 - C20- C21
19	20	60	1	1.0968e+02	3.9497e+02 ;C19 - C20- H27
19	20	61	1	1.0968e+02	3.9497e+02 ;C19 - C20- H28
20	19	71	1	1.1196e+02	5.7990e+02 ;C20 - C19- O1
20	19	72	1	1.2311e+02	5.6902e+02 ;C20 - C19- O2
20	21	22	1	1.1063e+02	5.2886e+02 ;C20 - C21- C22
20	21	58	1	1.1005e+02	3.8828e+02 ;C20 - C21- H25
20	21	59	1	1.1005e+02	3.8828e+02 ;C20 - C21- H26
21	20	60	1	1.1005e+02	3.8828e+02 ;C21 - C20- H27
21	20	61	1	1.1005e+02	3.8828e+02 ;C21 - C20- H28
21	22	23	1	1.1063e+02	5.2886e+02 ;C21 - C22- C23
21	22	56	1	1.1005e+02	3.8828e+02 ;C21 - C22- H23
21	22	57	1	1.1005e+02	3.8828e+02 ;C21 - C22- H24
22	21	58	1	1.1005e+02	3.8828e+02 ;C22 - C21- H25

22	21	59	1	1.1005e+02	3.8828e+02 ;C22 - C21- H26
22	23	24	1	1.1063e+02	5.2886e+02 ;C22 - C23- C24
22	23	54	1	1.1005e+02	3.8828e+02 ;C22 - C23- H21
22	23	55	1	1.1005e+02	3.8828e+02 ;C22 - C23- H22
23	22	56	1	1.1005e+02	3.8828e+02 ;C23 - C22- H23
23	22	57	1	1.1005e+02	3.8828e+02 ;C23 - C22- H24
23	24	25	1	1.1063e+02	5.2886e+02 ;C23 - C24- C25
23	24	52	1	1.1005e+02	3.8828e+02 ;C23 - C24- H19
23	24	53	1	1.1005e+02	3.8828e+02 ;C23 - C24- H20
24	23	54	1	1.1005e+02	3.8828e+02 ;C24 - C23- H21
24	23	55	1	1.1005e+02	3.8828e+02 ;C24 - C23- H22
24	25	26	1	1.1063e+02	5.2886e+02 ;C24 - C25- C26
24	25	50	1	1.1005e+02	3.8828e+02 ;C24 - C25- H17
24	25	51	1	1.1005e+02	3.8828e+02 ;C24 - C25- H18
25	24	52	1	1.1005e+02	3.8828e+02 ;C25 - C24- H19
25	24	53	1	1.1005e+02	3.8828e+02 ;C25 - C24- H20
25	26	27	1	1.1063e+02	5.2886e+02 ;C25 - C26- C27
25	26	48	1	1.1005e+02	3.8828e+02 ;C25 - C26- H15
25	26	49	1	1.1005e+02	3.8828e+02 ;C25 - C26- H16
26	25	50	1	1.1005e+02	3.8828e+02 ;C26 - C25- H17
26	25	51	1	1.1005e+02	3.8828e+02 ;C26 - C25- H18
26	27	28	1	1.1063e+02	5.2886e+02 ;C26 - C27- C28
26	27	46	1	1.1005e+02	3.8828e+02 ;C26 - C27- H13
26	27	47	1	1.1005e+02	3.8828e+02 ;C26 - C27- H14
27	26	48	1	1.1005e+02	3.8828e+02 ;C27 - C26- H15
27	26	49	1	1.1005e+02	3.8828e+02 ;C27 - C26- H16
27	28	29	1	1.1063e+02	5.2886e+02 ;C27 - C28- C29
27	28	44	1	1.1005e+02	3.8828e+02 ;C27 - C28- H11
27	28	45	1	1.1005e+02	3.8828e+02 ;C27 - C28- H12
28	27	46	1	1.1005e+02	3.8828e+02 ;C28 - C27- H13

28	27	47	1	1.1005e+02	3.8828e+02 ;C28 - C27- H14
28	29	42	1	1.1007e+02	3.8828e+02 ;C28 - C29- H9
28	29	43	1	1.1007e+02	3.8828e+02 ;C28 - C29- H10
28	29	70	1	1.1259e+02	5.5061e+02 ;C28 - C29- N1
29	28	44	1	1.1005e+02	3.8828e+02 ;C29 - C28- H11
29	28	45	1	1.1005e+02	3.8828e+02 ;C29 - C28- H12
29	70	31	1	1.2436e+02	5.2802e+02 ;C29 - N1 - C31
29	70	32	1	1.2436e+02	5.2802e+02 ;C29 - N1 - C32
30	18	32	1	1.1997e+02	5.6233e+02 ;C30 - C18- C32
30	18	37	1	1.2001e+02	4.0585e+02 ;C30 - C18- H4
30	33	31	1	1.1997e+02	5.6233e+02 ;C30 - C33- C31
30	33	39	1	1.2001e+02	4.0585e+02 ;C30 - C33- H6
31	33	39	1	1.2001e+02	4.0585e+02 ;C31 - C33- H6
31	70	32	1	1.1980e+02	5.6149e+02 ;C31 - N1 - C32
32	18	37	1	1.2001e+02	4.0585e+02 ;C32 - C18- H4
33	30	38	1	1.2001e+02	4.0585e+02 ;C33 - C30- H5
33	31	41	1	1.2109e+02	4.0334e+02 ;C33 - C31- H8
33	31	70	1	1.1834e+02	5.8743e+02 ;C33 - C31- N1
40	32	70	1	1.1465e+02	4.3430e+02 ; H7 - C32- N1
41	31	70	1	1.1465e+02	4.3430e+02 ; H8 - C31- N1
42	29	43	1	1.0955e+02	3.2803e+02 ; H9 - C29- H10
42	29	70	1	1.0945e+02	4.1756e+02 ; H9 - C29- N1
43	29	70	1	1.0945e+02	4.1756e+02 ;H10 - C29- N1
44	28	45	1	1.0835e+02	3.2970e+02 ;H11 - C28- H12
46	27	47	1	1.0835e+02	3.2970e+02 ;H13 - C27- H14
48	26	49	1	1.0835e+02	3.2970e+02 ;H15 - C26- H16
50	25	51	1	1.0835e+02	3.2970e+02 ;H17 - C25- H18
52	24	53	1	1.0835e+02	3.2970e+02 ;H19 - C24- H20
54	23	55	1	1.0835e+02	3.2970e+02 ;H21 - C23- H22
56	22	57	1	1.0835e+02	3.2970e+02 ;H23 - C22- H24

```
    58      21      59      1       1.0835e+02      3.2970e+02 ;H25 - C21- H26
    60      20      61      1       1.0835e+02      3.2970e+02 ;H27 - C20- H28
    67      12      68      1       1.0955e+02      3.2803e+02 ;H34 - C12- H35
    67      12      71      1       1.0882e+02      4.2509e+02 ;H34 - C12- O1
    68      12      71      1       1.0882e+02      4.2509e+02 ;H35 - C12- O1
    71      19      72      1       1.2243e+02      6.3764e+02 ; O1 - C19- O2

[ dihedrals ] ; propers

; treated as RBs in GROMACS to use combine multiple AMBER torsions per quartet

; i    j    k    l   func       C0         C1              C2              C3              C4              C5
  1    2    5    7     3    30.33400    0.00000 -30.33400    0.00000    0.00000 0.00000 ; C1- C2- C5- C7
  1    2    5 10     3    30.33400    0.00000 -30.33400    0.00000    0.00000 0.00000 ; C1- C2- C5-C10
  1    2    6    8     3    30.33400    0.00000 -30.33400    0.00000    0.00000 0.00000 ; C1- C2- C6- C8
  1    2    6    9     3    30.33400    0.00000 -30.33400    0.00000    0.00000 0.00000 ; C1- C2- C6- C9
  1    3 11    7     3    30.33400    0.00000 -30.33400    0.00000    0.00000 0.00000 ; C1- C3-C11- C7
  1    3 11 36     3    30.33400    0.00000 -30.33400    0.00000    0.00000 0.00000 ; C1- C3-C11- H3
  1    4 15    9     3    30.33400    0.00000 -30.33400    0.00000    0.00000 0.00000 ; C1- C4-C15- C9
  1    4 15 64     3    30.33400    0.00000 -30.33400    0.00000    0.00000 0.00000 ; C1- C4-C15-H31
  2    1    3 11     3    30.33400    0.00000 -30.33400    0.00000    0.00000 0.00000 ; C2- C1- C3-C11
  2    1    3 69     3    30.33400    0.00000 -30.33400    0.00000    0.00000 0.00000 ; C2- C1- C3-H36
  2    1    4 15     3    30.33400    0.00000 -30.33400    0.00000    0.00000 0.00000 ; C2- C1- C4-C15
  2    1    4 34     3    30.33400    0.00000 -30.33400    0.00000    0.00000 0.00000 ; C2- C1- C4- H1
  2    5    7 11     3    30.33400    0.00000 -30.33400    0.00000    0.00000 0.00000 ; C2- C5- C7-C11
  2    5    7 12     3    30.33400    0.00000 -30.33400    0.00000    0.00000 0.00000 ; C2- C5- C7-C12
  2    5 10 13     3    30.33400    0.00000 -30.33400    0.00000    0.00000 0.00000 ; C2- C5-C10-C13
  2    5 10 35     3    30.33400    0.00000 -30.33400    0.00000    0.00000 0.00000 ; C2- C5-C10- H2
  2    6    8 13     3    30.33400    0.00000 -30.33400    0.00000    0.00000 0.00000 ; C2- C6- C8-C13
  2    6    8 14     3    30.33400    0.00000 -30.33400    0.00000    0.00000 0.00000 ; C2- C6- C8-C14
  2    6    9 15     3    30.33400    0.00000 -30.33400    0.00000    0.00000 0.00000 ; C2- C6- C9-C15
  2    6    9 16     3    30.33400    0.00000 -30.33400    0.00000    0.00000 0.00000 ; C2- C6- C9-C16
  3    1    2    5     3    30.33400    0.00000 -30.33400    0.00000    0.00000 0.00000 ; C3- C1- C2- C5
```

3 1 2 6 3 30.33400 0.00000 -30.33400 0.00000 0.00000 0.00000 ; C3- C1- C2- C6

3 1 4 15 3 30.33400 0.00000 -30.33400 0.00000 0.00000 0.00000 ; C3- C1- C4-C15

3 1 4 34 3 30.33400 0.00000 -30.33400 0.00000 0.00000 0.00000 ; C3- C1- C4- H1

3 11 7 5 3 30.33400 0.00000 -30.33400 0.00000 0.00000 0.00000 ; C3-C11- C7- C5

3 11 7 12 3 30.33400 0.00000 -30.33400 0.00000 0.00000 0.00000 ; C3-C11- C7-C12

4 1 2 5 3 30.33400 0.00000 -30.33400 0.00000 0.00000 0.00000 ; C4- C1- C2- C5

4 1 2 6 3 30.33400 0.00000 -30.33400 0.00000 0.00000 0.00000 ; C4- C1- C2- C6

4 1 3 11 3 30.33400 0.00000 -30.33400 0.00000 0.00000 0.00000 ; C4- C1- C3-C11

4 1 3 69 3 30.33400 0.00000 -30.33400 0.00000 0.00000 0.00000 ; C4- C1- C3-H36

4 15 9 6 3 30.33400 0.00000 -30.33400 0.00000 0.00000 0.00000 ; C4-C15- C9- C6

4 15 9 16 3 30.33400 0.00000 -30.33400 0.00000 0.00000 0.00000 ; C4-C15- C9-C16

5 2 6 8 3 30.33400 0.00000 -30.33400 0.00000 0.00000 0.00000 ; C5- C2- C6- C8

5 2 6 9 3 30.33400 0.00000 -30.33400 0.00000 0.00000 0.00000 ; C5- C2- C6- C9

5 7 11 36 3 30.33400 0.00000 -30.33400 0.00000 0.00000 0.00000 ; C5- C7-C11- H3

5 7 12 67 3 0.000000 0.00000 0.00000 0.00000 0.00000 0.00000 ; C5- C7-C12-H34

5 7 12 68 3 0.000000 0.00000 0.00000 0.00000 0.00000 0.00000 ; C5- C7-C12-H35

5 7 12 71 3 1.737220 0.00000 -0.571642 0.00000 -1.21255 0.00000 ; C5- C7-C12- O1

5 10 13 8 3 30.33400 0.00000 -30.33400 0.00000 0.00000 0.00000 ; C5-C10-C13- C8

5 10 13 66 3 30.33400 0.00000 -30.33400 0.00000 0.00000 0.00000 ; C5-C10-C13-H33

6 2 5 7 3 30.33400 0.00000 -30.33400 0.00000 0.00000 0.00000 ; C6- C2- C5- C7

6 2 5 10 3 30.33400 0.00000 -30.33400 0.00000 0.00000 0.00000 ; C6- C2- C5-C10

6 8 13 10 3 30.33400 0.00000 -30.33400 0.00000 0.00000 0.00000 ; C6- C8-C13-C10

6 8 13 66 3 30.33400 0.00000 -30.33400 0.00000 0.00000 0.00000 ; C6- C8-C13-H33

6 8 14 17 3 30.33400 0.00000 -30.33400 0.00000 0.00000 0.00000 ; C6- C8-C14-C17

6 8 14 65 3 30.33400 0.00000 -30.33400 0.00000 0.00000 0.00000 ; C6- C8-C14-H32

6 9 15 64 3 30.33400 0.00000 -30.33400 0.00000 0.00000 0.00000 ; C6- C9-C15-H31

6 9 16 17 3 30.33400 0.00000 -30.33400 0.00000 0.00000 0.00000 ; C6- C9-C16-C17

6 9 16 63 3 30.33400 0.00000 -30.33400 0.00000 0.00000 0.00000 ; C6- C9-C16-H30

7 5 10 13 3 30.33400 0.00000 -30.33400 0.00000 0.00000 0.00000 ; C7- C5-C10-C13

7 5 10 35 3 30.33400 0.00000 -30.33400 0.00000 0.00000 0.00000 ; C7- C5-C10- H2

7 11 3 69 3 30.33400 0.00000 -30.33400 0.00000 0.00000 0.00000 ; C7-C11- C3-H36

7 12 71 19 3 1.60387 4.81160 0.00000 -6.41547 0.00000 0.00000 ; C7-C12- O1-C19

8 6 9 15 3 30.33400 0.00000 -30.33400 0.00000 0.00000 0.00000 ; C8- C6- C9-C15

8 6 9 16 3 30.33400 0.00000 -30.33400 0.00000 0.00000 0.00000 ; C8- C6- C9-C16

8 13 10 35 3 30.33400 0.00000 -30.33400 0.00000 0.00000 0.00000 ; C8-C13-C10- H2

8 14 17 16 3 30.33400 0.00000 -30.33400 0.00000 0.00000 0.00000 ; C8-C14-C17-C16

8 14 17 62 3 30.33400 0.00000 -30.33400 0.00000 0.00000 0.00000 ; C8-C14-C17-H29

9 6 8 13 3 30.33400 0.00000 -30.33400 0.00000 0.00000 0.00000 ; C9- C6- C8-C13

9 6 8 14 3 30.33400 0.00000 -30.33400 0.00000 0.00000 0.00000 ; C9- C6- C8-C14

9 15 4 34 3 30.33400 0.00000 -30.33400 0.00000 0.00000 0.00000 ; C9-C15- C4- H1

9 16 17 14 3 30.33400 0.00000 -30.33400 0.00000 0.00000 0.00000 ; C9-C16-C17-C14

9 16 17 62 3 30.33400 0.00000 -30.33400 0.00000 0.00000 0.00000 ; C9-C16-C17-H29

10 5 7 11 3 30.33400 0.00000 -30.33400 0.00000 0.00000 0.00000 ;C10- C5- C7-C11

10 5 7 12 3 30.33400 0.00000 -30.33400 0.00000 0.00000 0.00000 ;C10- C5- C7-C12

10 13 8 14 3 30.33400 0.00000 -30.33400 0.00000 0.00000 0.00000 ;C10-C13- C8-C14

11 7 12 67 3 0.000000 0.00000 0.00000 0.00000 0.00000 0.00000 ;C11- C7-C12-H34

11 7 12 68 3 0.000000 0.00000 0.00000 0.00000 0.00000 0.00000 ;C11- C7-C12-H35

11 7 12 71 3 1.737220 0.00000 -0.571642 0.00000 -1.21255 0.00000 ;C11- C7-C12- O1

12 7 11 36 3 30.33400 0.00000 -30.33400 0.00000 0.00000 0.00000 ;C12- C7-C11- H3

12 71 19 20 3 22.59360 0.00000 -22.59360 0.00000 0.00000 0.00000 ;C12- O1-C19-C20

12 71 19 72 3 28.45120 5.85760 -22.59360 0.00000 0.00000 0.00000 ;C12- O1-C19- O2

13 8 14 17 3 30.33400 0.00000 -30.33400 0.00000 0.00000 0.00000 ;C13- C8-C14-C17

13 8 14 65 3 30.33400 0.00000 -30.33400 0.00000 0.00000 0.00000 ;C13- C8-C14-H32

14 8 13 66 3 30.33400 0.00000 -30.33400 0.00000 0.00000 0.00000 ;C14- C8-C13-H33

14 17 16 63 3 30.33400 0.00000 -30.33400 0.00000 0.00000 0.00000 ;C14-C17-C16-H30

15 9 16 17 3 30.33400 0.00000 -30.33400 0.00000 0.00000 0.00000 ;C15- C9-C16-C17

15 9 16 63 3 30.33400 0.00000 -30.33400 0.00000 0.00000 0.00000 ;C15- C9-C16-H30

16 9 15 64 3 30.33400 0.00000 -30.33400 0.00000 0.00000 0.00000 ;C16- C9-C15-H31

16 17 14 65 3 30.33400 0.00000 -30.33400 0.00000 0.00000 0.00000 ;C16-C17-C14-H32

18 30 33 31 3 30.33400 0.00000 -30.33400 0.00000 0.00000 0.00000 ;C18-C30-C33-C31

18 30 33 39 3 30.33400 0.00000 -30.33400 0.00000 0.00000 0.00000 ;C18-C30-C33- H6

18 32 70 29 3 2.51040 0.00000 -2.51040 0.00000 0.00000 0.00000 ;C18-C32- N1-C29

18 32 70 31 3 2.51040 0.00000 -2.51040 0.00000 0.00000 0.00000 ;C18-C32- N1-C31

19 20 21 22 3 0.65084 1.95253 0.00000 -2.60338 0.00000 0.00000 ;C19-C20-C21-C22

19 20 21 58 3 0.65084 1.95253 0.00000 -2.60338 0.00000 0.00000 ;C19-C20-C21-H25

19 20 21 59 3 0.65084 1.95253 0.00000 -2.60338 0.00000 0.00000 ;C19-C20-C21-H26

19 71 12 67 3 1.60387 4.81160 0.00000 -6.41547 0.00000 0.00000 ;C19- O1-C12-H34

19 71 12 68 3 1.60387 4.81160 0.00000 -6.41547 0.00000 0.00000 ;C19- O1-C12-H35

20 21 22 23 3 3.68192 3.09616 -2.09200 -3.01248 0.00000 0.00000 ;C20-C21-C22-C23

20 21 22 56 3 0.66944 2.00832 0.00000 -2.67776 0.00000 0.00000 ;C20-C21-C22-H23

20 21 22 57 3 0.66944 2.00832 0.00000 -2.67776 0.00000 0.00000 ;C20-C21-C22-H24

21 20 19 71 3 0.00000 0.00000 0.00000 0.00000 0.00000 0.00000 ;C21-C20-C19- O1

21 20 19 72 3 0.00000 0.00000 0.00000 0.00000 0.00000 0.00000 ;C21-C20-C19- O2

21 22 23 24 3 3.68192 3.09616 -2.09200 -3.01248 0.00000 0.00000 ;C21-C22-C23-C24

21 22 23 54 3 0.66944 2.00832 0.00000 -2.67776 0.00000 0.00000 ;C21-C22-C23-H21

21 22 23 55 3 0.66944 2.00832 0.00000 -2.67776 0.00000 0.00000 ;C21-C22-C23-H22

22 21 20 60 3 0.66944 2.00832 0.00000 -2.67776 0.00000 0.00000 ;C22-C21-C20-H27

22 21 20 61 3 0.66944 2.00832 0.00000 -2.67776 0.00000 0.00000 ;C22-C21-C20-H28

22 23 24 25 3 3.68192 3.09616 -2.09200 -3.01248 0.00000 0.00000 ;C22-C23-C24-C25

22 23 24 52 3 0.66944 2.00832 0.00000 -2.67776 0.00000 0.00000 ;C22-C23-C24-H19

22 23 24 53 3 0.66944 2.00832 0.00000 -2.67776 0.00000 0.00000 ;C22-C23-C24-H20

23 22 21 58 3 0.66944 2.00832 0.00000 -2.67776 0.00000 0.00000 ;C23-C22-C21-H25

23 22 21 59 3 0.66944 2.00832 0.00000 -2.67776 0.00000 0.00000 ;C23-C22-C21-H26

23 24 25 26 3 3.68192 3.09616 -2.09200 -3.01248 0.00000 0.00000 ;C23-C24-C25-C26

23 24 25 50 3 0.66944 2.00832 0.00000 -2.67776 0.00000 0.00000 ;C23-C24-C25-H17

23 24 25 51 3 0.66944 2.00832 0.00000 -2.67776 0.00000 0.00000 ;C23-C24-C25-H18

24 23 22 56 3 0.66944 2.00832 0.00000 -2.67776 0.00000 0.00000 ;C24-C23-C22-H23

24 23 22 57 3 0.66944 2.00832 0.00000 -2.67776 0.00000 0.00000 ;C24-C23-C22-H24

24 25 26 27 3 3.68192 3.09616 -2.09200 -3.01248 0.00000 0.00000 ;C24-C25-C26-C27

24 25 26 48 3 0.66944 2.00832 0.00000 -2.67776 0.00000 0.00000 ;C24-C25-C26-H15

24 25 26 49 3 0.66944 2.00832 0.00000 -2.67776 0.00000 0.00000 ;C24-C25-C26-H16

25 24 23 54 3 0.66944 2.00832 0.00000 -2.67776 0.00000 0.00000 ;C25-C24-C23-H21

25 24 23 55 3 0.66944 2.00832 0.00000 -2.67776 0.00000 0.00000 ;C25-C24-C23-H22

25 26 27 28 3 3.68192 3.09616 -2.09200 -3.01248 0.00000 0.00000 ;C25-C26-C27-C28

25 26 27 46 3 0.66944 2.00832 0.00000 -2.67776 0.00000 0.00000 ;C25-C26-C27-H13

25 26 27 47 3 0.66944 2.00832 0.00000 -2.67776 0.00000 0.00000 ;C25-C26-C27-H14

26 25 24 52 3 0.66944 2.00832 0.00000 -2.67776 0.00000 0.00000 ;C26-C25-C24-H19

26 25 24 53 3 0.66944 2.00832 0.00000 -2.67776 0.00000 0.00000 ;C26-C25-C24-H20

26 27 28 29 3 3.68192 3.09616 -2.09200 -3.01248 0.00000 0.00000 ;C26-C27-C28-C29

26 27 28 44 3 0.66944 2.00832 0.00000 -2.67776 0.00000 0.00000 ;C26-C27-C28-H11

26 27 28 45 3 0.66944 2.00832 0.00000 -2.67776 0.00000 0.00000 ;C26-C27-C28-H12

27 26 25 50 3 0.66944 2.00832 0.00000 -2.67776 0.00000 0.00000 ;C27-C26-C25-H17

27 26 25 51 3 0.66944 2.00832 0.00000 -2.67776 0.00000 0.00000 ;C27-C26-C25-H18

27 28 29 42 3 0.65084 1.95253 0.00000 -2.60338 0.00000 0.00000 ;C27-C28-C29- H9

27 28 29 43 3 0.65084 1.95253 0.00000 -2.60338 0.00000 0.00000 ;C27-C28-C29-H10

27 28 29 70 3 0.65084 1.95253 0.00000 -2.60338 0.00000 0.00000 ;C27-C28-C29- N1

28 27 26 48 3 0.66944 2.00832 0.00000 -2.67776 0.00000 0.00000 ;C28-C27-C26-H15

28 27 26 49 3 0.66944 2.00832 0.00000 -2.67776 0.00000 0.00000 ;C28-C27-C26-H16

28 29 70 31 3 0.00000 0.00000 0.00000 0.00000 0.00000 0.00000 ;C28-C29- N1-C31

28 29 70 32 3 0.00000 0.00000 0.00000 0.00000 0.00000 0.00000 ;C28-C29- N1-C32

29 28 27 46 3 0.66944 2.00832 0.00000 -2.67776 0.00000 0.00000 ;C29-C28-C27-H13

29 28 27 47 3 0.66944 2.00832 0.00000 -2.67776 0.00000 0.00000 ;C29-C28-C27-H14

29 70 31 33 3 2.51040 0.00000 -2.51040 0.00000 0.00000 0.00000 ;C29- N1-C31-C33

29 70 31 41 3 2.51040 0.00000 -2.51040 0.00000 0.00000 0.00000 ;C29- N1-C31- H8

29 70 32 40 3 2.51040 0.00000 -2.51040 0.00000 0.00000 0.00000 ;C29- N1-C32- H7

30 18 32 40 3 30.33400 0.00000 -30.33400 0.00000 0.00000 0.00000 ;C30-C18-C32- H7

30 18 32 70 3 30.33400 0.00000 -30.33400 0.00000 0.00000 0.00000 ;C30-C18-C32- N1

30 33 31 41 3 30.33400 0.00000 -30.33400 0.00000 0.00000 0.00000 ;C30-C33-C31- H8

30 33 31 70 3 30.33400 0.00000 -30.33400 0.00000 0.00000 0.00000 ;C30-C33-C31- N1

31 33 30 38 3 30.33400 0.00000 -30.33400 0.00000 0.00000 0.00000 ;C31-C33-C30- H5

31 70 29 42 3 0.00000 0.00000 0.00000 0.00000 0.00000 0.00000 ;C31- N1-C29- H9

31 70 29 43 3 0.00000 0.00000 0.00000 0.00000 0.00000 0.00000 ;C31- N1-C29-H10

31 70 32 40 3 2.51040 0.00000 -2.51040 0.00000 0.00000 0.00000 ;C31- N1-C32- H7

32 18 30 33 3 30.33400 0.00000 -30.33400 0.00000 0.00000 0.00000 ;C32-C18-C30-C33

32 18 30 38 3 30.33400 0.00000 -30.33400 0.00000 0.00000 0.00000 ;C32-C18-C30- H5

32 70 29 42 3 0.00000 0.00000 0.00000 0.00000 0.00000 0.00000 ;C32- N1-C29- H9

32 70 29 43 3 0.00000 0.00000 0.00000 0.00000 0.00000 0.00000 ;C32- N1-C29-H10

32 70 31 33 3 2.51040 0.00000 -2.51040 0.00000 0.00000 0.00000 ;C32- N1-C31-C33

32 70 31 41 3 2.51040 0.00000 -2.51040 0.00000 0.00000 0.00000 ;C32- N1-C31- H8

33 30 18 37 3 30.33400 0.00000 -30.33400 0.00000 0.00000 0.00000 ;C33-C30-C18- H4

34 4 15 64 3 30.33400 0.00000 -30.33400 0.00000 0.00000 0.00000 ; H1- C4-C15-H31

35 10 13 66 3 30.33400 0.00000 -30.33400 0.00000 0.00000 0.00000 ; H2-C10-C13-H33

36 11 3 69 3 30.33400 0.00000 -30.33400 0.00000 0.00000 0.00000 ; H3-C11- C3-H36

37 18 30 38 3 30.33400 0.00000 -30.33400 0.00000 0.00000 0.00000 ; H4-C18-C30- H5

37 18 32 40 3 30.33400 0.00000 -30.33400 0.00000 0.00000 0.00000 ; H4-C18-C32- H7

37 18 32 70 3 30.33400 0.00000 -30.33400 0.00000 0.00000 0.00000 ; H4-C18-C32- N1

38 30 33 39 3 30.33400 0.00000 -30.33400 0.00000 0.00000 0.00000 ; H5-C30-C33- H6

39 33 31 41 3 30.33400 0.00000 -30.33400 0.00000 0.00000 0.00000 ; H6-C33-C31- H8

39 33 31 70 3 30.33400 0.00000 -30.33400 0.00000 0.00000 0.00000 ; H6-C33-C31- N1

42 29 28 44 3 0.65084 1.95253 0.00000 -2.60338 0.00000 0.00000 ; H9-C29-C28-H11

42 29 28 45 3 0.65084 1.95253 0.00000 -2.60338 0.00000 0.00000 ; H9-C29-C28-H12

43 29 28 44 3 0.65084 1.95253 0.00000 -2.60338 0.00000 0.00000 ;H10-C29-C28-H11

43 29 28 45 3 0.65084 1.95253 0.00000 -2.60338 0.00000 0.00000 ;H10-C29-C28-H12

44 28 27 46 3 0.62760 1.88280 0.00000 -2.51040 0.00000 0.00000 ;H11-C28-C27-H13

44 28 27 47 3 0.62760 1.88280 0.00000 -2.51040 0.00000 0.00000 ;H11-C28-C27-H14

44 28 29 70 3 0.65084 1.95253 0.00000 -2.60338 0.00000 0.00000 ;H11-C28-C29- N1

45 28 27 46 3 0.62760 1.88280 0.00000 -2.51040 0.00000 0.00000 ;H12-C28-C27-H13

45 28 27 47 3 0.62760 1.88280 0.00000 -2.51040 0.00000 0.00000 ;H12-C28-C27-H14

45 28 29 70 3 0.65084 1.95253 0.00000 -2.60338 0.00000 0.00000 ;H12-C28-C29- N1

46 27 26 48 3 0.62760 1.88280 0.00000 -2.51040 0.00000 0.00000 ;H13-C27-C26-H15

46 27 26 49 3 0.62760 1.88280 0.00000 -2.51040 0.00000 0.00000 ;H13-C27-C26-H16

47 27 26 48 3 0.62760 1.88280 0.00000 -2.51040 0.00000 0.00000 ;H14-C27-C26-H15

47 27 26 49 3 0.62760 1.88280 0.00000 -2.51040 0.00000 0.00000 ;H14-C27-C26-H16

48 26 25 50 3 0.62760 1.88280 0.00000 -2.51040 0.00000 0.00000 ;H15-C26-C25-H17

48 26 25 51 3 0.62760 1.88280 0.00000 -2.51040 0.00000 0.00000 ;H15-C26-C25-H18

49 26 25 50 3 0.62760 1.88280 0.00000 -2.51040 0.00000 0.00000 ;H16-C26-C25-H17

49 26 25 51 3 0.62760 1.88280 0.00000 -2.51040 0.00000 0.00000 ;H16-C26-C25-H18

50 25 24 52 3 0.62760 1.88280 0.00000 -2.51040 0.00000 0.00000 ;H17-C25-C24-H19

50 25 24 53 3 0.62760 1.88280 0.00000 -2.51040 0.00000 0.00000 ;H17-C25-C24-H20

51 25 24 52 3 0.62760 1.88280 0.00000 -2.51040 0.00000 0.00000 ;H18-C25-C24-H19

51 25 24 53 3 0.62760 1.88280 0.00000 -2.51040 0.00000 0.00000 ;H18-C25-C24-H20

52 24 23 54 3 0.62760 1.88280 0.00000 -2.51040 0.00000 0.00000 ;H19-C24-C23-H21

52 24 23 55 3 0.62760 1.88280 0.00000 -2.51040 0.00000 0.00000 ;H19-C24-C23-H22

53 24 23 54 3 0.62760 1.88280 0.00000 -2.51040 0.00000 0.00000 ;H20-C24-C23-H21

53 24 23 55 3 0.62760 1.88280 0.00000 -2.51040 0.00000 0.00000 ;H20-C24-C23-H22

54 23 22 56 3 0.62760 1.88280 0.00000 -2.51040 0.00000 0.00000 ;H21-C23-C22-H23

54 23 22 57 3 0.62760 1.88280 0.00000 -2.51040 0.00000 0.00000 ;H21-C23-C22-H24

55 23 22 56 3 0.62760 1.88280 0.00000 -2.51040 0.00000 0.00000 ;H22-C23-C22-H23

55 23 22 57 3 0.62760 1.88280 0.00000 -2.51040 0.00000 0.00000 ;H22-C23-C22-H24

56 22 21 58 3 0.62760 1.88280 0.00000 -2.51040 0.00000 0.00000 ;H23-C22-C21-H25

56 22 21 59 3 0.62760 1.88280 0.00000 -2.51040 0.00000 0.00000 ;H23-C22-C21-H26

57 22 21 58 3 0.62760 1.88280 0.00000 -2.51040 0.00000 0.00000 ;H24-C22-C21-H25

57 22 21 59 3 0.62760 1.88280 0.00000 -2.51040 0.00000 0.00000 ;H24-C22-C21-H26

58 21 20 60 3 0.62760 1.88280 0.00000 -2.51040 0.00000 0.00000 ;H25-C21-C20-H27

58 21 20 61 3 0.62760 1.88280 0.00000 -2.51040 0.00000 0.00000 ;H25-C21-C20-H28

59 21 20 60 3 0.62760 1.88280 0.00000 -2.51040 0.00000 0.00000 ;H26-C21-C20-H27

59 21 20 61 3 0.62760 1.88280 0.00000 -2.51040 0.00000 0.00000 ;H26-C21-C20-H28

60 20 19 71 3 0.00000 0.00000 0.00000 0.00000 0.00000 0.00000 ;H27-C20-C19- O1

60 20 19 72 3 3.68192 -4.35136 0.00000 1.33888 0.00000 0.00000 ;H27-C20-C19- O2

61 20 19 71 3 0.00000 0.00000 0.00000 0.00000 0.00000 0.00000 ;H28-C20-C19- O1

61 20 19 72 3 3.68192 -4.35136 0.00000 1.33888 0.00000 0.00000 ;H28-C20-C19- O2

62 17 14 65 3 30.33400 0.00000 -30.33400 0.00000 0.00000 0.00000 ;H29-C17-C14-H32

62 17 16 63 3 30.33400 0.00000 -30.33400 0.00000 0.00000 0.00000 ;H29-C17-C16-H30

[dihedrals] ; impropers

; treated as propers in GROMACS to use correct AMBER analytical function

;i j k l func phase kd pn

1 5 2 6 1 180.00 4.60240 2 ; C1- C5- C2- C6

1 11 3 69 1 180.00 4.60240 2 ; C1-C11- C3-H36

1 15 4 34 1 180.00 4.60240 2 ; C1-C15- C4- H1

2 7 5 10 1 180.00 4.60240 2 ; C2- C7- C5-C10

2 8 6 9 1 180.00 4.60240 2 ; C2- C8- C6- C9

3 7 11 36 1 180.00 4.60240 2 ; C3- C7- C11- H3

4 1 3 2 1 180.00 4.60240 2 ; C4- C1- C3- C2

4 9 15 64 1 180.00 4.60240 2 ; C4- C9- C15-H31

5 11 7 12 1 180.00 4.60240 2 ; C5-C11- C7-C12

5 13 10 35 1 180.00 4.60240 2 ; C5-C13- C10- H2

6 13 8 14 1 180.00 4.60240 2 ; C6-C13- C8-C14

6 15 9 16 1 180.00 4.60240 2 ; C6-C15- C9-C16

8 10 13 66 1 180.00 4.60240 2 ; C8-C10- C13-H33

8 17 14 65 1 180.00 4.60240 2 ; C8-C17- C14-H32

9 17 16 63 1 180.00 4.60240 2 ; C9-C17- C16-H30

14 16 17 62 1 180.00 4.60240 2 ; C14-C16- C17-H29

18 33 30 38 1 180.00 4.60240 2 ; C18-C33- C30- H5

18 40 32 70 1 180.00 4.60240 2 ; C18- H7- C32- N1

20 72 19 71 1 180.00 43.93200 2 ; C20- O2- C19- O1

30 31 33 39 1 180.00 4.60240 2 ; C30-C31- C33- H6

30 32 18 37 1 180.00 4.60240 2 ; C30-C32- C18- H4

31 32 70 29 1 180.00 4.60240 2 ; C31-C32- N1-C29

33 41 31 70 1 180.00 4.60240 2 ; C33- H8- C31- N1

[system]

PYR-AA

[molecules]

; Compound nmols

PYR 1

(2) Force field parameters for PYN in all atom resolution.

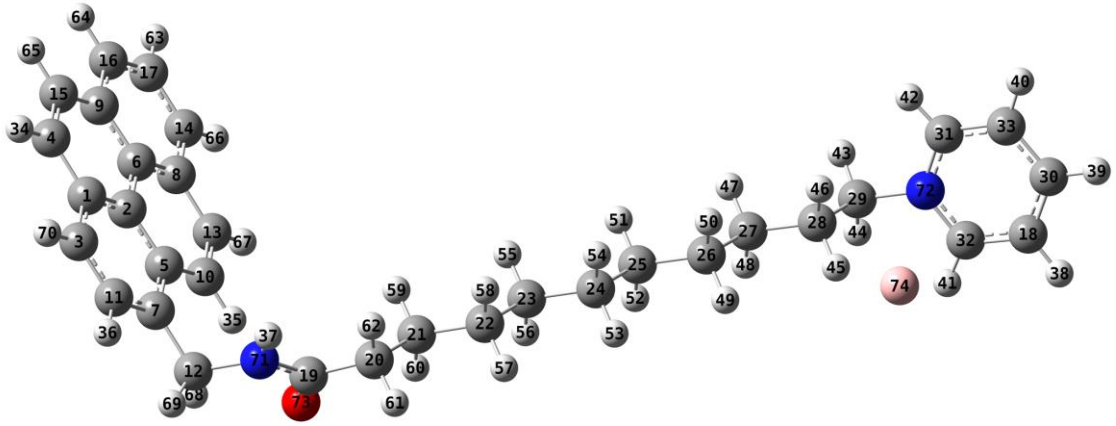

Snapshot of PYN in all atom representation (the index of each atom was also labeled in the above Figure).

The details of PYN force field in all atom resolution in Gromacs format are as follows:

; PYN_AA.top

[defaults]

; nbfunc	comb-rule	gen-pairs	fudgeLJ	fudgeQQ
1	2	yes	0.5	0.8333

[atomtypes]

;name	bond_type	mass	charge	ptype	sigma	epsilon
ca	ca	0.00000	0.00000	A	3.39967e-01	3.59824e-01
c3	c3	0.00000	0.00000	A	3.39967e-01	4.57730e-01
c	c	0.00000	0.00000	A	3.39967e-01	3.59824e-01
ha	ha	0.00000	0.00000	A	2.59964e-01	6.27600e-02
hn	hn	0.00000	0.00000	A	1.06908e-01	6.56888e-02
h4	h4	0.00000	0.00000	A	2.51055e-01	6.27600e-02
h1	h1	0.00000	0.00000	A	2.47135e-01	6.56888e-02
hc	hc	0.00000	0.00000	A	2.64953e-01	6.56888e-02
n	n	0.00000	0.00000	A	3.25000e-01	7.11280e-01
na	na	0.00000	0.00000	A	3.25000e-01	7.11280e-01
o	o	0.00000	0.00000	A	2.95992e-01	8.78640e-01
IM	IM	0.00000	0.00000	A	3.95559e-01	1.33888e+00

[moleculetype]

;name nrexcl

PYN 3

[atoms]

; nr type resi res atom cgnr charge mass

1	ca	1	PYN	C1	1	0.148714	12.01000
2	ca	1	PYN	C2	2	0.012487	12.01000
3	ca	1	PYN	C3	3	-0.268257	12.01000
4	ca	1	PYN	C4	4	-0.208393	12.01000
5	ca	1	PYN	C5	5	0.071333	12.01000
6	ca	1	PYN	C6	6	-0.057946	12.01000
7	ca	1	PYN	C7	7	-0.110168	12.01000
8	ca	1	PYN	C8	8	0.202794	12.01000
9	ca	1	PYN	C9	9	0.195936	12.01000
10	ca	1	PYN	C10	10	-0.158714	12.01000
11	ca	1	PYN	C11	11	-0.161158	12.01000
12	c3	1	PYN	C12	12	0.174765	12.01000
13	ca	1	PYN	C13	13	-0.274801	12.01000
14	ca	1	PYN	C14	14	-0.281660	12.01000
15	ca	1	PYN	C15	15	-0.255687	12.01000
16	ca	1	PYN	C16	16	-0.276622	12.01000
17	ca	1	PYN	C17	17	-0.104228	12.01000
18	ca	1	PYN	C18	18	-0.227299	12.01000
19	c	1	PYN	C19	19	0.742947	12.01000
20	c3	1	PYN	C20	20	-0.301848	12.01000
21	c3	1	PYN	C21	21	0.172830	12.01000
22	c3	1	PYN	C22	22	-0.010474	12.01000
23	c3	1	PYN	C23	23	-0.092764	12.01000
24	c3	1	PYN	C24	24	0.032877	12.01000
25	c3	1	PYN	C25	25	0.027829	12.01000
26	c3	1	PYN	C26	26	-0.097332	12.01000

27	c3	1	PYN	C27	27	0.001144	12.01000
28	c3	1	PYN	C28	28	0.094938	12.01000
29	c3	1	PYN	C29	29	-0.268569	12.01000
30	ca	1	PYN	C30	30	0.112013	12.01000
31	ca	1	PYN	C31	31	0.018785	12.01000
32	ca	1	PYN	C32	32	0.018785	12.01000
33	ca	1	PYN	C33	33	-0.227299	12.01000
34	ha	1	PYN	H1	34	0.156839	1.00800
35	ha	1	PYN	H2	35	0.167915	1.00800
36	ha	1	PYN	H3	36	0.156649	1.00800
37	hn	1	PYN	H4	37	0.367677	1.00800
38	ha	1	PYN	H5	38	0.198358	1.00800
39	ha	1	PYN	H6	39	0.163495	1.00800
40	ha	1	PYN	H7	40	0.198358	1.00800
41	h4	1	PYN	H8	41	0.211153	1.00800
42	h4	1	PYN	H9	42	0.211153	1.00800
43	h1	1	PYN	H10	43	0.141588	1.00800
44	h1	1	PYN	H11	44	0.141588	1.00800
45	hc	1	PYN	H12	45	0.013916	1.00800
46	hc	1	PYN	H13	46	0.013916	1.00800
47	hc	1	PYN	H14	47	0.025338	1.00800
48	hc	1	PYN	H15	48	0.025338	1.00800
49	hc	1	PYN	H16	49	0.028403	1.00800
50	hc	1	PYN	H17	50	0.028403	1.00800
51	hc	1	PYN	H18	51	0.004604	1.00800
52	hc	1	PYN	H19	52	0.004604	1.00800
53	hc	1	PYN	H20	53	0.000668	1.00800
54	hc	1	PYN	H21	54	0.000668	1.00800
55	hc	1	PYN	H22	55	0.025813	1.00800
56	hc	1	PYN	H23	56	0.025813	1.00800

57	hc	1	PYN	H24	57	0.009137	1.00800
58	hc	1	PYN	H25	58	0.009137	1.00800
59	hc	1	PYN	H26	59	-0.016373	1.00800
60	hc	1	PYN	H27	60	-0.016373	1.00800
61	hc	1	PYN	H28	61	0.070874	1.00800
62	hc	1	PYN	H29	62	0.070874	1.00800
63	ha	1	PYN	H30	63	0.147423	1.00800
64	ha	1	PYN	H31	64	0.168083	1.00800
65	ha	1	PYN	H32	65	0.167777	1.00800
66	ha	1	PYN	H33	66	0.168361	1.00800
67	ha	1	PYN	H34	67	0.162493	1.00800
68	h1	1	PYN	H35	68	0.065584	1.00800
69	h1	1	PYN	H36	69	0.065584	1.00800
70	ha	1	PYN	H37	70	0.170639	1.00800
71	n	1	PYN	N1	71	-0.692275	14.01000
72	na	1	PYN	N2	72	0.105280	14.01000
73	o	1	PYN	O1	73	-0.613442	16.00000
74	IM	1	PYR	Br-	74	-1.000000	79.90000

[bonds]

;	ai	aj	funct	r	k	
	1	2	1	1.3870e-01	4.0033e+05 ;	C1 - C2
	1	3	1	1.3870e-01	4.0033e+05 ;	C1 - C3
	1	4	1	1.3870e-01	4.0033e+05 ;	C1 - C4
	2	5	1	1.3870e-01	4.0033e+05 ;	C2 - C5
	2	6	1	1.3870e-01	4.0033e+05 ;	C2 - C6
	3	11	1	1.3870e-01	4.0033e+05 ;	C3 - C11
	3	70	1	1.0870e-01	2.8811e+05 ;	C3 - H37
	4	15	1	1.3870e-01	4.0033e+05 ;	C4 - C15
	4	34	1	1.0870e-01	2.8811e+05 ;	C4 - H1
	5	7	1	1.3870e-01	4.0033e+05 ;	C5 - C7

5	10	1	1.3870e-01	4.0033e+05 ;	C5 - C10
6	8	1	1.3870e-01	4.0033e+05 ;	C6 - C8
6	9	1	1.3870e-01	4.0033e+05 ;	C6 - C9
7	11	1	1.3870e-01	4.0033e+05 ;	C7 - C11
7	12	1	1.5130e-01	2.7070e+05 ;	C7 - C12
8	13	1	1.3870e-01	4.0033e+05 ;	C8 - C13
8	14	1	1.3870e-01	4.0033e+05 ;	C8 - C14
9	15	1	1.3870e-01	4.0033e+05 ;	C9 - C15
9	16	1	1.3870e-01	4.0033e+05 ;	C9 - C16
10	13	1	1.3870e-01	4.0033e+05 ;	C10 - C13
10	35	1	1.0870e-01	2.8811e+05 ;	C10 - H2
11	36	1	1.0870e-01	2.8811e+05 ;	C11 - H3
12	68	1	1.0930e-01	2.8108e+05 ;	C12 - H35
12	69	1	1.0930e-01	2.8108e+05 ;	C12 - H36
12	71	1	1.4600e-01	2.7665e+05 ;	C12 - N1
13	67	1	1.0870e-01	2.8811e+05 ;	C13 - H34
14	17	1	1.3870e-01	4.0033e+05 ;	C14 - C17
14	66	1	1.0870e-01	2.8811e+05 ;	C14 - H33
15	65	1	1.0870e-01	2.8811e+05 ;	C15 - H32
16	17	1	1.3870e-01	4.0033e+05 ;	C16 - C17
16	64	1	1.0870e-01	2.8811e+05 ;	C16 - H31
17	63	1	1.0870e-01	2.8811e+05 ;	C17 - H30
18	30	1	1.3870e-01	4.0033e+05 ;	C18 - C30
18	32	1	1.3870e-01	4.0033e+05 ;	C18 - C32
18	38	1	1.0870e-01	2.8811e+05 ;	C18 - H5
19	20	1	1.5080e-01	2.7472e+05 ;	C19 - C20
19	71	1	1.3450e-01	4.0016e+05 ;	C19 - N1
19	73	1	1.2140e-01	5.4225e+05 ;	C19 - O1
20	21	1	1.5350e-01	2.5363e+05 ;	C20 - C21
20	61	1	1.0920e-01	2.8225e+05 ;	C20 - H28

20	62	1	1.0920e-01	2.8225e+05 ;	C20 - H29
21	22	1	1.5350e-01	2.5363e+05 ;	C21 - C22
21	59	1	1.0920e-01	2.8225e+05 ;	C21 - H26
21	60	1	1.0920e-01	2.8225e+05 ;	C21 - H27
22	23	1	1.5350e-01	2.5363e+05 ;	C22 - C23
22	57	1	1.0920e-01	2.8225e+05 ;	C22 - H24
22	58	1	1.0920e-01	2.8225e+05 ;	C22 - H25
23	24	1	1.5350e-01	2.5363e+05 ;	C23 - C24
23	55	1	1.0920e-01	2.8225e+05 ;	C23 - H22
23	56	1	1.0920e-01	2.8225e+05 ;	C23 - H23
24	25	1	1.5350e-01	2.5363e+05 ;	C24 - C25
24	53	1	1.0920e-01	2.8225e+05 ;	C24 - H20
24	54	1	1.0920e-01	2.8225e+05 ;	C24 - H21
25	26	1	1.5350e-01	2.5363e+05 ;	C25 - C26
25	51	1	1.0920e-01	2.8225e+05 ;	C25 - H18
25	52	1	1.0920e-01	2.8225e+05 ;	C25 - H19
26	27	1	1.5350e-01	2.5363e+05 ;	C26 - C27
26	49	1	1.0920e-01	2.8225e+05 ;	C26 - H16
26	50	1	1.0920e-01	2.8225e+05 ;	C26 - H17
27	28	1	1.5350e-01	2.5363e+05 ;	C27 - C28
27	47	1	1.0920e-01	2.8225e+05 ;	C27 - H14
27	48	1	1.0920e-01	2.8225e+05 ;	C27 - H15
28	29	1	1.5350e-01	2.5363e+05 ;	C28 - C29
28	45	1	1.0920e-01	2.8225e+05 ;	C28 - H12
28	46	1	1.0920e-01	2.8225e+05 ;	C28 - H13
29	43	1	1.0930e-01	2.8108e+05 ;	C29 - H10
29	44	1	1.0930e-01	2.8108e+05 ;	C29 - H11
29	72	1	1.4560e-01	2.8008e+05 ;	C29 - N2
30	33	1	1.3870e-01	4.0033e+05 ;	C30 - C33
30	39	1	1.0870e-01	2.8811e+05 ;	C30 - H6

```
    31     33     1     1.3870e-01     4.0033e+05 ;     C31 - C33
    31     42     1     1.0880e-01     2.8694e+05 ;     C31 - H9
    31     72     1     1.3500e-01     3.9355e+05 ;     C31 - N2
    32     41     1     1.0880e-01     2.8694e+05 ;     C32 - H8
    32     72     1     1.3500e-01     3.9355e+05 ;     C32 - N2
    33     40     1     1.0870e-01     2.8811e+05 ;     C33 - H7
    37     71     1     1.0090e-01     3.4326e+05 ;      H4 - N1

[ pairs ]

;    ai      aj      funct

     1       7       1 ;      C1 - C7
     1       8       1 ;      C1 - C8
     1       9       1 ;      C1 - C9
     1      10       1 ;      C1 - C10
     1      36       1 ;      C1 - H3
     1      65       1 ;      C1 - H32
     2      11       1 ;      C2 - C11
     2      12       1 ;      C2 - C12
     2      13       1 ;      C2 - C13
     2      14       1 ;      C2 - C14
     2      15       1 ;      C2 - C15
     2      16       1 ;      C2 - C16
     2      34       1 ;      C2 - H1
     2      35       1 ;      C2 - H2
     2      70       1 ;      C2 - H37
     3       5       1 ;      C3 - C5
     3       6       1 ;      C3 - C6
     3      12       1 ;      C3 - C12
     3      15       1 ;      C3 - C15
     3      34       1 ;      C3 - H1
     4       5       1 ;      C4 - C5
```

4 6 1 ; C4 - C6

4 11 1 ; C4 - C11

4 16 1 ; C4 - C16

4 70 1 ; C4 - H37

5 8 1 ; C5 - C8

5 9 1 ; C5 - C9

5 36 1 ; C5 - H3

5 67 1 ; C5 - H34

5 68 1 ; C5 - H35

5 69 1 ; C5 - H36

5 71 1 ; C5 - N1

6 7 1 ; C6 - C7

6 10 1 ; C6 - C10

6 17 1 ; C6 - C17

6 64 1 ; C6 - H31

6 65 1 ; C6 - H32

6 66 1 ; C6 - H33

6 67 1 ; C6 - H34

7 13 1 ; C7 - C13

7 19 1 ; C7 - C19

7 35 1 ; C7 - H2

7 37 1 ; C7 - H4

7 70 1 ; C7 - H37

8 15 1 ; C8 - C15

8 16 1 ; C8 - C16

8 35 1 ; C8 - H2

8 63 1 ; C8 - H30

9 13 1 ; C9 - C13

9 14 1 ; C9 - C14

9 34 1 ; C9 - H1

9	63	1 ;	C9 - H30
10	11	1 ;	C10 - C11
10	12	1 ;	C10 - C12
10	14	1 ;	C10 - C14
11	68	1 ;	C11 - H35
11	69	1 ;	C11 - H36
11	71	1 ;	C11 - N1
12	20	1 ;	C12 - C20
12	36	1 ;	C12 - H3
12	73	1 ;	C12 - O1
13	17	1 ;	C13 - C17
13	66	1 ;	C13 - H33
14	64	1 ;	C14 - H31
14	67	1 ;	C14 - H34
15	17	1 ;	C15 - C17
15	64	1 ;	C15 - H31
16	65	1 ;	C16 - H32
16	66	1 ;	C16 - H33
18	29	1 ;	C18 - C29
18	31	1 ;	C18 - C31
18	40	1 ;	C18 - H7
19	22	1 ;	C19 - C22
19	59	1 ;	C19 - H26
19	60	1 ;	C19 - H27
19	68	1 ;	C19 - H35
19	69	1 ;	C19 - H36
20	23	1 ;	C20 - C23
20	37	1 ;	C20 - H4
20	57	1 ;	C20 - H24
20	58	1 ;	C20 - H25

21 24 1 ; C21 - C24

21 55 1 ; C21 - H22

21 56 1 ; C21 - H23

21 71 1 ; C21 - N1

21 73 1 ; C21 - O1

22 25 1 ; C22 - C25

22 53 1 ; C22 - H20

22 54 1 ; C22 - H21

22 61 1 ; C22 - H28

22 62 1 ; C22 - H29

23 26 1 ; C23 - C26

23 51 1 ; C23 - H18

23 52 1 ; C23 - H19

23 59 1 ; C23 - H26

23 60 1 ; C23 - H27

24 27 1 ; C24 - C27

24 49 1 ; C24 - H16

24 50 1 ; C24 - H17

24 57 1 ; C24 - H24

24 58 1 ; C24 - H25

25 28 1 ; C25 - C28

25 47 1 ; C25 - H14

25 48 1 ; C25 - H15

25 55 1 ; C25 - H22

25 56 1 ; C25 - H23

26 29 1 ; C26 - C29

26 45 1 ; C26 - H12

26 46 1 ; C26 - H13

26 53 1 ; C26 - H20

26 54 1 ; C26 - H21

27 43 1 ; C27 - H10

27 44 1 ; C27 - H11

27 51 1 ; C27 - H18

27 52 1 ; C27 - H19

27 72 1 ; C27 - N2

28 31 1 ; C28 - C31

28 32 1 ; C28 - C32

28 49 1 ; C28 - H16

28 50 1 ; C28 - H17

29 33 1 ; C29 - C33

29 41 1 ; C29 - H8

29 42 1 ; C29 - H9

29 47 1 ; C29 - H14

29 48 1 ; C29 - H15

30 41 1 ; C30 - H8

30 42 1 ; C30 - H9

30 72 1 ; C30 - N2

31 39 1 ; C31 - H6

31 41 1 ; C31 - H8

31 43 1 ; C31 - H10

31 44 1 ; C31 - H11

32 33 1 ; C32 - C33

32 39 1 ; C32 - H6

32 42 1 ; C32 - H9

32 43 1 ; C32 - H10

32 44 1 ; C32 - H11

33 38 1 ; C33 - H5

34 65 1 ; H1 - H32

35 67 1 ; H2 - H34

36 70 1 ; H3 - H37

37	68	1 ;	H4 - H35
37	69	1 ;	H4 - H36
37	73	1 ;	H4 - O1
38	39	1 ;	H5 - H6
38	41	1 ;	H5 - H8
38	72	1 ;	H5 - N2
39	40	1 ;	H6 - H7
40	42	1 ;	H7 - H9
40	72	1 ;	H7 - N2
43	45	1 ;	H10 - H12
43	46	1 ;	H10 - H13
44	45	1 ;	H11 - H12
44	46	1 ;	H11 - H13
45	47	1 ;	H12 - H14
45	48	1 ;	H12 - H15
45	72	1 ;	H12 - N2
46	47	1 ;	H13 - H14
46	48	1 ;	H13 - H15
46	72	1 ;	H13 - N2
47	49	1 ;	H14 - H16
47	50	1 ;	H14 - H17
48	49	1 ;	H15 - H16
48	50	1 ;	H15 - H17
49	51	1 ;	H16 - H18
49	52	1 ;	H16 - H19
50	51	1 ;	H17 - H18
50	52	1 ;	H17 - H19
51	53	1 ;	H18 - H20
51	54	1 ;	H18 - H21
52	53	1 ;	H19 - H20

```
    52      54      1 ;     H19 - H21
    53      55      1 ;     H20 - H22
    53      56      1 ;     H20 - H23
    54      55      1 ;     H21 - H22
    54      56      1 ;     H21 - H23
    55      57      1 ;     H22 - H24
    55      58      1 ;     H22 - H25
    56      57      1 ;     H23 - H24
    56      58      1 ;     H23 - H25
    57      59      1 ;     H24 - H26
    57      60      1 ;     H24 - H27
    58      59      1 ;     H25 - H26
    58      60      1 ;     H25 - H27
    59      61      1 ;     H26 - H28
    59      62      1 ;     H26 - H29
    60      61      1 ;     H27 - H28
    60      62      1 ;     H27 - H29
    61      71      1 ;     H28 - N1
    61      73      1 ;     H28 - O1
    62      71      1 ;     H29 - N1
    62      73      1 ;     H29 - O1
    63      64      1 ;     H30 - H31
    63      66      1 ;     H30 - H33
[ angles ]
;   ai      aj      ak      funct   theta           cth
     1       2       5       1     1.1997e+02    5.6233e+02 ;     C1 - C2   - C5
     1       2       6       1     1.1997e+02    5.6233e+02 ;     C1 - C2   - C6
     1       3      11       1     1.1997e+02    5.6233e+02 ;     C1 - C3   - C11
     1       3      70       1     1.2001e+02    4.0585e+02 ;     C1 - C3   - H37
     1       4      15       1     1.1997e+02    5.6233e+02 ;     C1 - C4   - C15
```

1	4	34	1	1.2001e+02	4.0585e+02 ;	C1 - C4 - H1
2	1	3	1	1.1997e+02	5.6233e+02 ;	C2 - C1 - C3
2	1	4	1	1.1997e+02	5.6233e+02 ;	C2 - C1 - C4
2	5	7	1	1.1997e+02	5.6233e+02 ;	C2 - C5 - C7
2	5	10	1	1.1997e+02	5.6233e+02 ;	C2 - C5 - C10
2	6	8	1	1.1997e+02	5.6233e+02 ;	C2 - C6 - C8
2	6	9	1	1.1997e+02	5.6233e+02 ;	C2 - C6 - C9
3	1	4	1	1.1997e+02	5.6233e+02 ;	C3 - C1 - C4
3	11	7	1	1.1997e+02	5.6233e+02 ;	C3 - C11 - C7
3	11	36	1	1.2001e+02	4.0585e+02 ;	C3 - C11 - H3
4	15	9	1	1.1997e+02	5.6233e+02 ;	C4 - C15 - C9
4	15	65	1	1.2001e+02	4.0585e+02 ;	C4 - C15 - H32
5	2	6	1	1.1997e+02	5.6233e+02 ;	C5 - C2 - C6
5	7	11	1	1.1997e+02	5.6233e+02 ;	C5 - C7 - C11
5	7	12	1	1.2063e+02	5.3388e+02 ;	C5 - C7 - C12
5	10	13	1	1.1997e+02	5.6233e+02 ;	C5 - C10 - C13
5	10	35	1	1.2001e+02	4.0585e+02 ;	C5 - C10 - H2
6	8	13	1	1.1997e+02	5.6233e+02 ;	C6 - C8 - C13
6	8	14	1	1.1997e+02	5.6233e+02 ;	C6 - C8 - C14
6	9	15	1	1.1997e+02	5.6233e+02 ;	C6 - C9 - C15
6	9	16	1	1.1997e+02	5.6233e+02 ;	C6 - C9 - C16
7	5	10	1	1.1997e+02	5.6233e+02 ;	C7 - C5 - C10
7	11	36	1	1.2001e+02	4.0585e+02 ;	C7 - C11 - H3
7	12	68	1	1.1095e+02	3.9162e+02 ;	C7 - C12 - H35
7	12	69	1	1.1095e+02	3.9162e+02 ;	C7 - C12 - H36
7	12	71	1	1.1314e+02	5.5026e+02 ;	C7 - C12 - N1
8	6	9	1	1.1997e+02	5.6233e+02 ;	C8 - C6 - C9
8	13	10	1	1.1997e+02	5.6233e+02 ;	C8 - C13 - C10
8	13	67	1	1.2001e+02	4.0585e+02 ;	C8 - C13 - H34
8	14	17	1	1.1997e+02	5.6233e+02 ;	C8 - C14 - C17

8	14	66	1	1.2001e+02	4.0585e+02 ;	C8 - C14 - H33
9	15	65	1	1.2001e+02	4.0585e+02 ;	C9 - C15 - H32
9	16	17	1	1.1997e+02	5.6233e+02 ;	C9 - C16 - C17
9	16	64	1	1.2001e+02	4.0585e+02 ;	C9 - C16 - H31
10	13	67	1	1.2001e+02	4.0585e+02 ;	C10 - C13 - H34
11	3	70	1	1.2001e+02	4.0585e+02 ;	C11 - C3 - H37
11	7	12	1	1.2063e+02	5.3388e+02 ;	C11 - C7 - C12
12	71	19	1	1.2135e+02	5.3472e+02 ;	C12 - N1 - C19
12	71	37	1	1.1678e+02	3.8493e+02 ;	C12 - N1 - H4
13	8	14	1	1.1997e+02	5.6233e+02 ;	C13 - C8 - C14
13	10	35	1	1.2001e+02	4.0585e+02 ;	C13 - C10 - H2
14	17	16	1	1.1997e+02	5.6233e+02 ;	C14 - C17 - C16
14	17	63	1	1.2001e+02	4.0585e+02 ;	C14 - C17 - H30
15	4	34	1	1.2001e+02	4.0585e+02 ;	C15 - C4 - H1
15	9	16	1	1.1997e+02	5.6233e+02 ;	C15 - C9 - C16
16	17	63	1	1.2001e+02	4.0585e+02 ;	C16 - C17 - H30
17	14	66	1	1.2001e+02	4.0585e+02 ;	C17 - C14 - H33
17	16	64	1	1.2001e+02	4.0585e+02 ;	C17 - C16 - H31
18	30	33	1	1.1997e+02	5.6233e+02 ;	C18 - C30 - C33
18	30	39	1	1.2001e+02	4.0585e+02 ;	C18 - C30 - H6
18	32	41	1	1.2109e+02	4.0334e+02 ;	C18 - C32 - H8
18	32	72	1	1.1834e+02	5.8743e+02 ;	C18 - C32 - N2
19	20	21	1	1.1053e+02	5.3388e+02 ;	C19 - C20 - C21
19	20	61	1	1.0968e+02	3.9497e+02 ;	C19 - C20 - H28
19	20	62	1	1.0968e+02	3.9497e+02 ;	C19 - C20 - H29
19	71	37	1	1.1846e+02	4.1171e+02 ;	C19 - N1 - H4
20	19	71	1	1.1515e+02	5.6819e+02 ;	C20 - C19 - N1
20	19	73	1	1.2311e+02	5.6902e+02 ;	C20 - C19 - O1
20	21	22	1	1.1063e+02	5.2886e+02 ;	C20 - C21 - C22
20	21	59	1	1.1005e+02	3.8828e+02 ;	C20 - C21 - H26

20	21	60	1	1.1005e+02	3.8828e+02 ;	C20 - C21 - H27
21	20	61	1	1.1005e+02	3.8828e+02 ;	C21 - C20 - H28
21	20	62	1	1.1005e+02	3.8828e+02 ;	C21 - C20 - H29
21	22	23	1	1.1063e+02	5.2886e+02 ;	C21 - C22 - C23
21	22	57	1	1.1005e+02	3.8828e+02 ;	C21 - C22 - H24
21	22	58	1	1.1005e+02	3.8828e+02 ;	C21 - C22 - H25
22	21	59	1	1.1005e+02	3.8828e+02 ;	C22 - C21 - H26
22	21	60	1	1.1005e+02	3.8828e+02 ;	C22 - C21 - H27
22	23	24	1	1.1063e+02	5.2886e+02 ;	C22 - C23 - C24
22	23	55	1	1.1005e+02	3.8828e+02 ;	C22 - C23 - H22
22	23	56	1	1.1005e+02	3.8828e+02 ;	C22 - C23 - H23
23	22	57	1	1.1005e+02	3.8828e+02 ;	C23 - C22 - H24
23	22	58	1	1.1005e+02	3.8828e+02 ;	C23 - C22 - H25
23	24	25	1	1.1063e+02	5.2886e+02 ;	C23 - C24 - C25
23	24	53	1	1.1005e+02	3.8828e+02 ;	C23 - C24 - H20
23	24	54	1	1.1005e+02	3.8828e+02 ;	C23 - C24 - H21
24	23	55	1	1.1005e+02	3.8828e+02 ;	C24 - C23 - H22
24	23	56	1	1.1005e+02	3.8828e+02 ;	C24 - C23 - H23
24	25	26	1	1.1063e+02	5.2886e+02 ;	C24 - C25 - C26
24	25	51	1	1.1005e+02	3.8828e+02 ;	C24 - C25 - H18
24	25	52	1	1.1005e+02	3.8828e+02 ;	C24 - C25 - H19
25	24	53	1	1.1005e+02	3.8828e+02 ;	C25 - C24 - H20
25	24	54	1	1.1005e+02	3.8828e+02 ;	C25 - C24 - H21
25	26	27	1	1.1063e+02	5.2886e+02 ;	C25 - C26 - C27
25	26	49	1	1.1005e+02	3.8828e+02 ;	C25 - C26 - H16
25	26	50	1	1.1005e+02	3.8828e+02 ;	C25 - C26 - H17
26	25	51	1	1.1005e+02	3.8828e+02 ;	C26 - C25 - H18
26	25	52	1	1.1005e+02	3.8828e+02 ;	C26 - C25 - H19
26	27	28	1	1.1063e+02	5.2886e+02 ;	C26 - C27 - C28
26	27	47	1	1.1005e+02	3.8828e+02 ;	C26 - C27 - H14

26	27	48	1	1.1005e+02	3.8828e+02 ;	C26 - C27 - H15
27	26	49	1	1.1005e+02	3.8828e+02 ;	C27 - C26 - H16
27	26	50	1	1.1005e+02	3.8828e+02 ;	C27 - C26 - H17
27	28	29	1	1.1063e+02	5.2886e+02 ;	C27 - C28 - C29
27	28	45	1	1.1005e+02	3.8828e+02 ;	C27 - C28 - H12
27	28	46	1	1.1005e+02	3.8828e+02 ;	C27 - C28 - H13
28	27	47	1	1.1005e+02	3.8828e+02 ;	C28 - C27 - H14
28	27	48	1	1.1005e+02	3.8828e+02 ;	C28 - C27 - H15
28	29	43	1	1.1007e+02	3.8828e+02 ;	C28 - C29 - H10
28	29	44	1	1.1007e+02	3.8828e+02 ;	C28 - C29 - H11
28	29	72	1	1.1259e+02	5.5061e+02 ;	C28 - C29 - N2
29	28	45	1	1.1005e+02	3.8828e+02 ;	C29 - C28 - H12
29	28	46	1	1.1005e+02	3.8828e+02 ;	C29 - C28 - H13
29	72	31	1	1.2436e+02	5.2802e+02 ;	C29 - N2 - C31
29	72	32	1	1.2436e+02	5.2802e+02 ;	C29 - N2 - C32
30	18	32	1	1.1997e+02	5.6233e+02 ;	C30 - C18 - C32
30	18	38	1	1.2001e+02	4.0585e+02 ;	C30 - C18 - H5
30	33	31	1	1.1997e+02	5.6233e+02 ;	C30 - C33 - C31
30	33	40	1	1.2001e+02	4.0585e+02 ;	C30 - C33 - H7
31	33	40	1	1.2001e+02	4.0585e+02 ;	C31 - C33 - H7
31	72	32	1	1.1980e+02	5.6149e+02 ;	C31 - N2 - C32
32	18	38	1	1.2001e+02	4.0585e+02 ;	C32 - C18 - H5
33	30	39	1	1.2001e+02	4.0585e+02 ;	C33 - C30 - H6
33	31	42	1	1.2109e+02	4.0334e+02 ;	C33 - C31 - H9
33	31	72	1	1.1834e+02	5.8743e+02 ;	C33 - C31 - N2
41	32	72	1	1.1465e+02	4.3430e+02 ;	H8 - C32 - N2
42	31	72	1	1.1465e+02	4.3430e+02 ;	H9 - C31 - N2
43	29	44	1	1.0955e+02	3.2803e+02 ;	H10 - C29 - H11
43	29	72	1	1.0945e+02	4.1756e+02 ;	H10 - C29 - N2
44	29	72	1	1.0945e+02	4.1756e+02 ;	H11 - C29 - N2

```
    45      28      46      1       1.0835e+02      3.2970e+02 ;    H12 - C28 - H13
    47      27      48      1       1.0835e+02      3.2970e+02 ;    H14 - C27 - H15
    49      26      50      1       1.0835e+02      3.2970e+02 ;    H16 - C26 - H17
    51      25      52      1       1.0835e+02      3.2970e+02 ;    H18 - C25 - H19
    53      24      54      1       1.0835e+02      3.2970e+02 ;    H20 - C24 - H21
    55      23      56      1       1.0835e+02      3.2970e+02 ;    H22 - C23 - H23
    57      22      58      1       1.0835e+02      3.2970e+02 ;    H24 - C22 - H25
    59      21      60      1       1.0835e+02      3.2970e+02 ;    H26 - C21 - H27
    61      20      62      1       1.0835e+02      3.2970e+02 ;    H28 - C20 - H29
    68      12      69      1       1.0955e+02      3.2803e+02 ;    H35 - C12 - H36
    68      12      71      1       1.0932e+02      4.1673e+02 ;    H35 - C12 - N1
    69      12      71      1       1.0932e+02      4.1673e+02 ;    H36 - C12 - N1
    71      19      73      1       1.2203e+02      6.3429e+02 ;     N1 - C19 - O1

[ dihedrals ] ; propers

;i      j       k       l       func    C0          C1          C2          C3          C4          C5
  1     2       5       7       3       30.33400    0.00000 -30.33400   0.00000     0.00000     0.00000 ; C1- C2- C5- C7
  1     2       5       10      3       30.33400    0.00000 -30.33400   0.00000     0.00000     0.00000 ; C1- C2- C5-C10
  1     2       6       8       3       30.33400    0.00000 -30.33400   0.00000     0.00000     0.00000 ; C1- C2- C6- C8
  1     2       6       9       3       30.33400    0.00000 -30.33400   0.00000     0.00000     0.00000 ; C1- C2- C6- C9
  1     3       11      7       3       30.33400    0.00000 -30.33400   0.00000     0.00000     0.00000 ; C1- C3-C11- C7
  1     3       11      36      3       30.33400    0.00000 -30.33400   0.00000     0.00000     0.00000 ; C1- C3-C11- H3
  1     4       15      9       3       30.33400    0.00000 -30.33400   0.00000     0.00000     0.00000 ; C1- C4-C15- C9
  1     4       15      65      3       30.33400    0.00000 -30.33400   0.00000     0.00000     0.00000 ; C1- C4-C15-H32
  2     1       3       11      3       30.33400    0.00000 -30.33400   0.00000     0.00000     0.00000 ; C2- C1- C3-C11
  2     1       3       70      3       30.33400    0.00000 -30.33400   0.00000     0.00000     0.00000 ; C2- C1- C3-H37
  2     1       4       15      3       30.33400    0.00000 -30.33400   0.00000     0.00000     0.00000 ; C2- C1- C4-C15
  2     1       4       34      3       30.33400    0.00000 -30.33400   0.00000     0.00000     0.00000 ; C2- C1- C4- H1
  2     5       7       11      3       30.33400    0.00000 -30.33400   0.00000     0.00000     0.00000 ; C2- C5- C7-C11
  2     5       7       12      3       30.33400    0.00000 -30.33400   0.00000     0.00000     0.00000 ; C2- C5- C7-C12
  2     5       10      13      3       30.33400    0.00000 -30.33400   0.00000     0.00000     0.00000 ; C2- C5-C10-C13
```

2 5 10 35 3 30.33400 0.00000 -30.33400 0.00000 0.00000 0.00000 ; C2- C5-C10- H2

2 6 8 13 3 30.33400 0.00000 -30.33400 0.00000 0.00000 0.00000 ; C2- C6- C8-C13

2 6 8 14 3 30.33400 0.00000 -30.33400 0.00000 0.00000 0.00000 ; C2- C6- C8-C14

2 6 9 15 3 30.33400 0.00000 -30.33400 0.00000 0.00000 0.00000 ; C2- C6- C9-C15

2 6 9 16 3 30.33400 0.00000 -30.33400 0.00000 0.00000 0.00000 ; C2- C6- C9-C16

3 1 2 5 3 30.33400 0.00000 -30.33400 0.00000 0.00000 0.00000 ; C3- C1- C2- C5

3 1 2 6 3 30.33400 0.00000 -30.33400 0.00000 0.00000 0.00000 ; C3- C1- C2- C6

3 1 4 15 3 30.33400 0.00000 -30.33400 0.00000 0.00000 0.00000 ; C3- C1- C4-C15

3 1 4 34 3 30.33400 0.00000 -30.33400 0.00000 0.00000 0.00000 ; C3- C1- C4- H1

3 11 7 5 3 30.33400 0.00000 -30.33400 0.00000 0.00000 0.00000 ; C3-C11- C7- C5

3 11 7 12 3 30.33400 0.00000 -30.33400 0.00000 0.00000 0.00000 ; C3-C11- C7-C12

4 1 2 5 3 30.33400 0.00000 -30.33400 0.00000 0.00000 0.00000 ; C4- C1- C2- C5

4 1 2 6 3 30.33400 0.00000 -30.33400 0.00000 0.00000 0.00000 ; C4- C1- C2- C6

4 1 3 11 3 30.33400 0.00000 -30.33400 0.00000 0.00000 0.00000 ; C4- C1- C3-C11

4 1 3 70 3 30.33400 0.00000 -30.33400 0.00000 0.00000 0.00000 ; C4- C1- C3-H37

4 15 9 6 3 30.33400 0.00000 -30.33400 0.00000 0.00000 0.00000 ; C4-C15- C9- C6

4 15 9 16 3 30.33400 0.00000 -30.33400 0.00000 0.00000 0.00000 ; C4-C15- C9-C16

5 2 6 8 3 30.33400 0.00000 -30.33400 0.00000 0.00000 0.00000 ; C5- C2- C6- C8

5 2 6 9 3 30.33400 0.00000 -30.33400 0.00000 0.00000 0.00000 ; C5- C2- C6- C9

5 7 11 36 3 30.33400 0.00000 -30.33400 0.00000 0.00000 0.00000 ; C5- C7-C11- H3

5 7 12 68 3 0.00000 0.00000 0.00000 0.00000 0.00000 0.00000 ; C5- C7-C12-H35

5 7 12 69 3 0.00000 0.00000 0.00000 0.00000 0.00000 0.00000 ; C5- C7-C12-H36

5 7 12 71 3 0.00000 0.00000 0.00000 0.00000 0.00000 0.00000 ; C5- C7-C12- N1

5 10 13 8 3 30.33400 0.00000 -30.33400 0.00000 0.00000 0.00000 ; C5-C10-C13- C8

5 10 13 67 3 30.33400 0.00000 -30.33400 0.00000 0.00000 0.00000 ; C5-C10-C13-H34

6 2 5 7 3 30.33400 0.00000 -30.33400 0.00000 0.00000 0.00000 ; C6- C2- C5- C7

6 2 5 10 3 30.33400 0.00000 -30.33400 0.00000 0.00000 0.00000 ; C6- C2- C5-C10

6 8 13 10 3 30.33400 0.00000 -30.33400 0.00000 0.00000 0.00000 ; C6- C8-C13-C10

6 8 13 67 3 30.33400 0.00000 -30.33400 0.00000 0.00000 0.00000 ; C6- C8-C13-H34

6 8 14 17 3 30.33400 0.00000 -30.33400 0.00000 0.00000 0.00000 ; C6- C8-C14-C17

6 8 14 66 3 30.33400 0.00000 -30.33400 0.00000 0.00000 0.00000 ; C6- C8-C14-H33

6 9 15 65 3 30.33400 0.00000 -30.33400 0.00000 0.00000 0.00000 ; C6- C9-C15-H32

6 9 16 17 3 30.33400 0.00000 -30.33400 0.00000 0.00000 0.00000 ; C6- C9-C16-C17

6 9 16 64 3 30.33400 0.00000 -30.33400 0.00000 0.00000 0.00000 ; C6- C9-C16-H31

7 5 10 13 3 30.33400 0.00000 -30.33400 0.00000 0.00000 0.00000 ; C7- C5-C10-C13

7 5 10 35 3 30.33400 0.00000 -30.33400 0.00000 0.00000 0.00000 ; C7- C5-C10- H2

7 11 3 70 3 30.33400 0.00000 -30.33400 0.00000 0.00000 0.00000 ; C7-C11- C3-H37

7 12 71 19 3 0.00000 0.00000 0.00000 0.00000 0.00000 0.00000 ; C7-C12- N1-C19

7 12 71 37 3 0.00000 0.00000 0.00000 0.00000 0.00000 0.00000 ; C7-C12- N1- H4

8 6 9 15 3 30.33400 0.00000 -30.33400 0.00000 0.00000 0.00000 ; C8- C6- C9-C15

8 6 9 16 3 30.33400 0.00000 -30.33400 0.00000 0.00000 0.00000 ; C8- C6- C9-C16

8 13 10 35 3 30.33400 0.00000 -30.33400 0.00000 0.00000 0.00000 ; C8-C13-C10- H2

8 14 17 16 3 30.33400 0.00000 -30.33400 0.00000 0.00000 0.00000 ; C8-C14-C17-C16

8 14 17 63 3 30.33400 0.00000 -30.33400 0.00000 0.00000 0.00000 ; C8-C14-C17-H30

9 6 8 13 3 30.33400 0.00000 -30.33400 0.00000 0.00000 0.00000 ; C9- C6- C8-C13

9 6 8 14 3 30.33400 0.00000 -30.33400 0.00000 0.00000 0.00000 ; C9- C6- C8-C14

9 15 4 34 3 30.33400 0.00000 -30.33400 0.00000 0.00000 0.00000 ; C9-C15- C4- H1

9 16 17 14 3 30.33400 0.00000 -30.33400 0.00000 0.00000 0.00000 ; C9-C16-C17-C14

9 16 17 63 3 30.33400 0.00000 -30.33400 0.00000 0.00000 0.00000 ; C9-C16-C17-H30

10 5 7 11 3 30.33400 0.00000 -30.33400 0.00000 0.00000 0.00000 ;C10- C5- C7-C11

10 5 7 12 3 30.33400 0.00000 -30.33400 0.00000 0.00000 0.00000 ;C10- C5- C7-C12

10 13 8 14 3 30.33400 0.00000 -30.33400 0.00000 0.00000 0.00000 ;C10-C13- C8-C14

11 7 12 68 3 0.00000 0.00000 0.00000 0.00000 0.00000 0.00000 ;C11- C7-C12-H35

11 7 12 69 3 0.00000 0.00000 0.00000 0.00000 0.00000 0.00000 ;C11- C7-C12-H36

11 7 12 71 3 0.00000 0.00000 0.00000 0.00000 0.00000 0.00000 ;C11- C7-C12- N1

12 7 11 36 3 30.33400 0.00000 -30.33400 0.00000 0.00000 0.00000 ;C12- C7-C11- H3

12 71 19 20 3 20.92000 0.00000 -20.92000 0.00000 0.00000 0.00000 ;C12- N1-C19-C20

12 71 19 73 3 20.92000 0.00000 -20.92000 0.00000 0.00000 0.00000 ;C12- N1-C19- O1

13 8 14 17 3 30.33400 0.00000 -30.33400 0.00000 0.00000 0.00000 ;C13- C8-C14-C17

13 8 14 66 3 30.33400 0.00000 -30.33400 0.00000 0.00000 0.00000 ;C13- C8-C14-H33

14 8 13 67 3 30.33400 0.00000 -30.33400 0.00000 0.00000 0.00000 ;C14- C8-C13-H34

14 17 16 64 3 30.33400 0.00000 -30.33400 0.00000 0.00000 0.00000 ;C14-C17-C16-H31

15 9 16 17 3 30.33400 0.00000 -30.33400 0.00000 0.00000 0.00000 ;C15- C9-C16-C17

15 9 16 64 3 30.33400 0.00000 -30.33400 0.00000 0.00000 0.00000 ;C15- C9-C16-H31

16 9 15 65 3 30.33400 0.00000 -30.33400 0.00000 0.00000 0.00000 ;C16- C9-C15-H32

16 17 14 66 3 30.33400 0.00000 -30.33400 0.00000 0.00000 0.00000 ;C16-C17-C14-H33

18 30 33 31 3 30.33400 0.00000 -30.33400 0.00000 0.00000 0.00000 ;C18-C30-C33-C31

18 30 33 40 3 30.33400 0.00000 -30.33400 0.00000 0.00000 0.00000 ;C18-C30-C33- H7

18 32 72 29 3 2.51040 0.00000 -2.51040 0.00000 0.00000 0.00000 ;C18-C32- N2-C29

18 32 72 31 3 2.51040 0.00000 -2.51040 0.00000 0.00000 0.00000 ;C18-C32- N2-C31

19 20 21 22 3 0.65084 1.95253 0.00000 -2.60338 0.00000 0.00000 ;C19-C20-C21-C22

19 20 21 59 3 0.65084 1.95253 0.00000 -2.60338 0.00000 0.00000 ;C19-C20-C21-H26

19 20 21 60 3 0.65084 1.95253 0.00000 -2.60338 0.00000 0.00000 ;C19-C20-C21-H27

19 71 12 68 3 0.00000 0.00000 0.00000 0.00000 0.00000 0.00000 ;C19- N1-C12-H35

19 71 12 69 3 0.00000 0.00000 0.00000 0.00000 0.00000 0.00000 ;C19- N1-C12-H36

20 19 71 37 3 20.92000 0.00000 -20.92000 0.00000 0.00000 0.00000 ;C20-C19- N1- H4

20 21 22 23 3 3.68192 3.09616 -2.09200 -3.01248 0.00000 0.00000 ;C20-C21-C22-C23

20 21 22 57 3 0.66944 2.00832 0.00000 -2.67776 0.00000 0.00000 ;C20-C21-C22-H24

20 21 22 58 3 0.66944 2.00832 0.00000 -2.67776 0.00000 0.00000 ;C20-C21-C22-H25

21 20 19 71 3 0.83680 0.00000 -2.76144 0.00000 3.34720 0.00000 ;C21-C20-C19- N1

21 20 19 73 3 0.00000 0.00000 0.00000 0.00000 0.00000 0.00000 ;C21-C20-C19- O1

21 22 23 24 3 3.68192 3.09616 -2.09200 -3.01248 0.00000 0.00000 ;C21-C22-C23-C24

21 22 23 55 3 0.66944 2.00832 0.00000 -2.67776 0.00000 0.00000 ;C21-C22-C23-H22

21 22 23 56 3 0.66944 2.00832 0.00000 -2.67776 0.00000 0.00000 ;C21-C22-C23-H23

22 21 20 61 3 0.66944 2.00832 0.00000 -2.67776 0.00000 0.00000 ;C22-C21-C20-H28

22 21 20 62 3 0.66944 2.00832 0.00000 -2.67776 0.00000 0.00000 ;C22-C21-C20-H29

22 23 24 25 3 3.68192 3.09616 -2.09200 -3.01248 0.00000 0.00000 ;C22-C23-C24-C25

22 23 24 53 3 0.66944 2.00832 0.00000 -2.67776 0.00000 0.00000 ;C22-C23-C24-H20

22 23 24 54 3 0.66944 2.00832 0.00000 -2.67776 0.00000 0.00000 ;C22-C23-C24-H21

23 22 21 59 3 0.66944 2.00832 0.00000 -2.67776 0.00000 0.00000 ;C23-C22-C21-H26

23 22 21 60 3 0.66944 2.00832 0.00000 -2.67776 0.00000 0.00000 ;C23-C22-C21-H27

23 24 25 26 3 3.68192 3.09616 -2.09200 -3.01248 0.00000 0.00000 ;C23-C24-C25-C26

23 24 25 51 3 0.66944 2.00832 0.00000 -2.67776 0.00000 0.00000 ;C23-C24-C25-H18

23 24 25 52 3 0.66944 2.00832 0.00000 -2.67776 0.00000 0.00000 ;C23-C24-C25-H19

24 23 22 57 3 0.66944 2.00832 0.00000 -2.67776 0.00000 0.00000 ;C24-C23-C22-H24

24 23 22 58 3 0.66944 2.00832 0.00000 -2.67776 0.00000 0.00000 ;C24-C23-C22-H25

24 25 26 27 3 3.68192 3.09616 -2.09200 -3.01248 0.00000 0.00000 ;C24-C25-C26-C27

24 25 26 49 3 0.66944 2.00832 0.00000 -2.67776 0.00000 0.00000 ;C24-C25-C26-H16

24 25 26 50 3 0.66944 2.00832 0.00000 -2.67776 0.00000 0.00000 ;C24-C25-C26-H17

25 24 23 55 3 0.66944 2.00832 0.00000 -2.67776 0.00000 0.00000 ;C25-C24-C23-H22

25 24 23 56 3 0.66944 2.00832 0.00000 -2.67776 0.00000 0.00000 ;C25-C24-C23-H23

25 26 27 28 3 3.68192 3.09616 -2.09200 -3.01248 0.00000 0.00000 ;C25-C26-C27-C28

25 26 27 47 3 0.66944 2.00832 0.00000 -2.67776 0.00000 0.00000 ;C25-C26-C27-H14

25 26 27 48 3 0.66944 2.00832 0.00000 -2.67776 0.00000 0.00000 ;C25-C26-C27-H15

26 25 24 53 3 0.66944 2.00832 0.00000 -2.67776 0.00000 0.00000 ;C26-C25-C24-H20

26 25 24 54 3 0.66944 2.00832 0.00000 -2.67776 0.00000 0.00000 ;C26-C25-C24-H21

26 27 28 29 3 3.68192 3.09616 -2.09200 -3.01248 0.00000 0.00000 ;C26-C27-C28-C29

26 27 28 45 3 0.66944 2.00832 0.00000 -2.67776 0.00000 0.00000 ;C26-C27-C28-H12

26 27 28 46 3 0.66944 2.00832 0.00000 -2.67776 0.00000 0.00000 ;C26-C27-C28-H13

27 26 25 51 3 0.66944 2.00832 0.00000 -2.67776 0.00000 0.00000 ;C27-C26-C25-H18

27 26 25 52 3 0.66944 2.00832 0.00000 -2.67776 0.00000 0.00000 ;C27-C26-C25-H19

27 28 29 43 3 0.65084 1.95253 0.00000 -2.60338 0.00000 0.00000 ;C27-C28-C29-H10

27 28 29 44 3 0.65084 1.95253 0.00000 -2.60338 0.00000 0.00000 ;C27-C28-C29-H11

27 28 29 72 3 0.65084 1.95253 0.00000 -2.60338 0.00000 0.00000 ;C27-C28-C29- N2

28 27 26 49 3 0.66944 2.00832 0.00000 -2.67776 0.00000 0.00000 ;C28-C27-C26-H16

28 27 26 50 3 0.66944 2.00832 0.00000 -2.67776 0.00000 0.00000 ;C28-C27-C26-H17

28 29 72 31 3 0.00000 0.00000 0.00000 0.00000 0.00000 0.00000 ;C28-C29- N2-C31

28 29 72 32 3 0.00000 0.00000 0.00000 0.00000 0.00000 0.00000 ;C28-C29- N2-C32

29 28 27 47 3 0.66944 2.00832 0.00000 -2.67776 0.00000 0.00000 ;C29-C28-C27-H14

29 28 27 48 3 0.66944 2.00832 0.00000 -2.67776 0.00000 0.00000 ;C29-C28-C27-H15

29 72 31 33 3 2.51040 0.00000 -2.51040 0.00000 0.00000 0.00000 ;C29- N2-C31-C33

29 72 31 42 3 2.51040 0.00000 -2.51040 0.00000 0.00000 0.00000 ;C29- N2-C31- H9

29 72 32 41 3 2.51040 0.00000 -2.51040 0.00000 0.00000 0.00000 ;C29- N2-C32- H8

30 18 32 41 3 30.33400 0.00000 -30.33400 0.00000 0.00000 0.00000 ;C30-C18-C32- H8

30 18 32 72 3 30.33400 0.00000 -30.33400 0.00000 0.00000 0.00000 ;C30-C18-C32- N2

30 33 31 42 3 30.33400 0.00000 -30.33400 0.00000 0.00000 0.00000 ;C30-C33-C31- H9

30 33 31 72 3 30.33400 0.00000 -30.33400 0.00000 0.00000 0.00000 ;C30-C33-C31- N2

31 33 30 39 3 30.33400 0.00000 -30.33400 0.00000 0.00000 0.00000 ;C31-C33-C30- H6

31 72 29 43 3 0.00000 0.00000 0.00000 0.00000 0.00000 0.00000 ;C31- N2-C29-H10

31 72 29 44 3 0.00000 0.00000 0.00000 0.00000 0.00000 0.00000 ;C31- N2-C29-H11

31 72 32 41 3 2.51040 0.00000 -2.51040 0.00000 0.00000 0.00000 ;C31- N2-C32- H8

32 18 30 33 3 30.33400 0.00000 -30.33400 0.00000 0.00000 0.00000 ;C32-C18-C30-C33

32 18 30 39 3 30.33400 0.00000 -30.33400 0.00000 0.00000 0.00000 ;C32-C18-C30- H6

32 72 29 43 3 0.00000 0.00000 0.00000 0.00000 0.00000 0.00000 ;C32- N2-C29-H10

32 72 29 44 3 0.00000 0.00000 0.00000 0.00000 0.00000 0.00000 ;C32- N2-C29-H11

32 72 31 33 3 2.51040 0.00000 -2.51040 0.00000 0.00000 0.00000 ;C32- N2-C31-C33

32 72 31 42 3 2.51040 0.00000 -2.51040 0.00000 0.00000 0.00000 ;C32- N2-C31- H9

33 30 18 38 3 30.33400 0.00000 -30.33400 0.00000 0.00000 0.00000 ;C33-C30-C18- H5

34 4 15 65 3 30.33400 0.00000 -30.33400 0.00000 0.00000 0.00000 ; H1- C4-C15-H32

35 10 13 67 3 30.33400 0.00000 -30.33400 0.00000 0.00000 0.00000 ; H2-C10-C13-H34

36 11 3 70 3 30.33400 0.00000 -30.33400 0.00000 0.00000 0.00000 ; H3-C11- C3-H37

37 71 12 68 3 0.00000 0.00000 0.00000 0.00000 0.00000 0.00000 ; H4- N1-C12-H35

37 71 12 69 3 0.00000 0.00000 0.00000 0.00000 0.00000 0.00000 ; H4- N1-C12-H36

37 71 19 73 3 29.28800 -8.36800 -20.92000 0.00000 0.00000 0.00000 ; H4- N1-C19- O1

38 18 30 39 3 30.33400 0.00000 -30.33400 0.00000 0.00000 0.00000 ; H5-C18-C30- H6

38 18 32 41 3 30.33400 0.00000 -30.33400 0.00000 0.00000 0.00000 ; H5-C18-C32- H8

38 18 32 72 3 30.33400 0.00000 -30.33400 0.00000 0.00000 0.00000 ; H5-C18-C32- N2

39 30 33 40 3 30.33400 0.00000 -30.33400 0.00000 0.00000 0.00000 ; H6-C30-C33- H7

40 33 31 42 3 30.33400 0.00000 -30.33400 0.00000 0.00000 0.00000 ; H7-C33-C31- H9

40 33 31 72 3 30.33400 0.00000 -30.33400 0.00000 0.00000 0.00000 ; H7-C33-C31- N2

43 29 28 45 3 0.65084 1.95253 0.00000 -2.60338 0.00000 0.00000 ;H10-C29-C28-H12

43 29 28 46 3 0.65084 1.95253 0.00000 -2.60338 0.00000 0.00000 ;H10-C29-C28-H13

44 29 28 45 3 0.65084 1.95253 0.00000 -2.60338 0.00000 0.00000 ;H11-C29-C28-H12

44 29 28 46 3 0.65084 1.95253 0.00000 -2.60338 0.00000 0.00000 ;H11-C29-C28-H13

45 28 27 47 3 0.62760 1.88280 0.00000 -2.51040 0.00000 0.00000 ;H12-C28-C27-H14

45 28 27 48 3 0.62760 1.88280 0.00000 -2.51040 0.00000 0.00000 ;H12-C28-C27-H15

45 28 29 72 3 0.65084 1.95253 0.00000 -2.60338 0.00000 0.00000 ;H12-C28-C29- N2

46 28 27 47 3 0.62760 1.88280 0.00000 -2.51040 0.00000 0.00000 ;H13-C28-C27-H14

46 28 27 48 3 0.62760 1.88280 0.00000 -2.51040 0.00000 0.00000 ;H13-C28-C27-H15

46 28 29 72 3 0.65084 1.95253 0.00000 -2.60338 0.00000 0.00000 ;H13-C28-C29- N2

47 27 26 49 3 0.62760 1.88280 0.00000 -2.51040 0.00000 0.00000 ;H14-C27-C26-H16

47 27 26 50 3 0.62760 1.88280 0.00000 -2.51040 0.00000 0.00000 ;H14-C27-C26-H17

48 27 26 49 3 0.62760 1.88280 0.00000 -2.51040 0.00000 0.00000 ;H15-C27-C26-H16

48 27 26 50 3 0.62760 1.88280 0.00000 -2.51040 0.00000 0.00000 ;H15-C27-C26-H17

49 26 25 51 3 0.62760 1.88280 0.00000 -2.51040 0.00000 0.00000 ;H16-C26-C25-H18

49 26 25 52 3 0.62760 1.88280 0.00000 -2.51040 0.00000 0.00000 ;H16-C26-C25-H19

50 26 25 51 3 0.62760 1.88280 0.00000 -2.51040 0.00000 0.00000 ;H17-C26-C25-H18

50 26 25 52 3 0.62760 1.88280 0.00000 -2.51040 0.00000 0.00000 ;H17-C26-C25-H19

51 25 24 53 3 0.62760 1.88280 0.00000 -2.51040 0.00000 0.00000 ;H18-C25-C24-H20

51 25 24 54 3 0.62760 1.88280 0.00000 -2.51040 0.00000 0.00000 ;H18-C25-C24-H21

52 25 24 53 3 0.62760 1.88280 0.00000 -2.51040 0.00000 0.00000 ;H19-C25-C24-H20

52 25 24 54 3 0.62760 1.88280 0.00000 -2.51040 0.00000 0.00000 ;H19-C25-C24-H21

53 24 23 55 3 0.62760 1.88280 0.00000 -2.51040 0.00000 0.00000 ;H20-C24-C23-H22

53 24 23 56 3 0.62760 1.88280 0.00000 -2.51040 0.00000 0.00000 ;H20-C24-C23-H23

54 24 23 55 3 0.62760 1.88280 0.00000 -2.51040 0.00000 0.00000 ;H21-C24-C23-H22

54 24 23 56 3 0.62760 1.88280 0.00000 -2.51040 0.00000 0.00000 ;H21-C24-C23-H23

55 23 22 57 3 0.62760 1.88280 0.00000 -2.51040 0.00000 0.00000 ;H22-C23-C22-H24

55 23 22 58 3 0.62760 1.88280 0.00000 -2.51040 0.00000 0.00000 ;H22-C23-C22-H25

56 23 22 57 3 0.62760 1.88280 0.00000 -2.51040 0.00000 0.00000 ;H23-C23-C22-H24

56 23 22 58 3 0.62760 1.88280 0.00000 -2.51040 0.00000 0.00000 ;H23-C23-C22-H25

57 22 21 59 3 0.62760 1.88280 0.00000 -2.51040 0.00000 0.00000 ;H24-C22-C21-H26

57 22 21 60 3 0.62760 1.88280 0.00000 -2.51040 0.00000 0.00000 ;H24-C22-C21-H27

58 22 21 59 3 0.62760 1.88280 0.00000 -2.51040 0.00000 0.00000 ;H25-C22-C21-H26

58 22 21 60 3 0.62760 1.88280 0.00000 -2.51040 0.00000 0.00000 ;H25-C22-C21-H27

59 21 20 61 3 0.62760 1.88280 0.00000 -2.51040 0.00000 0.00000 ;H26-C21-C20-H28

59 21 20 62 3 0.62760 1.88280 0.00000 -2.51040 0.00000 0.00000 ;H26-C21-C20-H29

60 21 20 61 3 0.62760 1.88280 0.00000 -2.51040 0.00000 0.00000 ;H27-C21-C20-H28

60 21 20 62 3 0.62760 1.88280 0.00000 -2.51040 0.00000 0.00000 ;H27-C21-C20-H29

61 20 19 71 3 0.00000 0.00000 0.00000 0.00000 0.00000 0.00000 ;H28-C20-C19- N1

61 20 19 73 3 3.68192 -4.35136 0.00000 1.33888 0.00000 0.00000 ;H28-C20-C19- O1

62 20 19 71 3 0.00000 0.00000 0.00000 0.00000 0.00000 0.00000 ;H29-C20-C19- N1

62 20 19 73 3 3.68192 -4.35136 0.00000 1.33888 0.00000 0.00000 ;H29-C20-C19- O1

63 17 14 66 3 30.33400 0.00000 -30.33400 0.00000 0.00000 0.00000 ;H30-C17-C14-H33

63 17 16 64 3 30.33400 0.00000 -30.33400 0.00000 0.00000 0.00000 ;H30-C17-C16-H31

[dihedrals] ; impropers

; i j k l func phase kd pn

1 5 2 6 1 180.00 4.60240 2 ; C1- C5- C2- C6

1 11 3 70 1 180.00 4.60240 2 ; C1-C11- C3-H37

1 15 4 34 1 180.00 4.60240 2 ; C1-C15- C4- H1

2 7 5 10 1 180.00 4.60240 2 ; C2- C7- C5-C10

2 8 6 9 1 180.00 4.60240 2 ; C2- C8- C6- C9

3 7 11 36 1 180.00 4.60240 2 ; C3- C7-C11- H3

4 1 3 2 1 180.00 4.60240 2 ; C4- C1- C3- C2

4 9 15 65 1 180.00 4.60240 2 ; C4- C9-C15-H32

5 11 7 12 1 180.00 4.60240 2 ; C5-C11- C7-C12

5 13 10 35 1 180.00 4.60240 2 ; C5-C13-C10- H2

6 13 8 14 1 180.00 4.60240 2 ; C6-C13- C8-C14

6 15 9 16 1 180.00 4.60240 2 ; C6-C15- C9-C16

8 10 13 67 1 180.00 4.60240 2 ; C8-C10-C13-H34

8 17 14 66 1 180.00 4.60240 2 ; C8-C17-C14-H33

9 17 16 64 1 180.00 4.60240 2 ; C9-C17-C16-H31

14 16 17 63 1 180.00 4.60240 2 ; C14-C16-C17-H30

18 33 30 39 1 180.00 4.60240 2 ; C18-C33-C30- H6

18 41 32 72 1 180.00 4.60240 2 ; C18- H8-C32- N2

19 12 71 37 1 180.00 4.60240 2 ; C19-C12- N1- H4

20 71 19 73 1 180.00 43.93200 2 ; C20- N1-C19- O1

30 31 33 40 1 180.00 4.60240 2 ; C30-C31-C33- H7

30 32 18 38 1 180.00 4.60240 2 ; C30-C32-C18- H5

31 32 72 29 1 180.00 4.60240 2 ; C31-C32- N2-C29

33 42 31 72 1 180.00 4.60240 2 ; C33- H9-C31- N2

[system]

PYN-AA

[molecules]

; Compound nmols

PYN 1

(3) Force field parameters for PYR in coarse grained resolution.

Here, for both PYR and PYN, the non-bonded parameters were inherited from the martini_v2.2.itp directly.

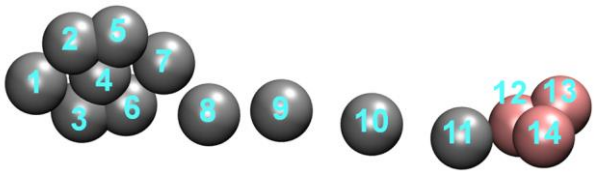

Snapshot of PYR in all atom representation (the index of each atom was also labeled in the above Figure).

The details of PYR force field in all atom resolution in Gromacs format are as follows:

PYR-CG.itp

[moleculetype]

;molname nrexcl

PYR-CG 1

[atoms]

;id	type	resnr	residu	atom	cgnr	charge	mass
1	SC3	1	PYR	B1	1	0.0000	0.000
2	SC3	1	PYR	B2	2	0.0000	56.545
3	SC3	1	PYR	B3	3	0.0000	56.545
4	SC3	1	PYR	B4	4	0.0000	0.000
5	SC3	1	PYR	B5	5	0.0000	0.000
6	SC3	1	PYR	B6	6	0.0000	0.000
7	SC3	1	PYR	B7	7	0.0000	88.062
8	Na	1	PYR	B8	8	0.0000	58.036
9	C2	1	PYR	B9	9	0.0000	42.078
10	C1	1	PYR	B10	10	0.0000	56.104
11	C2	1	PYR	B11	11	0.0000	42.078
12	SQ0	1	PYR	B12	12	1.0000	27.028
13	SC5	1	PYR	B13	13	0.0000	26.036
14	SC5	1	PYR	B14	14	0.0000	26.036

[bonds]

```
;   i    j     funct    length   force.c.
    7    8       1       0.3720       1250
    8    9       1       0.3937       1250
    9   10       1       0.3902       1250
   10   11       1       0.3972       1250
   11   12       1       0.3530       1250

#ifndef FLEXIBLE
[ constraints ]
#endif
    2    3    1        0.382     1000000
    2    7    1        0.460     1000000
    3    7    1        0.460     1000000
   12   13    1        0.270     1000000
   12   14    1        0.270     1000000
   13   14    1        0.270     1000000

[ angles ]
;   i    j    k       funct    angle    force.c.
    5    7    8         2       75.0       25.0
    6    7    8         2      160.0      25.0
    7    8    9         2      125.0      25.0
    8    9   10         2      180.0      25.0
    9   10   11         2      180.0      25.0
   10   11   12         2      180.0      25.0
   11   12   13         2      150.0      25.0
   11   12   14         2      150.0      25.0

[ virtual_sites3 ]
; virtual sites    funct            a            b
```

1	7	3	2	1	0.746411	0.746411
4	7	3	2	1	0.373206	0.373206
5	3	2	7	1	0.746411	0.507178
6	2	7	3	1	0.507178	0.746411

[exclusions]

1 2 3 4 5 6 7

2 3 4 5 6 7

3 4 5 6 7

4 5 6 7

5 6 7

6 7

(4) Force field parameters for PYN in coarse grained resolution.

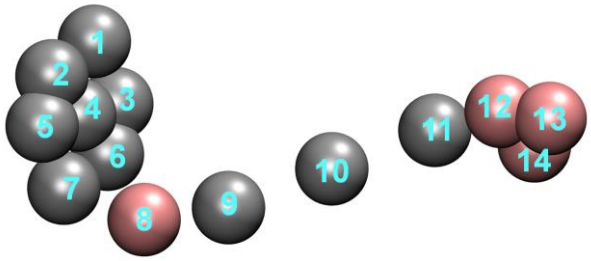

Snapshot of PYN in all atom representation (the index of each atom was also labeled in the above Figure).

The details of PYN force field in all atom resolution in Gromacs format are as follows:

; PYN-CG.top

[moleculetype]

;molname nrexcl

PYN-CG 1

[atoms]

; id	type	resnr	residu	atom	cgnr	charge	mass
1	SC3	1	PYN	B1	1	0.0000	0.000
2	SC3	1	PYN	B2	2	0.0000	56.545
3	SC3	1	PYN	B3	3	0.0000	56.545
4	SC3	1	PYN	B4	4	0.0000	0.000
5	SC3	1	PYN	B5	5	0.0000	0.000
6	SC3	1	PYN	B6	6	0.0000	0.000
7	SC3	1	PYN	B7	7	0.0000	88.062
8	P5	1	PYN	B8	8	0.0000	57.054
9	C2	1	PYN	B9	9	0.0000	42.078
10	C1	1	PYN	B10	10	0.0000	56.104
11	C2	1	PYN	B11	11	0.0000	42.078
12	SQ0	1	PYN	B12	12	1.0000	27.028
13	SC5	1	PYN	B13	13	0.0000	26.036
14	SC5	1	PYN	B14	14	0.0000	26.036

[bonds]

; i	j	funct	length	force.c.
7	8	1	0.3720	1250
8	9	1	0.3937	1250
9	10	1	0.3902	1250
10	11	1	0.3972	1250
11	12	1	0.3530	1250

#ifndef FLEXIBLE

[constraints]

#endif

2	3	1	0.382	1000000
2	7	1	0.460	1000000
3	7	1	0.460	1000000
12	13	1	0.270	1000000
12	14	1	0.270	1000000
13	14	1	0.270	1000000

[angles]

; i j k	funct	angle	force.c.
5 7 8	2	50.0	25.0
6 7 8	2	130.0	25.0
7 8 9	2	125.0	25.0
8 9 10	2	180.0	25.0
9 10 11	2	180.0	25.0
10 11 12	2	180.0	25.0
11 12 13	2	150.0	25.0
11 12 14	2	150.0	25.0

[virtual_sites3]

; virtual site funct a b

1 7 3 2 1 0.746411 0.746411

4 7 3 2 1 0.373206 0.373206

5 3 2 7 1 0.746411 0.507178

6 2 7 3 1 0.507178 0.746411

[exclusions]

1 2 3 4 5 6 7

2 3 4 5 6 7

3 4 5 6 7

4 5 6 7

5 6 7

6 7

Supplementary References

(1) Israelachvili, J. N.; Mitchell, D. J.; Ninham, B. W. Theory of Self-Assembly of Hydrocarbon Amphiphiles into Micelles and Bilayers. *J. Chem. Soc., Faraday Trans. 2: Mol. Chem. Phys.* **1976,** *72*, 1525-1568.

(2) Khalil, R. A.; Zarari, A.-h. A. Theoretical Estimation of the Critical Packing Parameter of Amphiphilic Self-Assembled Aggregates. *Appl. Surf. Sci.* **2014,** *318*, 85-89.

(3) Wang, J. M.; Wolf, R. M.; Caldwell, J. W.; Kollman, P. A.; Case, D. A. Development and Testing of a General Amber Force Field. *J. Comput. Chem.* **2004,** *25*, 1157-1174.

(4) Frisch, M. J.; Trucks, G. W.; Schlegel, H. B.; Scuseria, G. E.; Robb, M. A.; Cheeseman, J. R.; Scalmani, G.; Barone, V.; Mennucci, B.; Petersson, G. A. *et al*. *Gaussian, Inc.* Wallingford CT, 2009.

(5) Bayly, C. I.; Cieplak, P.; Cornell, W.; Kollman, P. A. A Well-Behaved Electrostatic Potential Based Method Using Charge Restraints for Deriving Atomic Charges: The Resp Model. *J. Phys. Chem.* **1993,** *97*, 10269-10280.

(6) Cornell, W. D.; Cieplak, P.; Bayly, C. I.; Kollmann, P. A. Application of Resp Charges to Calculate Conformational Energies, Hydrogen Bond Energies, and Free Energies of Solvation. *J. Am. Chem. Soc.* **1993,** *115*, 9620-9631.

(7) Ryckaert, J.-P.; Bellemans, A. Molecular Dynamics of Liquid Alkanes. *Faraday Discuss. Chem. Soc.* **1978,** *66*, 95-106.

(8) Bussi, G.; Donadio, D.; Parrinello, M. Canonical Sampling through Velocity Rescaling. *J. Chem. Phys.* **2007,** *126*, 014101.

(9) Parrinello, M.; Rahman, A. Polymorphic Transitions in Single Crystals: A New Molecular Dynamics Method. *J. Appl. Phys.* **1981,** *52*, 7182-7190.

(10) Darden, T.; York, D.; Pedersen, L. Particle Mesh Ewald: An N·log(N) Method for Ewald Sums in Large Systems. *J. Chem. Phys.* **1993,** *98*, 10089-10092.

(11) Essmann, U.; Perera, L.; Berkowitz, M. L.; Darden, T.; Lee, H.; Pedersen, L. G. A Smooth Particle Mesh Ewald Method. *J. Phys. Chem.* **1995,** *103*, 8577-8593.

(12) Hess, B.; Kutzner, C.; van der Spoel, D.; Lindahl, E. Gromacs 4: Algorithms for Highly Efficient, Load-Balanced, and Scalable Molecular Simulation. *J Chem. Theory Comput.* **2008,** *4*, 435-447.

(13) Marrink, S. J.; Risselada, H. J.; Yefimov, S.; Tieleman, D. P.; de Vries, A. H. The Martini Force Field: Coarse Grained Model for Biomolecular Simulations. *J. Phys. Chem. B* **2007,** *111*, 7812-7824.

(14) Wang, C.; Chen, Q.; Xu, H.; Wang, Z.; Zhang, X. Photoresponsive Supramolecular Amphiphiles for Controlled Self-Assembly of Nanofibers and Vesicles. *Adv. Mater.* **2010,** *22*, 2553-2555.

(15) Wang, C.; Yin, S.; Chen, S.; Xu, H.; Wang, Z.; Zhang, X. Controlled Self-Assembly Manipulated by Charge-Transfer Interactions: From Tubes to Vesicles. *Angew. Chem. Int. Ed.* **2008,** *47*, 9049-9052.

(16) Berendsen, H. J. C.; Postma, J. P. M.; van Gunsteren, W. F.; DiNola, A.; Haak, J. R. Molecular Dynamics with Coupling to an External Bath. *J. Chem. Phys.* **1984,** *81*, 3684-3690.

(17) Hess, B.; Bekker, H.; Berendsen, H. J.; Fraaije, J. G. LINCS: A Linear Constraint Solver for Molecular Simulations. *J. Comput. Chem.* **1997,** *18*, 1463-1472.

(18) Zhu, J.; Jiang, Y.; Liang, H.; Jiang, W. Self-Assembly of Aba Amphiphilic Triblock Copolymers into Vesicles in Dilute Solution. *J. Phys. Chem. B* **2005,** *109*, 8619-8625.

(19) Zhang, L.; Eisenberg, A. Multiple Morphologies and Characteristics of "Crew-Cut" Micelle-Like Aggregates of Polystyrene-B-Poly(Acrylic Acid) Diblock Copolymers in Aqueous Solutions. *J Am. Chem. Soc.* **1996,** *118*, 3168-3181.

(20) Yu, Y.; Zhang, L.; Eisenberg, A. Morphogenic Effect of Solvent on Crew-Cut Aggregates of Apmphiphilic Diblock Copolymers. *Macromolecules* **1998,** *31*, 1144-1154.

(21) Perkett, M. R.; Hagan, M. F. Using Markov State Models to Study Self-Assembly. *J. Chem. Phys.* **2014,** *140*, 214101.

(22) Han, Y.; Yu, H.; Du, H.; Jiang, W. Effect of Selective Solvent Addition Rate on the Pathways for Spontaneous

Vesicle Formation of Aba Amphiphilic Triblock Copolymers. *J. Am. Chem. Soc.* **2010,** *132*, 1144-1150.
(23) Han, M.; Hong, M.; Sim, E. Influence of the Block Hydrophilicity of Ab2 Miktoarm Star Copolymers on Cluster Formation in Solutions. *J. Chem. Phys.* **2011,** *134*, 204901.
(24) Choucair, A.; Eisenberg, A. Control of Amphiphilic Block Copolymer Morphologies Using Solution Conditions. *Eur. Phys. J E* **2003,** *10*, 37-44.
(25) Noguchi, H.; Yoshikawa, K. Morphological Variation in a Collapsed Single Homopolymer Chain. *J. Chem. Phys.* **1998,** *109*, 5070-5077.
(26) Rudnick, J.; Gaspari, G. The Aspherity of Random Walks. *J. Phys. A: Math. Gen.* **1986,** *19*, L191.
(27) Zifferer, G. Shape Asymmetry of Star‐Branched Random Walks with Many Arms. *J. Chem. Phys.* **1995,** *102* (9), 3720-3726.
(28) Noguchi, H.; Yoshikawa, K. Morphological Variation in a Collapsed Single Homopolymer Chain. *J. Chem. Phys.* **1998,** *109*, 5070-5077.
(29) Lin, C.-M.; Chen, Y.-Z.; Sheng, Y.-J.; Tsao, H.-K. Effects of Macromolecular Architecture on the Micellization Behavior of Complex Block Copolymers. *React. Funct. Polym.* **2009,** *69*, 539-545.
(30) Zhang, J.; Lu, Z.-Y.; Sun, Z.-Y. A Possible Route to Fabricate Patchy Nanoparticles Via Self-Assembly of a Multiblock Copolymer Chain in One Step. *Soft Matter* **2011,** *7*, 9944-9950.
(31) Li, B.; Zhu, Y.-L.; Liu, H.; Lu, Z.-Y. Brownian Dynamics Simulation Study on the Self-Assembly of Incompatible Star-Like Block Copolymers in Dilute Solution. *Phys. Chem. Chem. Phys.* **2012,** *14*, 4964-4970.
(32) Li, B.; Zhao, L.; Qian, H.-J.; Lu, Z.-Y. Coarse-Grained Simulation Study on the Self-Assembly of Miktoarm Star-Like Block Copolymers in Various Solvent Conditions. *Soft Matter* **2014,** *10*, 2245-2252.
(33) Zhao, Y.; Sheong, F. K.; Sun, J.; Sander, P.; Huang, X. A Fast Parallel Clustering Algorithm for Molecular Simulation Trajectories. *J. Comput. Chem.* **2013,** *34*, 95-104.
(34) Weinan, E.; Vanden-Eijnden, E. Towards a Theory of Transition Paths. *J. Stat. Phy.* **2006,** *123*, 503-523.
(35) Metzner, P.; Schütte, C.; Vanden-Eijnden, E. Transition Path Theory for Markov Jump Processes. *Multiscale Model. Simul.* **2009,** *7*, 1192-1219.
(36) Zeng, X.; Li, B.; Qiao, Q.; Zhu, L.; Lu, Z.-Y.; Huang, X. Elucidating Dominant Pathways of the Nano-Particle Self-Assembly Process. *Phys. Chem. Chem. Phys.* **2016,** *18*, 23494-23499.
(37) Noe, F.; Schutte, C.; Vanden-Eijnden, E.; Reich, L.; Weikl, T. R. Constructing the Equilibrium Ensemble of Folding Pathways from Short Off-Equilibrium Simulations. *Proc. Natl. Acad. Sci. U S A* **2009,** *106*, 19011-6.
(38) Ng, A. Y.; Jordan, M. I.; Weiss, Y. On Spectral Clustering: Analysis and an Algorithm. *Adv. Neural Inf. Process. Syst.* **2002,** *14*, 849-856.
(39) Eisenhaber, F.; Lijnzaad, P.; Argos, P.; Sander, C.; Scharf, M. The Double Cubic Lattice Method: Efficient Approaches to Numerical Integration of Surface Area and Volume and to Dot Surface Contouring of Molecular Assemblies. *J. Comput. Chem.* **1995,** *16*, 273-284.
(40) Humphrey, W.; Dalke, A.; Schulten, K. Vmd: Visual Molecular Dynamics. *J. Mol. Graphics* **1996,** *14*, 33-38.